Check for updates

RESEARCH ARTICLE

Inverted rift-orthogonal thrust systems in the Greenland–Iceland–Faroe Ridge: implications for the nature of the crust and plate tectonics

[version 1; peer review: awaiting peer review]

Jean-Baptiste Koehl

Grannes terrasse 107 U, Hafrsfjord, Rogaland, 4044, Norway

v1 **First published:** 24 Sep 2026, **6**:376
https://doi.org/10.12688/openreseurope.24284.1
Latest published: 24 Sep 2026, **6**:376
https://doi.org/10.12688/openreseurope.24284.1

Abstract

Background

The thickened character of the crust at the Greenland–Iceland–Faroe Ridge has thus far been attributed to extensive magmatism related to a mantle plume. However, the plume hypothesis does not satisfy all the available data, and more recently a continental nature has been suggested for the middle–lower crust at the Greenland–Iceland–Faroe Ridge.

Methods

We further test this hypothesis by using recent advances in interpreting major tectonic structures and magmatic features in the crust at the Greenland–Iceland–Faroe Ridge using seismic reflection and magnetic data.

Results

Seismic reflection interpretation suggests that late Paleoproterozoic (to Neoarchean?), WNW–ESE-striking thrust systems of the Laxfordian Orogen (or Badcallian–Inverian belt) extend from northern Scotland and off the Faroe Islands to Iceland and are capped by a few km thick Cenozoic lavas. These were mildly reworked into NE–SW-striking folds during the Caledonian Orogeny, which were inverted during Cenozoic rifting.

Conclusions

Open Peer Review

Approval Status *AWAITING PEER REVIEW*

Any reports and responses or comments on the article can be found at the end of the article.

The mid–lower crust at the Greenland–Iceland–Faroe Ridge is continental and truncated of late Paleoproterozoic thrust systems of the Laxfordian Orogen–Ammassalik Belt. These thrust systems hindered the development of NE–SW-striking, rift-parallel structures during subsequent tectonic episodes, which led to a relatively inefficient thinning of the crust during rifting and delayed breakup at the Greenland–Iceland–Faroe Ridge. This elongated rift-orthogonal ribbon of thinned orogenic crust flanked by oceanic crustal domains is interpreted as an orogenic bridge. This suggests a long-lived connection between Laurentia, Baltica, and Avalonia from ca. 1.8 (up to 2.6 Gyr), thus providing a new anchor for future plate reconstructions.

Plain Language summary
The crust in Iceland and nearby regions between Iceland and Greenland and Iceland and the Faroe Islands is anomalously thick (25–40 km), which differs from regular oceanic crust (c. 6–8 km). Thus far, this anomalous thickness was ascribed to excess magmatism generated by a mantle plume (magma influx from the core–mantle boundary) under Iceland. Reinterpretation of existing seismic reflection and magnetic data at the Iceland–Faroe Ridge suggests that 1.8 Gyr old, NW–SE-striking fault zones onshore northern Scotland and around the Faroe Islands continue into the Iceland–Faroe Ridge. Since these fault zones are older than the North Atlantic rift and related oceanic crust, the crust between Iceland and the Faroe Islands is therefore proposed to be continental. The potential occurrence of ribbons of 1.8 Gyr old continental crust between the Faroe Islands and Iceland and possibly between Iceland and Greenland suggest long-term connections between these continents, despite repeated cycles of oceanic opening (e.g., Iapetus Ocean, Atlantic Ocean). This has implications for the reconstruction of past supercontinent cycles.

Keywords
Greenland–Iceland–Faroe Ridge, Paleoproterozoic, orogen, Laxfordian, Ammassalik, rifting, Caledonian, Paleozoic, Cenozoic, fault, thrust, fold, tectonic, magma pathway, continental, crust, seismic reflection, magnetic, orogenic bridge, Laurentia, Baltica, Avalonia, plate reconstruction, Atlantic

H2020
This article is included in the Horizon 2020 gateway.

This article is included in the Marie-Sklodowska-Curie Actions (MSCA) gateway.

Corresponding author: Jean-Baptiste Koehl (jeanbaptiste.koehl@gmail.com)

Author roles: Koehl JB: Conceptualization, Data Curation, Formal Analysis, Funding Acquisition, Investigation, Methodology, Project Administration, Resources, Validation, Visualization, Writing – Original Draft Preparation, Writing – Review & Editing

Competing interests: No competing interests were disclosed.

Grant information: This project has received funding from the European Union's Horizon 2020 research and innovation programme under the Marie Skłodowska-Curie grant agreement No 101023439. In addition, the project received funding from Hilsen Geological & Psychological Consulting & Training Services (GeoPS).
The funders had no role in study design, data collection and analysis, decision to publish, or preparation of the manuscript.

Copyright: © 2026 Koehl JB. This is an open access article distributed under the terms of the Creative Commons Attribution License, which permits unrestricted use, distribution, and reproduction in any medium, provided the original work is properly cited.

How to cite this article: Koehl JB. **Inverted rift-orthogonal thrust systems in the Greenland–Iceland–Faroe Ridge: implications for the nature of the crust and plate tectonics [version 1; peer review: awaiting peer review]** Open Research Europe 2026, **6**:376 https://doi.org/10.12688/openreseurope.24284.1

First published: 24 Sep 2026, **6**:376 https://doi.org/10.12688/openreseurope.24284.1

Introduction

Despite decades of investigations, the 25–40 km thick crust and extensive magmatism at the Greenland–Iceland–Faroe Ridge remain controversial. These have been notoriously explained by the presence of a mantle plume rising from the core–mantle boundary to the base of the lithosphere (e.g., Morgan, 1971; Schilling, 1973; White & McKenzie, 1995). This is believed to have resulted in intense, dominantly mafic magmatism and an anomalously thick oceanic crust.

Tomographic studies suggest the presence of a low-velocity zone in the upper mantle under Iceland (e.g., Zhang *et al.*, 2024). However, the geometry, shape, and extent of this zone are highly debated (e.g., Bransðóttir & Menke, 2008; Foulger, 2025 and references therein). An emerging competing hypothesis (plate model) involves large remnants of continental crust and partial melting of the upper mantle due to decompression during exhumation (Anderson, 2000; Foulger, 2021; Foulger *et al.*, 2020; Foulger *et al.*, 2021; Hole & Natland, 2020).

In addition, various inconsistencies around the plume hypothesis have cast doubt on the nature of the crust and whether a dominantly mafic crust in the Greenland–Iceland–Faroe Ridge and other areas with anomalously thick crust offshore (e.g., Walvis, Rio Grande, Mozambique, Madagascar, Chagos–Laccadive, Gunnerus, and Astrid ridges; Koehl & Foulger, 2025) is sustainable. In Iceland, important inconsistencies include, e.g., a relatively cold crust under Iceland (Foulger *et al.*, 2003; Menke & Levin, 1994; Menke *et al.*, 1995), a much larger distance between the oldest rocks Icelandic rift zones (c. 500 km instead of 290 km) than what is predicted by the full-plate spreading rate in the northeastern Atlantic (Foulger, 2006), and non-linear, disrupted magnetic anomalies, which are atypical in oceanic crust (e.g., Foulger *et al.*, 2020).

It does not help that the substratum to the several km thick basaltic upper crust in Iceland still eludes scientists. The deepest wells onshore Iceland (IDDP and Reyðarfjörður wellbores; Friðleifsson, 1982; Friðleifsson *et al.*, 2017; Robinson *et al.*, 1982) and the Faroe Islands (Lopra wellbore; Waagstein *et al.*, 1982) all terminated in Cenozoic lavas (Figure 1a–b), which have been suggested to be up to 10 km thick in places (e.g., Jolley *et al.*, 2021; Layfield *et al.*, 2023; Richardson *et al.*, 1998; Williamson & Ziska, 2018).

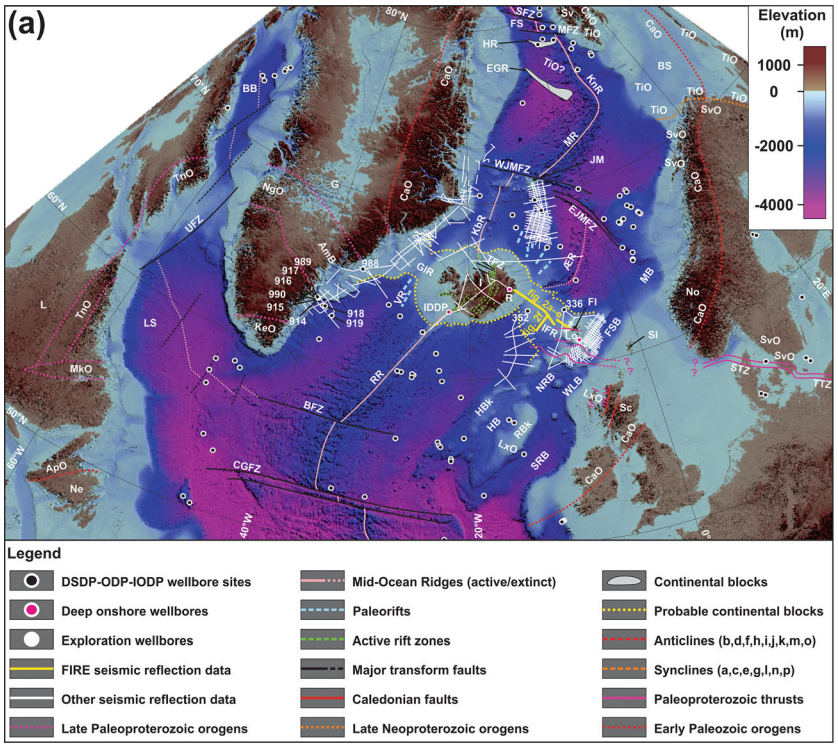
Furthermore, seaward-dipping reflectors are typically accepted as the continent–ocean boundary. However, recent seismic reflection mapping around the Faroe Islands have showed the existence of a network of WNW–ESE-striking brittle–ductile thrust systems (Koehl *et al.*, 2024a; Figure 1a–b). These were reworked mildly into NE–SW-striking folds and, in places, localized the formation of relatively shallow Caledonian thrusts (Koehl *et al.*, 2024a their Figure 2a, e, h, and i). These thrust systems strike parallel to the Greenland–Iceland–Faroe Ridge and were traced below seaward-dipping reflectors northwest of the Faroe Islands. The present work investigates potential tectonic structures in the Iceland–Faroe Ridge, their possible connection to structures around the Faroe Islands and onshore northern Scotland, and their impact on potential paleo rift centers (e.g., c).

Geological setting

Southeastern greenland

In southeastern Greenland, Archean–Paleoproterozoic basement rocks were deformed in the late Paleoproterozoic and form the WNW–ESE-striking Ammassalik Belt (Bridgewater & Myers, 1979; Chadwick & Vasudev, 1989; Chadwick *et al.*, 1989; Kalsbeek *et al.*, 1993a). Deformation in the Ammassalik Belt is strongly partitioned, with abrupt boundaries between zones of intensely deformed and near undeformed rocks (Bridgewater & Myers, 1979). This orogen is dominated by SSW-verging folds and thrusts crosscutting sinistral shear zones deformed under granulite-facies metamorphism and retrogressed to greenschist–amphibolite facies (Bridgewater & Myers, 1979; Chadwick *et al.*, 1989; Chadwick & Vasudev, 1989; Dawes *et al.*, 1989). Thrust systems in the Ammassalik Belt show mylonitic fabrics and sheared mafic intrusions, while fold structures are asymmetric (up to isoclinal) and are typically hundreds of meters wide (Chadwick & Vasudev, 1989). There is no evidence of Caledonian reworking in the Ammassalik Belt (Kalsbeek *et al.*, 1993a). Caledonian deformation was restricted to eastern and northeastern Greenland, where it reworked late Paleoproterozoic basement rocks and structures (Kalsbeek *et al.*, 1993b; Kalsbeek *et al.*, 2008), which partly retained their initial geometries (e.g., Thrane, 2004).

Archean–Mesoproterozoic basement and late Paleozoic–Mesozoic sedimentary rocks in southeastern Greenland are intruded by Cenozoic igneous rocks of the North Atlantic Igneous Province, most of which yielded mid Paleogene to mid Eocene geochronological ages (62.15–43.77 Ma; e.g., Brooks, 2011; Larsen *et al.*, 2014; Storey *et al.*, 2007; Tegner & Duncan, 1999; Tegner *et al.*, 2008; Wilkinson *et al.*, 2016). Onshore Cenozoic igneous rocks include basaltic dykes, syenite–gabbro intrusions, tuffs, volcaniclastics, pyroclastic flows, and seaward-dipping lava flows (e.g., Geoffroy, 2005; Guarnieri, 2011; Larsen *et al.*, 1999). The thickest Cenozoic lava flows are up to 3.5 km, but total volcanic thickness estimates are in the range of 6–7 km (Larsen *et al.*, 1989; Larsen *et al.*, 1999; Nilsen & Brooks, 1981).



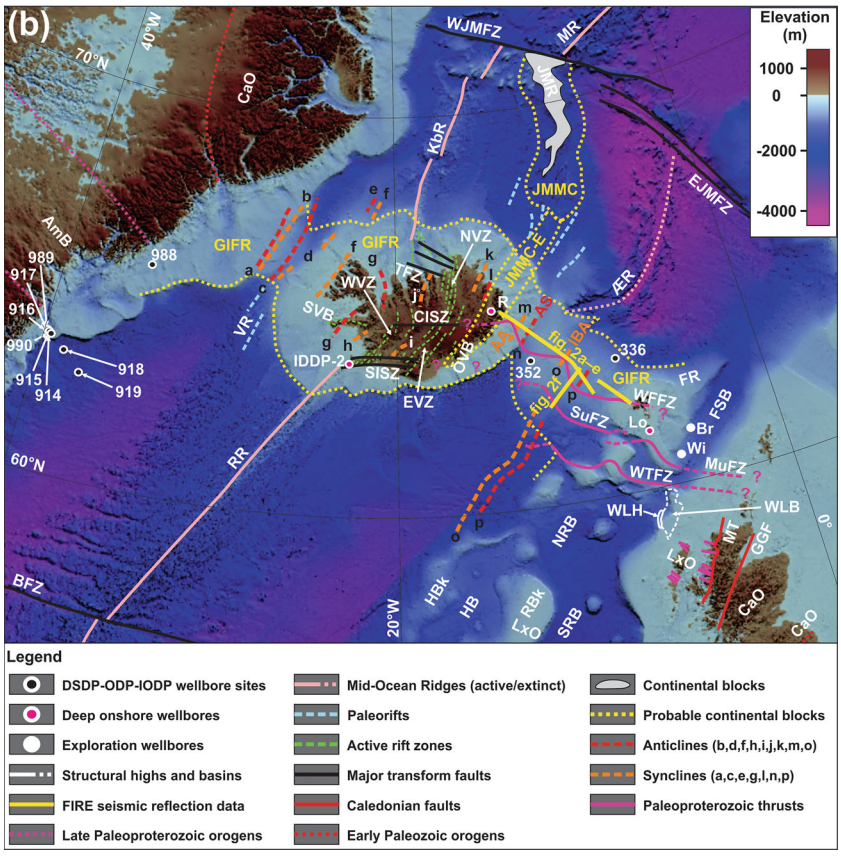


Figure 1. Caption continued on next page.

Offshore, seismic reflection studies have shown that Cenozoic igneous rocks include both intrusives (dykes and sills) and subaerial and subaqueous basaltic flows (Hovikoski *et al.*, 2021). Seaward-dipping reflectors are believed to be widespread at the Greenland–Iceland Ridge and possibly extend to Iceland (e.g., Dahl-Jensen *et al.*, 1997; Geoffroy *et al.*, 2021; Hopper *et al.*, 1998; Larsen & Jakobsðottir, 1988; Parson *et al.*, 1988). Basaltic seaward-dipping reflectors were drilled during ODP 152 and 163 (wellbores 915, 917, 918, 989, and 990; Figure 1a–b) and included dacite, which are absent onshore (Brooks, 2011; Tegner & Duncan, 1999). The thickest Cenozoic volcanic unit was penetrated by wellbore 915, which drilled through 779 m of basalt before terminating in pre-rift, likely lower Paleogene sedimentary rocks (Brooks, 2011).

Iceland

Outcrops onshore Iceland are dominated by Cenozoic–Quaternary lavas and igneous rocks intercalated with sparse contemporaneous sediments (e.g., Johannesson, 2014; Sæmundson, 1979). The oldest lavas onshore Iceland are c. 17 Ma and occur in the west and northwest (Harðarson *et al.*, 1997; McDougall *et al.*, 1984; Moorbath *et al.*, 1968). Lavas in northeastern Iceland are somewhat younger with ages up to 14.7 ± 0.4 Ma (Berg, 2016; Burchardt *et al.*, 2022; Jancin *et al.*, 1985; Martin *et al.*, 2011). Anorthosite inclusions were found locally in Cenozoic dolerite in western Iceland (Snæfellsnes; Griffin *et al.*, 1974; Kristmannsdóttir, 1971).

Icelandic lavas dip both inward and outward (with regards to the center of the island), which results in overall NE–SW- to NNE–SSW-striking synclinal and anticlinal geometries (e.g., Bourgeois *et al.*, 2005; Jancin *et al.*, 1985; Johannesson, 1980; Sæmundsson, 1979). Some of these structures were interpreted as potential fault-related rollover folds with syn-folding lava flows thinning away from syncline hinge zones and felsic intrusions in the footwall of related normal faults (e.g., Bourgeois *et al.*, 2005). Similarly, Icelandic lavas have been interpreted as (extensional-detachment-bounded) seaward-dipping reflectors (e.g., Geoffroy, 2005; Larsen & Jakobsðottir, 1988). At some anticlines, older lavas are separated from overlying younger lavas by (tilted) unconformities (e.g., Garcia *et al.*, 2003; Garcia *et al.*, 2008; Hjartarson, 2003; Johannesson, 1980; Johannesson, 2014; Sæmundsson, 1979). Adjacent synclines are thus typically interpreted as paleo rift centers (e.g., Boðvarsson & Walker, 1964; Harðarson *et al.*, 1997; Hjartarson, 2003; Hjartarson *et al.*, 2017).

Figure 1. (a) Bathymetric map of the North Atlantic region showing the main orogens, mid-ocean ridges, structural elements, and related faults. Notice the alignment of the Teisseyre–Tornquist Zone (TTZ) and Sorgenfrei–Tornquist Zone (STZ) with the late Paleoproterozoic thrust systems around the Faroe Islands and onshore northern Scotland (fuchsia lines). The basemap is from GEBCO Compilation Group (2023; displayed in projection UTM27). Abbreviations: AmB: Ammassalik Belt; ApO: Appalachian Orogen; BB: Baffin Bay; BFZ: Bight fault zone; BS: Barents Sea; CaO: Caledonian Orogen; CGFZ: Charlie Gibbs fault zone; DS: Davis Strait; EGR: East Greenland Ridge; EJMFZ: East Jan Mayen fault zone; FI: Faroe Islands; FS: Fram Strait; FSB: Faroe–Shetland Basin; G: Greenland; GIR: Greenland–Iceland Ridge; HB: Hatton Basin; HBk: Hatton Bank; HR: Hovgård Ridge; I: Iceland; IDDP-2: Iceland Deep Drilling Project wellbore 2; IFR: Iceland–Faroe Ridge; JM: Jan Mayen; KbR: Kolbeinsey Ridge; KeO: Ketilidian Orogen; KnR: Knipovich Ridge; L: Labrador; Lo: Lopra wellbore; LS: Labrador Sea; LxO: Laxfordian Orogen; MB: Møre Basin; MFZ: Molloy fault zone; MkO: Makkovikian Orogen; MR: Mohns Ridge; Ne: Newfoundland; NgO: Nagssugtoqiian Orogen; No: Norway; NRB: Northern Rockall Basin; R: Reyðarfjörður wellbore; RBk: Rockall Bank; RR: Reykjanes Ridge; Sc: Scotland; SFZ: Spitsbergen fault zone; SI: Shetland Islands; SRB: Southern Rockall Basin; STZ: Sorgenfrei–Tornquist Zone; Sv: Svalbard; SvO: Svecofennian Orogen; TFZ: Tjörnes fault zone; TiO: Timanian Orogen; TnO: Torngat Orogen; TTZ: Teisseyre–Tornquist Zone; UFZ: Ungava Fault Zone; WJMFZ: West Jan Mayen fault zone; ÆR: Ægir Ridge. (b) Zoom in the Greenland–Iceland–Faroe Ridge and nearby areas showing the continuation of potential (Neoarchean?–) late Paleoproterozoic thrust systems from northern Scotland and around the Faroe Islands to Iceland (e.g., West Faroe and Suðurøy fault zones; WFFZ and SuFZ). Notice the alignment of these thrust systems with the Southern Iceland Seismic Zone (SISZ) and Central Iceland Shear Zone (CISZ). The basemap is from GEBCO Compilation Group (2023; displayed in projection UTM27). Notice the extended Jan Mayen Microcontinent suggested by Torsvik et al. (2015) in eastern Iceland. Anticlines and synclines in the Greenland–Iceland–Faroe Ridge (a–p) are from Hjartarson et al. (2017) and the present study. Anticlines "m" and "o" and syncline "n" were named Austurbrún Anticline (AA), Iceland Basin Anticline (IBA), and Austurbrún Syncline (AS) respectively by Hjartarson et al. (2017). Abbreviations: AA: Austurbrún Anticline; AmB: Ammassalik Belt; AS: Austurbrún Syncline; BFZ: Bight fault zone; Br: Brugdan wellbore; EJMFZ: East Jan Mayen fault zone; EVZ: East Volcanic Zone; FR: Fugløy Ridge; FSB: Faroe–Shetland Basin; GGF: Great Glen Fault; IBA: Iceland Basin Anticline; IDDP-2: Iceland Deep Drilling Project wellbore 2; JMMC: Jan Mayen Microcontinent; JMMC-E: Jan Mayen Microcontinent extended; JMR: Jan Mayen Ridge; KbR: Kolbeinsey Ridge; Lo: Lopra wellbore; LxO: Laxfordian Orogen; MR: Mohns Ridge; MT: Moine Thrust; MuFZ: Munkagrunnur fault zone; NVZ: North Volcanic Zone; ÖVB: Öræfi Volcanic Belt; R: Reyðarfjörður wellbore; SVB: Snæfellsnes Volcanic Belt; SuFZ: Suðurøy fault zone; TFZ: Tjörnes fault zone; VR: Versturdjupet Rift; WFFZ: West Faroe fault zone; Wi: William wellbore; WJMFZ: West Jan Mayen fault zone; WLB: West Lewis Basin; WLH: West Lewis High; WTFZ: Wyville–Thomson fault zone; WVZ: West Volcanic Zone; ÆR: Ægir Ridge.

Structural trends onshore Iceland include rift-parallel, NE–SW- to NNE–SSW-striking normal faults and rift-orthogonal, WNW–ESE- to E–W-striking normal and strike-slip faults. While the former dominate in active volcanic zones along the rift axis, the latter are well developed in northern to southern central Iceland (e.g., Tjörnes fault zone, Central Iceland Shear Zone, and Southern Iceland Seismic Zone) and in western Iceland at Snæfellsnes (Snæfellsnes Volcanic Zone; Bergerat & Angelier, 2008; Khodayar, 2018; Khodayar & Einarsson, 2002; Khodayar *et al.*, 2020; Liotta *et al.*, 2021; Tryggvason, 1973; Villemin *et al.*, 1994; Young *et al.*, 1985; Figure 1b).

Seismic studies suggest that the Icelandic crust is 25–40 km thick (e.g., Darbyshire *et al.*, 1998; Du & Foulger, 2001; Foulger *et al.*, 2003). It is typically thought to comprise a few kilometers thick upper crustal layer consisting primarily of basaltic lavas (e.g., Tryggvason & Båth, 1961), which were drilled down to a depth of 4.5 km by the Iceland Deep Drilling Project wellbore in southwestern Iceland (Friðleifsson *et al.*, 2017) and c. 3.5 km in eastern Iceland (Friðleifsson, 1982; Robinson *et al.*, 1982).

The nature of the lower is, however, disputed and two main hypotheses are generally favored by geochemical studies. The first is a magma-inflated mafic lower crust related to a potential mantle plume below Iceland (e.g., Morgan, 1971; Schilling, 1973; White & McKenzie, 1995). The second is a (partly?) continental lower crust (e.g., Day, 2016; Jonasson, 2007; Natland, 2007; Torsvik *et al.*, 2015). The latter is supported by the relatively large proportion of silicic (i.e., felsic to intermediate) magmatism in Iceland (up to 21%; e.g., Jonasson, 2007; Natland, 2007; Thordarson & Larsen, 2007; Walker, 1964), which contrasts with mid-ocean ridge magmatism (c. 6% at the East Pacific Rise; Natland, 2007). This is further supported by evidence of extensive crustal contamination of lavas in southeastern Iceland (East Volcanic Zone; Figure 1b), which is the most productive magmatic zone in Iceland (80% of total erupted volume in the past 1130 years; Thordarson & Larsen, 2007) and displays a similar contamination crustal trend as lavas in the Jan Mayen Microcontinent Complex (Torsvik *et al.*, 2015).

Magnetotelluric studies have long shown evidence of a deep conductive layer at a depth of 5–20 km under Iceland (e.g., Arnason et al., 2025). This layer domes up under central volcanoes and geothermal fields. Although it is compatible with the presence of melt below active volcanoes in Iceland, it is not elsewhere, thus suggesting solid-state conduction. Arnason *et al.* (2025) thus suggested the presence of iron- and titanium-rich and/or hydrated minerals in the deep conductive layer.

Greenland–Iceland–Faroe Ridge

Seismic studies have shown that the Greenland–Iceland–Faroe Ridge is 23–40 km thick (Bohnhoff & Makris, 2004; Darbyshire *et al.*, 1998; Foulger *et al.*, 2003; Funck *et al.*, 2014). This anomalously thick crust in presumed oceanic crustal domain is typically attributed to intense magmatism due to a putative mantle plume under Iceland, thus resulting in a magma-inflated mafic crust (Morgan, 1971; White & McKenzie, 1995). Recent studies have however pointed at probable occurrences of continental crust in parts of the Greenland–Iceland–Faroe Ridge (e.g., Bohnhoff & Makris, 2004; Foulger *et al.*, 2020; Torsvik *et al.*, 2015).

Regardless, the upper crustal layer in the Greenland–Iceland–Faroe Ridge consists of several km thick Cenozoic lavas arranged in seaward-dipping reflectors (e.g., Geoffroy *et al.*, 2021; Hjartarson *et al.*, 2017). Near the center of the Iceland–Faroe Ridge, seismic data suggest that the crust is thinnest (c. 23 km) and that Cenozoic lavas are up to 3 km thick (Bohnhoff & Makris, 2004). Two DSDP 38 wellbores were drilled in the Iceland–Faroe Ridge and terminated in Cenozoic sediments and basalts (wellbores 336 and 352 in Figure 1a–b; Talwani *et al.*, 1976). Noteworthy, the 3 km estimate for Cenozoic volcanics is a maximum and includes the <1 km thick, low-velocity layer below the high-velocity basaltic unit penetrated in wellbore 336 (Bohnhoff & Makris, 2004). The low-velocity layer may represent a volcaniclastic endmember of the Cenozoic volcanics (e.g., hyaloclastites). This is suggested by results from the Brugdan and William wells in the Faroe–Shetland Basin (location in Figure 1b), which penetrated a similar low-velocity, 300–400 m thick layer of hyaloclastites below high-velocity basaltic lavas (Ólavsdóttir *et al.*, 2021; Schuler *et al.*, 2013). Wellbore 336 showed evidence of paleosols above basaltic flows dated to 43 ± 3.3 Ma (Talwani *et al.*, 1976), thus indicating that the Iceland–Faroe Ridge was exposed above sea level in the mid–late Eocene (Nilsen & Kerr, 1978).

Recently, the seismic reflection study by Hjartarson *et al.* (2017) has suggested that large, hundreds km wide, NE–SW- to NNE–SSW-striking folds occur below the Cenozoic lavas in the Greenland–Iceland and Iceland–Faroe ridges. Like onshore Iceland, these were interpreted as abandoned rift centers, e.g., Vesturdjupet Rift (Figure 1a–b; Hjartarson *et al.*, 2017).

Faroe Islands

Most Cenozoic igneous rocks onshore the Faroe Islands intruded the continental margin at ca. 60.8–50.5 Ma (i.e., mid Paleogene–early Eocene; e.g., Hansen & Ganerød, 2023; Storey *et al.*, 2007; Wilkinson *et al.*, 2016). They are generally believed to be c. 6.6 km thick (Passey & Jolley, 2008; Waagstein *et al.*, 1982), but seismic interpretation in the Faroe–Shetland Basin suggests that they could be >10 km thick, e.g., at the Brugdan wellbore and the Fugløy Ridge (Jolley *et al.*, 2021 their Figure 9; Layfield *et al.*, 2023 their Figure 2; Richardson *et al.*, 1998; Williamson & Ziska, 2018 their Figures 6–10).

Offshore, Cenozoic volcanics occur as thick successions of lava flows (including lava deltas), hyaloclastites, and volcaniclastics (e.g., Ellefsen *et al.*, 2009; Jolley *et al.*, 2021; Schuler *et al.*, 2013; Williamson & Ziska, 2018). Intrusions include dykes and (saucer-shaped) sills (e.g., Ellefsen *et al.*, 2009; Hansen *et al.*, 2004; Koehl *et al.*, 2024a; Layfield *et al.*, 2023). Seaward-dipping reflectors occur to the north and west of the Faroe Islands (e.g., Davison *et al.*, 2010; Koehl *et al.*, 2024a; Parson *et al.*, 1988; Smythe, 1983).

The nature of the substratum below the Cenozoic volcanics in the Faroe region is uncertain. The deepest well onshore the Faroe Islands (Lopra wellbore) terminated into pre-breakup basalts at a depth of 2178 m (Waagstein *et al.*, 1982), whereas offshore drilling in the Faroe–Shetland Basin terminated into sub-basalt hyaloclastites (e.g., Brugdan well) and basalt (e.g., William well; Jolley *et al.*, 2021; Schuler *et al.*, 2013; Williamson & Ziska, 2018). Nevertheless, recent seismic interpretation around the Faroe Islands suggests the occurrence of deep-seated, several to tens of km thick, WNW–ESE-striking thrust systems, which were reworked into hundreds km wide, NNE–SSW- to NE–SW-striking folds possibly during Caledonian and early Cenozoic contraction and, in places, localized the formation of Caledonian thrusts (Koehl *et al.*, 2024a). These were tentatively correlated with the WNW–ESE-striking, late Paleoproterozoic shear zones in northern Scotland and were traced below and beyond the seaward-dipping reflectors northwest of the Faroe Islands (Koehl *et al.*, 2024a).

Rockall

The Rockall region north of Ireland and west of Scotland consists of various Phanerozoic sedimentary basins and Precambrian basement highs with respective crustal thicknesses of 10–15 km and > 15–25 km, except in the Southern Rockall Basin where the crust may be as thin as 5–6 km in places (Funck *et al.*, 2014 their Figure 6.6; Kimbell *et al.*, 2016 their Figures 3–4). The entire region is believed to be underpinned by (hyper-) extended continental crust (Funck *et al.*, 2014 their Figure 6.6; Kimbell *et al.*, 2016 their Figures 3–4). Crustal thinning in the Rockall region is believed to be the result of successive periods of extension, including late–post-Caledonian collapse, and Permian–Triassic, Jurassic–Early Cretaceous, and Cenozoic rifting, as suggested by related sedimentary basins and tens of km wide Cenozoic igneous centers appearing as dominantly negative circular magnetic anomalies (e.g., Bird *et al.*, 2016; Coward *et al.*, 1989; Jolley *et al.*, 2021; Kimbell *et al.*, 2005; Musgrove & Mitchener, 1996; Waddams & Cordingley, 1999).

The NNE–SSW-striking Rockall Bank and West Lewis High are cored by Precambrian metamorphic rocks, which crop out on the seafloor where Cenozoic lavas are absent (Figure 1a–b). These are rocks recorded late Paleoproterozoic Laxfordian metamorphism and are comparable to rocks of the Lewisian Complex in Scotland (Dickin, 1992; Hitchen, 2004; Morton & Taylor, 1991; Roberts *et al.*, 1973; Waddams & Cordingley, 1999). Hatton Bank is characterized by a mild positive gravimetric anomaly, which is less intense than the high positive anomaly of upper Archean–Paleoproterozoic rocks at Rockall High (Hitchen, 2004). This structural high is separated from the Hatton Basin (Figure 1a–b) in the southeast by four igneous centers and is generally covered by Cenozoic lavas, except in a few places where mid Cretaceous sedimentary rocks were penetrated by exploration wells (Hitchen, 2004; Johnson *et al.*, 2005). There, the Mesozoic sedimentary succession is deformed into several km wide, dome- and trough-shaped folds warping around the Cenozoic igneous centers, thus suggesting that deformation is related to Cenozoic magmatism (Hitchen, 2004; Johnson *et al.*, 2005).

The Southern Rockall Basin (previously known as Rockall Trough and Rockall Basin) is an up to 6 km thick, late Paleozoic–Mesozoic sedimentary basin with an asymmetric, dominantly down–southeast, half-graben geometry (Kimbell *et al.*, 2016; Musgrove & Mitchener, 1996; Shannon *et al.*, 1999; Shannon *et al.*, 2020). Cenozoic lavas are generally thin or absent. Instead, the center of the basin was intruded by Cenozoic sills (Edwards, 2002; Musgrove & Mitchener, 1996). In contrast, the Northern Rockall, West Lewis, and possibly Hatton basins are covered by a few km thick succession of Cenozoic lava flows (Hitchen & Stoker, 1993; Hitchen *et al.*, 1997; Kimbell *et al.*, 2016; Musgrove & Mitchener, 1996; Waddams & Cordingley, 1999). These basins consist of up to several km thick upper Paleozoic–Mesozoic sedimentary rocks partly penetrated by exploration wells below the Cenozoic lavas. The Northern Rockall Basin defines a left step (i.e., to the northwest) with the main branch of the Permian–Triassic to Mesozoic rift system in the south, the Southern Rockall Basin (Figure 1a–b; Davison *et al.*, 2010; Hitchen, 2004; Waddams & Cordingley, 1999).

Northern Scotland

The bedrock in northern Scotland consists dominantly of Archean–Paleoproterozoic rocks of the Lewisian Complex such as gneiss, anorthosite, granulite, charnockite, and amphibolite (e.g., Evans, 1965; Evans & Lambert, 1974; Frazer, 1977; Sutton & Watson, 1950; Tarney & Weaver, 1987; Weaver & Tarney, 1980). These were first affected by granulite-facies metamorphism during the Badcallian event at ca. 2.8–2.7 Ga (Corfu *et al.*, 1994; Park, 1970; Zirkler *et al.*, 2012). They were partly retrogressed to amphibolite facies during the Inverian event at ca. 2.6–2.4 Ga (e.g., Attfield, 1987; Barooah & Bowes, 2009; Corfu *et al.*, 1994; Coward & Park, 1987; Evans & Lambert, 1974; Park, 1970; Storey *et al.*, 2010), which might be part of the Badcallian event, reflecting cooling to amphibolite-facies conditions (e.g., Love *et al.*, 2004; Zirkler *et al.*, 2012). Badcallian–Inverian contraction initiated the formation of major, WNW–ESE-striking, ductile fabrics, including tens of km-wide thrusts (Attfield, 1974; Corfu *et al.*, 1994; Evans & Lambert, 1974; Love *et al.*, 2004; Sutton & Watson, 1950). These were later reactivated into subvertical strike-slip shear zones during the late Paleoproterozoic during the Laxfordian Orogeny (e.g., Attfield, 1987; Coward & Park, 1987; Zirkler *et al.*, 2012). Further tectonic reworking and overprinting, including mylonitization, occurred in the (late) Neoproterozoic (Storey *et al.*, 2004). During the Caledonian Orogeny, preexisting structures and rocks of the Lewisian Complex were partly reactivated, truncated, and/or reworked by NE–SW- to NNE–SSW-striking folds and thrusts (e.g., Bird *et al.*, 2016; Brewer & Smythe, 1984; Coward, 1980; Coward, 1990; Coward *et al.*, 1980). Further folding occurred in the Cenozoic around igneous centers (e.g., Friend *et al.*, 1963; Longman & Coward, 1979).

Methods

The present study uses 2D seismic reflection data from TGS (e.g., Koehl *et al.*, 2024a) and the British Geological Survey (e.g., Smallwood *et al.*, 1998; Staples *et al.*, 1997), and magnetic data from the NAG-TEC consortium (Gaina *et al.*, 2017; Hopper *et al.*, 2014; Nasuti & Olesen, 2014a; Nasuti & Olesen, 2014b). Seismic reflection data were interpreted using Petrel (version 2021.3). An open-source alternative is OpendTect. Magnetic data were interpreted using GlobalMapper (version 13.0). The figures were designed with CorelDraw (version 2017). QGIS and GIMP are open-source alternative software.

The seismic and magnetic facies of the interpreted tectonic structures are described in previous studies, in which they were tied to structural trends onshore and to offshore exploration wellbores (Koehl, 2021; Koehl, 2025; Koehl *et al.*, 2019; Koehl *et al.*, 2022; Koehl *et al.*, 2023a; Koehl *et al.*, 2023b; Koehl *et al.*, 2024a; Koehl & Stokmo, 2024). The reader is referred to these studies for more detailed descriptions of the interpreted structures.

Sub-basalt units in Iceland and the Greenland–Iceland–Faroe Ridge are yet to be penetrated by drilling. The deepest wells onshore Iceland terminated in Cenozoic basaltic lavas (IDDP and Reyðarfjörður wellbores in Figure 1a–b; Friðleifsson, 1982; Friðleifsson *et al.*, 2017; Robinson *et al.*, 1982). Offshore, two DSDP 38 wellbores were drilled in the Iceland–Faroe Ridge and terminated in Cenozoic sediments and basalts (wellbores 336 and 352 in Figure 1a–b; Talwani *et al.*, 1976). Correlations in the study area are thus based on the geology of adjacent onshore areas (e.g., northern Scotland, southeastern Greenland, Iceland, and the Faroe Islands) and previous offshore studies (e.g., Koehl *et al.*, 2024a). Our interpretation is based on the previous detailed description of the internal geometry of thrust systems (Koehl *et al.*, 2022; Koehl *et al.*, 2023a; Koehl, 2025; Koehl and Stokmo, 2024) and mylonitic thrusts in metamorphosed basement rocks in seismic reflection data (Christensen, 1965; Fazlikhani *et al.*, 2017; Fountain *et al.*, 1984; Hedin *et al.*, 2016; Hurich *et al.*, 1985; Koehl *et al.*, 2018; Phillips *et al.*, 2016). The structural orientations refer to present-day coordinates. High-resolution versions of the seismic transects (Figure 2a–f) are available on Zenodo (https://doi.org/10.5281/zenodo.20606344; Koehl, 2025) and of the data around the Faroe Islands on DataverseNO (https://doi.org/10.18710/780M9P; Koehl, 2024).

The frequency of the FIRE (Faroe–Iceland Reflection Experiment) 2D seismic reflection data from the BIRPS (British Institutes Reflection Profiling Syndicate; now at the British Geological Survey) at a depth of 10 km is 30 Hz (Western Geco, 1996) and seismic velocity within Paleoproterozoic metamorphic rock units overall 6300–6500 $m.s^{-1}$ (i.e., c. 6400 $m.s^{-1}$; Bamford, 1979; Luckett & Baptie, 2015; Watson & Dunning, 1979) and up to 6300–6800 $m.s^{-1}$ in mylonites (Kästner et al., 2020 their table 2; Siegesmund *et al.*, 1991). These indicate that the vertical resolution of the seismic data (1/4 of the wavelength) is c. 53.3 m (6400/30/4). In places, the vertical resolution of seismic data may be as good as 1/32 of the wavelength (Kallweit & Wood, 1982; Li & Zhu, 2000), i.e., up to c. 6.7 m in the present case (6400/30/32). The horizontal resolution of the data at a depth of 5000 m is c. 730 m $((5000 \times (6400/30/2))^{1/2}$; Geldart & Sheriff, 2004). The studied structures (e.g., asymmetric folds in major shear zones and thrusts) are >500 meters wide and > 150 meters thick. They are thus well within the vertical and horizontal resolution of the dataset even at depth > 5000 m. The vertical and horizontal resolution of 2D seismic survey OF95RE11 (TGS) are respectively c. 39 m (up to c. 5 m) and c. 627 m (Koehl *et al.*, 2024a; Nicholson, 2012).

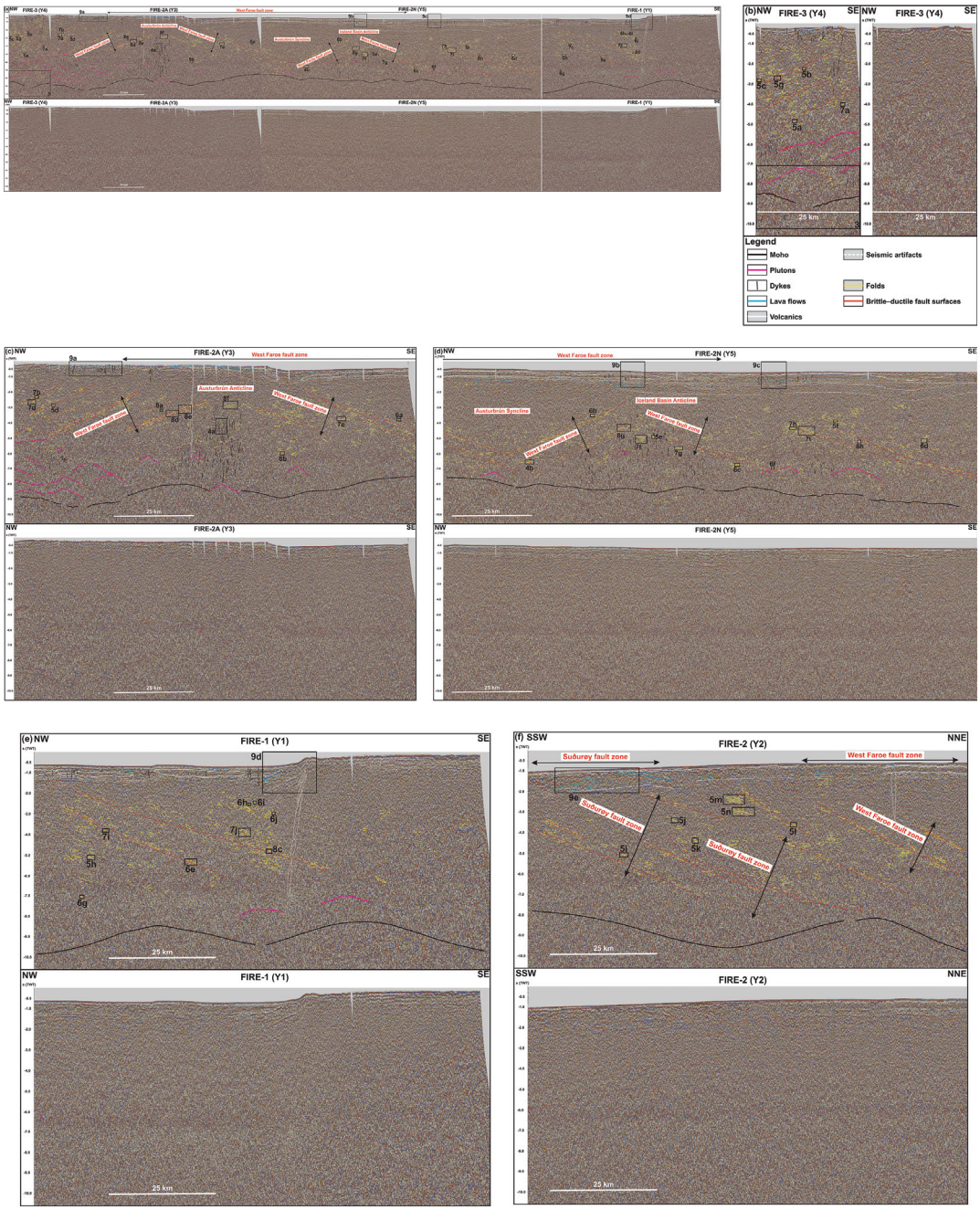


Figure 2. (a) NW–SE-striking FIRE seismic reflection transect along the Iceland–Faroe Ridge (lines FIRE-3 – Y4, FIRE-2A – Y3, FIRE-2 N –Y5, and FIRE-1 – Y1 from northwest to southeast). Legend is shown in (b) and location in Figure 1a–b. (b) Zoom in line FIRE-3 – Y4. (c) Zoom in line FIRE-2A – Y3. Legend is shown in (b). (d) Zoom in line FIRE-2 N – Y5. Legend is shown in (b). (e) Zoom in line FIRE-1 – Y1. Legend is shown in (b). (f) NNE–SSW-striking FIRE seismic reflection transect across the Iceland–Faroe Ridge (line FIRE-2 –Y2). Legend is shown in (b) and location in Figure 1a–b.

The NAG-TEC magnetic dataset is compiled from surveys acquired with different line spacing (from 200 m to 50 km) and flying altitude (from near sea level to 4100 m above sea level (Nasuti & Olesen, 2014a). More details about the data are included in Hopper *et al.* (2014).

Results

Seismic reflection data

Description

Moho

In the northwesternmost part of the Iceland–Faroe Ridge, a set of 10 km wide, bright, high-amplitude, undulating reflections occurs at a depth of 8.5–9.5 seconds (TWT; fuchsia lines in Figure 2a–e and Figure 3). This equates to a depth of c. 25.5–33.3 km assuming an average seismic velocity of 6–7 km.s^{-1} for the entire crust at the Iceland–Faroe Ridge; Bohnhoff & Makris, 2004). These reflections are abundant up to 50–55 km southeast of Iceland but are sparse farther southeast (Figure 2a–e).

Mid–lower crust

Directly above the high-amplitude undulating reflections at 8.5–9.5 seconds (TWT) depth southeast of Iceland, seismic reflection data show 5–10 km wide, c. 1.0 second (TWT) thick, dome-like, lensoidal packages of slightly increased reflectivity at depths of 5.0 to 8.5–9.5 seconds (TWT; Figure 2a–e). In the northwest, these lensoidal packages are stacked onto one another but become more difficult to track farther southeast due to decreasing reflectivity (Figure 2a–e).

Above the 8.5–9.5 second-deep, high-amplitude, undulating reflections and dominantly at depths of 8.0 seconds up to 3.0–4.0 seconds (TWT), the crust consists dominantly of moderate- to high-amplitude reflections showing asymmetric (subsidiary symmetric), curving-up or Z- to S-shaped geometries (yellow lines in Figure 2a–f). Such reflections are also found in places below the 8.5–9.5 second-deep, high-amplitude, undulating reflections (Figure 2a–f). These reflections display a wide range of geometrical variations, ranging from open symmetric (Figure 3 and Figure 4a–b) to tight recumbent isoclinal (Figure 4a–b, Figure 5a–n, Figure 6a–j, Figure 7a–j, and Figure 8a–h), including double-vergence geometry (Figure 5e). In the northwest, some curving-up reflections are observed at a depth of 0.5 second (TWT; i.e., c.

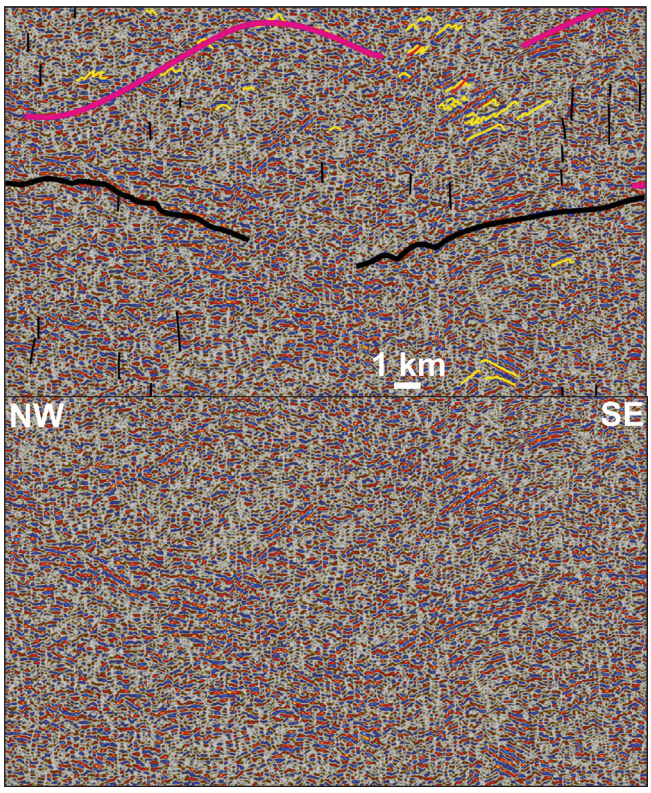


Figure 3. Interpreted (up) and uninterpreted (down) zoom in the northwestern end of the NW–SE-striking FIRE seismic transect showing a relatively reflective Moho near Iceland and lensoidal, upward-curving packages interpreted as possible plutons. The transect also shows potential folding of the mantle rocks (yellow lines below the Moho). Location is shown in Figure 2a–b.

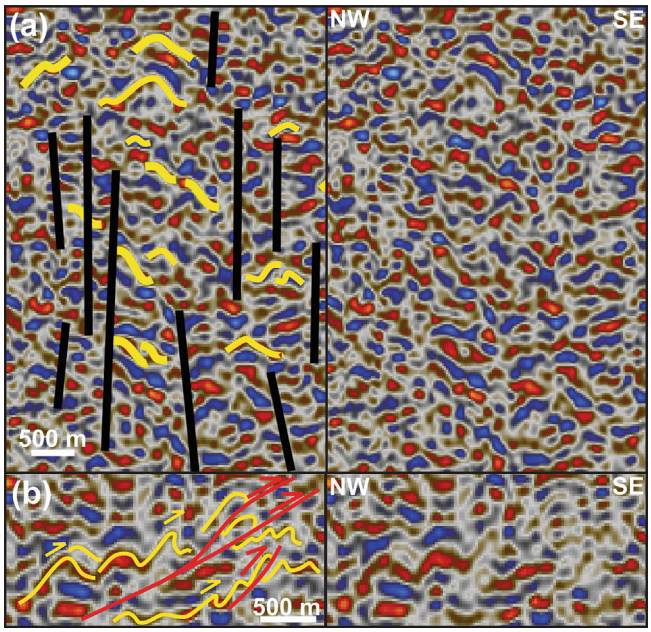


Figure 4. Interpreted (left hand side) and uninterpreted (right hand side) zoom in (a) symmetric folds truncated by subvertical disruptions interpreted as dykes in the hinge of the Austurbrún Anticline (anticline "m" in Figure 1b), and (b) symmetric folds (lower right corner) transitioning to top-southeast asymmetric folds offset by minor top-southeast brittle thrusts, including a floor décollement and a ramp thrust (McClay, 1992). Locations are shown in Figure 2a and c–d.

1.5 km assuming an average seismic velocity of 6 km.s^{-1} for lava-dominated upper crust at the Iceland–Faroe Ridge – Bohnhoff & Makris, 2004; Figure 2a–e), where the seabed reflection displays a rugose to undulating geometry (Figure 9a).

In places, these reflections are disrupted by tens of km wide, gently southeast-, northwest-, and NNE-dipping surfaces, which occur at depths of 1.5 to 8.0 seconds (TWT; red lines in Figure 2a–f and Figure 5g and l, Figure 6e, Figure 7d and i, and Figure 8c–e and g). In NW–SE-striking seismic cross section, these oppositely-dipping surfaces define hundred-km wide domes and troughs (Figure 2a–e). A-few-km- to tens-of-km-wide packages of hundreds of meters to km-scale S- and Z-shaped reflections are typically found adjacent to the tens-of-km-wide disruption surfaces (Figure 2a–f, Figure 5g, i–j, and l–n, Figure 6c and e, Figure 7a–j, and Figure 8a–h). S-shaped reflections occur both along NNE- and southeast-dipping disruption surfaces, whereas Z-shaped reflections are found near northwest-dipping disruption surfaces (Figure 2a–f, Figure 5g, i–j, and l–n, Figure 6c and e, Figure 7a–j, and Figure 8a–h).

In NE–SW-trending seismic cross section, the asymmetry of the hundred-meter- to km-scale, curving-up reflections typically consists of a long, more gently dipping, northeastern edge and a narrow, steeply dipping southwestern edge, thus conferring them a dominantly southwest-leaning geometry (Figure 2f). In contrast, their asymmetry in NW–SE-trending cross section alternates from southeast-leaning in the northwestern flank of the hundred-km-wide domes to northwest-leaning in the southeastern flank (Figure 2a–e). In the core of the hundred-km-wide domes, curving-up reflections become increasingly symmetric (Figure 2a–e, Figure 3, and Figure 4a–b). Curving-up reflections are also locally truncated by small (km wide), ≤0.2 second (TWT) thick disruptions (Figure 4b, Figure 5c, g, and l, Figure 6b, and Figure 7e and j). Offset along these disruptions are reverse (i.e., upper side up).

Typically <1.0 second thick, subvertical, in place merging/anastomosing disruptions and shadow areas are found ubiquitously in the seismic reflection data (i.e., areas in which seismic reflection amplitudes decrease significantly; Figure 4a, Figure 7f, and Figure 9a–c). These subvertical features truncate all reflections, though with no apparent offset (Figure 2a–f). Their frequency increases in the central part of the two domes defined by the gently southeast- and northwest-dipping disruption surfaces (Figure 2a–e and Figure 4a).

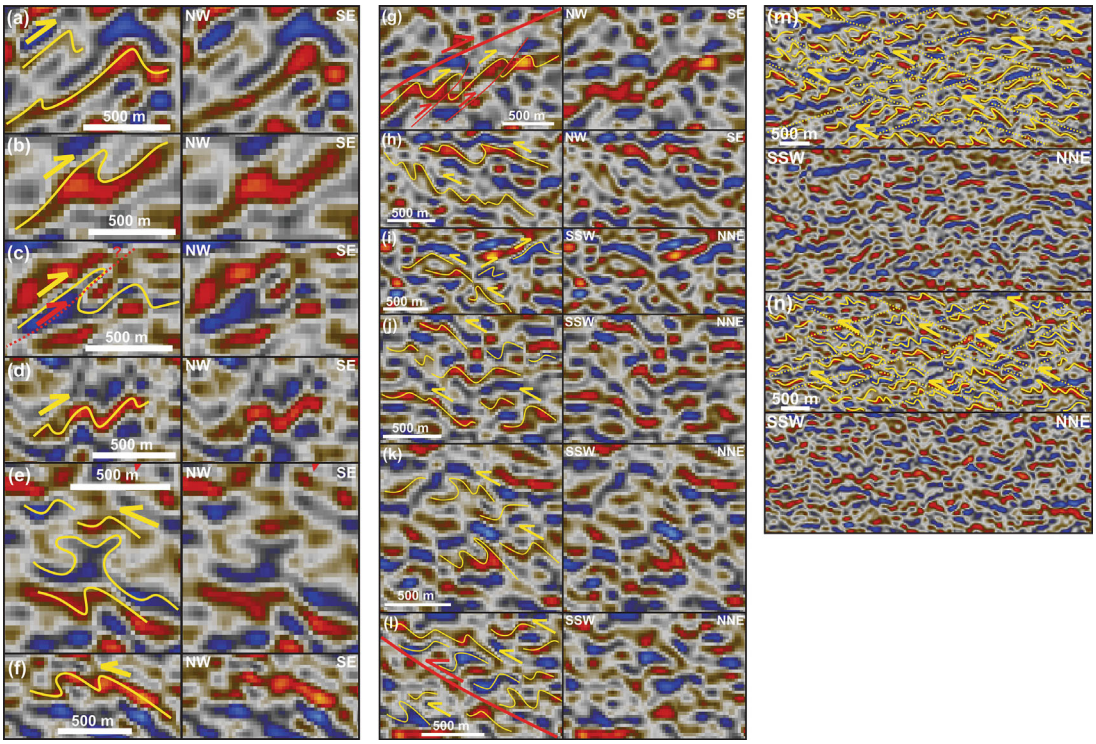


Figure 5. Interpreted (left hand side in a–l and up in m–n) and uninterpreted (right hand side in a–l and down in m–n) zoom in seismic reflection data showing various asymmetric fold geometries. Dominant fold vergence is towards the southeast on the northwestern limb of major anticlines like the Austurbrún and Iceland Basin anticlines (a–d and g) and towards the northwest on the southeastern limb (e–f), and towards the south-southwest in NNE–SSW-trending cross section (i–n). Notice the possible onset of brittle thrusting in the hinge of the fold in (c) (dotted red line), the double-vergence fold geometry in (e), potential top-southeast offsets along brittle thrusts below a major, northwest-dipping (mylonitic?) thrust surface in (g), arrangement of asymmetric folds into top-SSW, forward-dipping duplexes in (i–j and l–m; Boyer & Elliott, 1982; Koehl, 2021; McClay & Insley, 1986) including above a major, NNE-dipping (mylonitic?) thrust surface in (l), the transition from asymmetric to isoclinal overturned folds towards the south-southwest in (k), and the S–C fabrics created by duplexes' NNE-dipping top- and floor-décollements and the SSW-dipping, long flanks of the duplex horses (dotted yellow lines) in (m–n). Locations are shown in Figure 2a–f.

Upper crust

The upper 1.5–3.0 seconds (TWT) of the data show a large number of seismic artifacts, including several multiples and potential diffraction rays (e.g., Figure 9b–d), especially near the Faroe Islands in the southeast where the seafloor is shallowest (Figure 2a and e and Figure 9d). Nonetheless, in the upper 0.5–1.0 second (TWT), the seismic data typically show gently to moderately southeast- or northwest-dipping reflections, which can be traced for a few hundred meters to a few km (Figure 2a–e and Figure 9a–d). In places, some of these are stacked and arranged into packages of prograding reflections (Figure 9b–d). The uppermost 1.5 second (TWT) also displays 0.2–1.0 second-thick, up to hundred km wide layers of more chaotic reflections, which pinch out laterally (Figure 9b–c and e). The relatively chaotic character of these layers is associated with large numbers of disruption of apparently flat to moderately-dipping internal reflections (Figure 9b–c and e). Near southeastern Iceland, the seabed reflection shows a rugose geometry, which coincides with the occurrence of southeast-dipping, moderate- to high-amplitude reflections at and just below (<0.5 second TWT) the seafloor (Figure 9a).

Recent mid–upper Cenozoic sediments appear as thin (< 0.5 second TWT) layers of generally flat-lying to gently-dipping, moderate-amplitude reflections. These are not relevant to the present study and are thus not further discussed.

Interpretation

Moho

Given the c. 28–30 km thickness of the crust in easternmost Iceland (e.g., Foulger *et al.*, 2003), the 8.5–9.5 second-deep, high-amplitude, undulating reflections are tentatively interpreted as lower-crustal intrusions above the Moho (Figure 2a–f

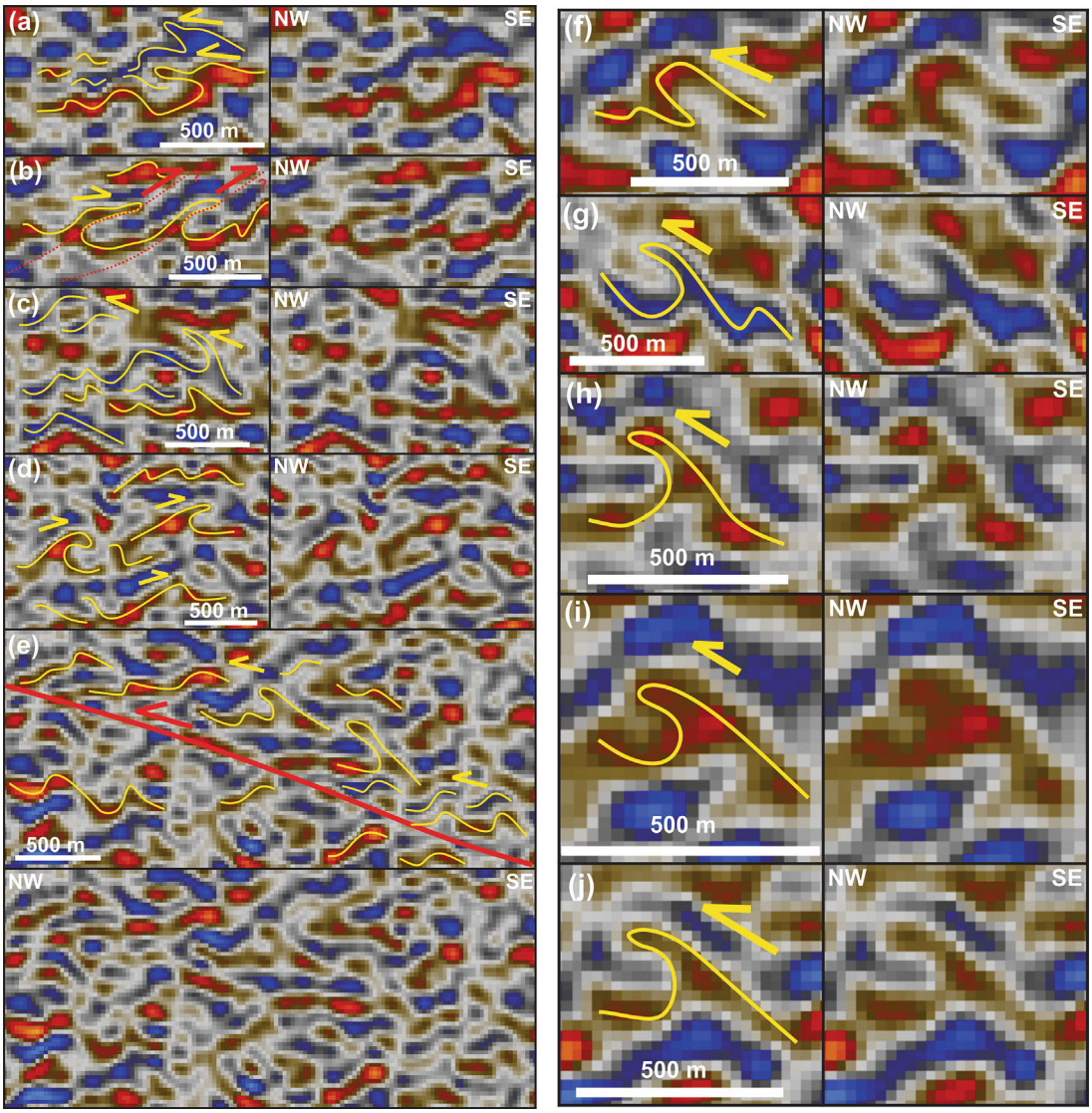


Figure 6. Interpreted (left hand side in a–d and f–j up in e) and uninterpreted (right hand side in a–d and f–j and down in e) zoom in seismic reflection data showing southeast- (b and d) and northwest-verging tight fold geometries (a, c, and e–j) respectively in the northwestern and southeastern limbs of the hundreds of km wide anticlines (e.g., Austurbrún and Iceland Basin anticlines). Geometries range from overturned to isoclinal recumbent. Notice the near separation of the fold hinges from the base of the two overturned anticlines in the southeast in (a), the possible initiation of top-southeast thrusting in (b), the occurrence of recumbent isoclinal folds in conjunction with a major, southeast-dipping (mylonitic?) thrust surface and related contractional, forward-dipping duplexes in (e), and the classic λ (lambda) shape of the isoclinal, overturned to recumbent folds in (g–j). Locations are shown in Figure 2a–e.

and Figure 3). This estimate is in agreement with the 23 km thickness of the crust farther southeast along the Iceland–Faroe Ridge (Bohnhoff & Makris, 2004). The negative-amplitude character of the Moho reflection suggests the occurrence of relatively weak rocks at the interface between the crust and mantle. Potential candidates include partially melted peridotite and related intrusions and serpentinite (density c. 2.6; Birch, 1960; Birch, 1961; Hyndman & Drury, 1977; Table 1). Given the high amounts of recent magmatism in Iceland and the difficulty in channeling water to hydrate mantle peridotite at great depth (c. 28–30 km), it is more probable that the negative amplitude of these reflections reflects the presence of partial melt and intrusions. The apparent increase of potential deep-crustal intrusions towards Iceland (fuchsia lines in Figure 2a–e) is consistent with the magmatic history of the region with gradually younger magmatism (i.e., potentially including partially molten rocks) towards Iceland.

Farther southeast, the Moho is diffuse and cannot be tied to any specific set of reflections (Figure 2a–f). The lack of high acoustic impedance contrast suggests the absence of partial melt in the uppermost mantle away from Iceland and that the lower crust at the Iceland–Faroe Ridge consists of rocks with a density comparable to that of peridotite (c. 3.3), e.g.,

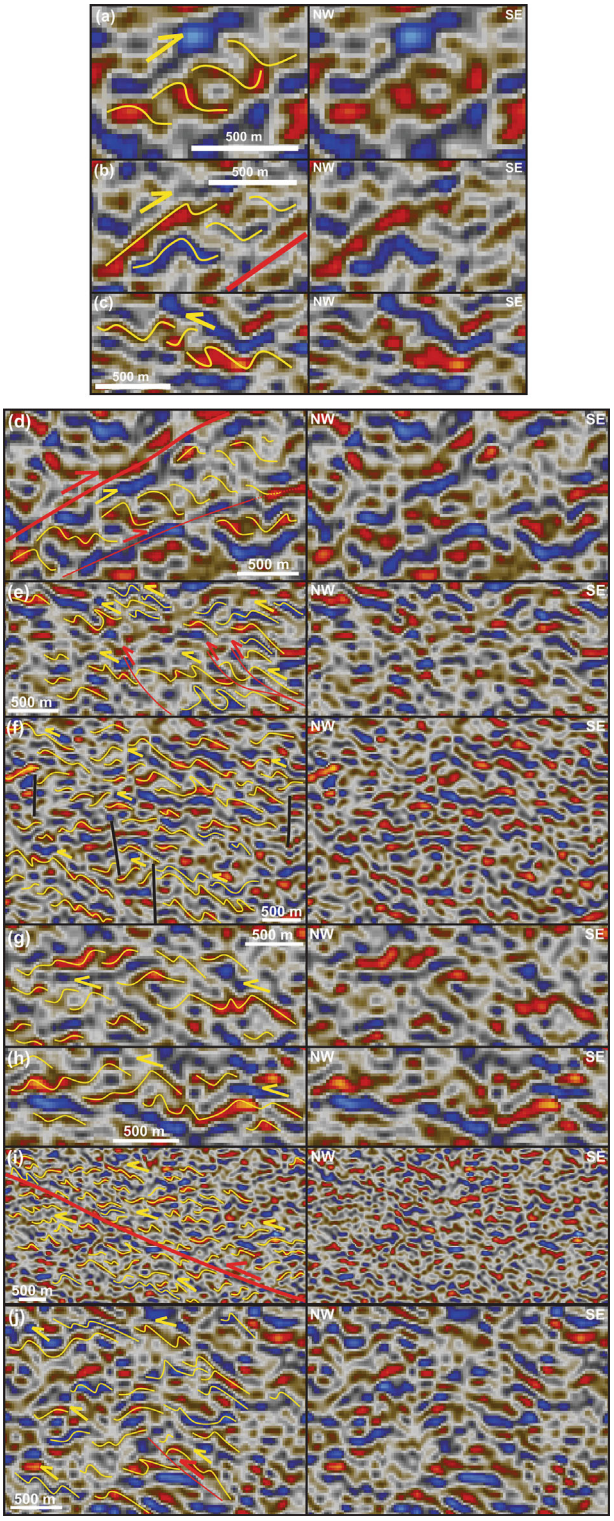


Figure 7. Caption continued on next page.

eclogite (c. 3.4), and/or migmatite (c. 3.0, up to 3.2), and/or granulite (c. 3.0, up to 3.2), and/or charnockite (c. 3.0, up to 3.4), and/or gabbro (c. 3.0), and/or diorite (up to 3.1), and/or amphibolite (c. 3.0, up to 3.2), and/or blueschist (c. 3.0, up to 3.3), and/or mafic gneiss (up to 3.2; Birch, 1960; Birch, 1961; Boyd & McCallister, 1976 and references therein; Cao *et al.*, 2013; Christensen, 1965; Coleman & Lanphere, 1971; Eshaghi *et al.*, 2019; Glen *et al.*, 2007; Henkel, 1976; Henkel, 1991; Hyndman & Drury, 1977; Ito & Kennedy, 1970; Jones, 2015 and references therein; Nilsen, 1973; Ott *et al.*, 2024; Ringwood & Green, 1966; Smithson, 1971; Subrahmanyam & Verma, 1981; van der Straaten, 2008; Ye *et al.*, 2022 and references therein; Table 1).

Mid–lower crust

The offset of hundreds-of-meter- to km-scale, asymmetric, curving-up reflections by km-scale disruption surfaces with reverse offset (Figure 4b, Figure 5c, g, and l, Figure 6b, and Figure 7e and j), their geometries ranging from open to overturned and tight recumbent isoclinal (e.g., Figure 5a–n and Figure 6a–j), and their consistent vergence on the limbs of the major, hundred-km-wide domes (Figure 2a–e, Figure 5a–n, Figure 6a–j, and Figure 7a–j) suggest that they reflect tectonic deformation. They are therefore interpreted as asymmetric contractional folds indicating the direction of tectonic transport during thrusting. Their size (hundreds of meters to km) and range of geometries (open to tight recumbent isoclinal) are comparable to that of well-studied onshore structures in fold-and-thrust belts (e.g., Fitz-Diaz *et al.*, 2011; Goscombe *et al.*, 2017; Mosqueira Gonzalez e*t al.*, 2021; Rutter *et al.*, 2007). The moderate acoustic impedance contrast creating these reflections may reflect alternating felsic and mafic rock units folded and/or sheared together.

Alternatively, the curving-up reflections may represent (folded?) mafic intrusions in a dominantly felsic crust or (folded?) felsic intrusions in a dominantly mafic crust. However, plutons are generally relatively isotropic and, thus, appear as large zones with lower reflectivity on seismic reflection data because of the lack of rock type variations (i.e., lack of acoustic impedance contrast), which is not consistent with the interpreted data. It is therefore more probable that the asymmetric reflections correspond to folded metaigneous and metasedimentary rocks.

The hundred-km wide domes and troughs flanked by the gently northwest- and southeast-dipping disruption surfaces (Figure 2a–f, Figure 5g and l, Figure 6e, Figure 7d and i, and Figure 8c–e and g) correlate with anticlines and synclines in previous seismic studies, e.g., Austurbrún anticline, Austurbrún syncline, and Iceland Basin Anticline (Hjartarson *et al.*, 2017; Figure 1b). The gently-dipping, tens of km wide disruption surfaces and their occurrence together with curving-up asymmetry fold reflections of opposite vergence (i.e., northwest-dipping disruption surfaces occurring with southeast-verging folds) and packages of Z- and S-shaped reflections suggest that they correspond to crustal-scale, potentially mylonitic, thrust surfaces (e.g., Figure 5g and l, Figure 6e, Figure 7d and i, and Figure 8c–e and g).

The occurrence of S- and Z-shaped reflections together with asymmetric folds suggest and their transitional nature with the latter suggest that they represent more intensely deformed rocks. The occurrence of S- and Z-shaped reflections along major, gently-dipping disruption surfaces and their arrangement into antiformal stacks suggest that they correspond to duplex horses (Figure 2a–f, Figure 5g, i–j, and l–n, Figure 6c and e, Figure 7a–j, and Figure 8a–h; e.g., Boyer & Elliott, 1982). While some Z- and S-shaped duplex reflections are transitional with nearby asymmetric fold geometries, e.g., at antiformal (thrust) stacks where they indicate reverse movement along the main disruption thrust surfaces (Figure 5g, i–j, and l–n, Figure 6c and e, Figure 7a–j, and Figure 8a–h), others show smoother S- and Z-like shapes, which indicate normal movement (Figure 8a–h).

The interpreted mylonitic thrusts and related asymmetric folds and duplexes (Figure 2a–f and Figure 4a–b, Figure 5a–n, Figure 6a–j, Figure 7a–j, and Figure 8a–h) are similar to other well-documented examples of fold-and-thrust belts on seismic reflection data worldwide (e.g., Calvert & Doublier, 2019; Fazlikhani *et al.*, 2022; Freeman *et al.*, 1988; Koehl

Figure 7. Interpreted (left hand side) and uninterpreted (right hand side) zoom in seismic reflection data showing contractional, dominantly forward-dipping duplexes (Boyer & Elliott, 1982; Koehl, 2021; McClay & Insley, 1986) indicating top-northwest (c and e–j) and top-southeast (a–b and d) kinematics respectively on the southeastern and northwestern limbs of the major, hundreds of km wide, open anticlines (e.g., Austurbrún and Iceland Basin anticlines). Notice the characteristic S- and Z-like geometries of the duplex horses respectively in top-southeast (a–b and d) and top-northwest duplexes (c and e–j), the northwestwards transition from asymmetric folds to overturned folds and to duplexes in (c), the occurrence of top-southeast and top-northwest contractional duplexes in conjunction with respectively northwest- and southeast-dipping (mylonitic?) thrust surfaces in (d) and (i), the occurrence of potential top-northwest, possibly imbricate brittle thrusts in (e) and (j), and the truncation of folds and related structures by subvertical disruption interpreted as potential dykes in (f). Locations are shown in Figure 2a–e.

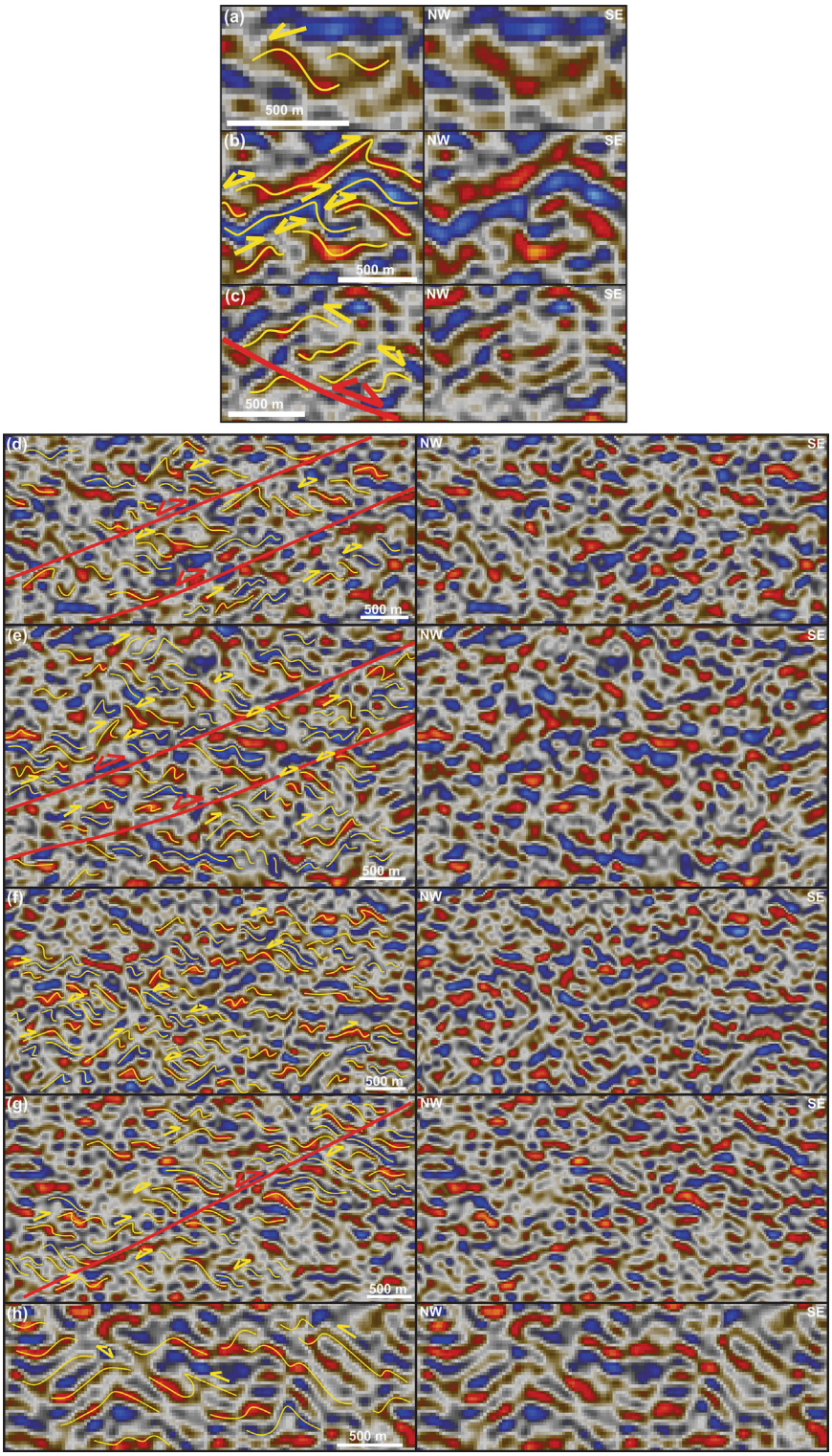


Figure 8. Interpreted (left hand side) and uninterpreted (right hand side) zoom in seismic reflection data showing potentially inverted (double yellow half arrows) contractional duplexes. Notice that the preservation of the initial top-southeast vergence of the fold in the lower left corner in (b) and the initial top-northwest vergence of the fold in the lower right corner in (c), and the occurrence of potentially inverted (double red half arrows) contractional duplexes adjacent and in between major (myltonitic?) thrust fault surfaces in (c), (d), (e), and (g). Traces of initial contraction are preserved in places as asymmetric to overturned folds in (d–h). Locations are shown in Figure 2a–e.

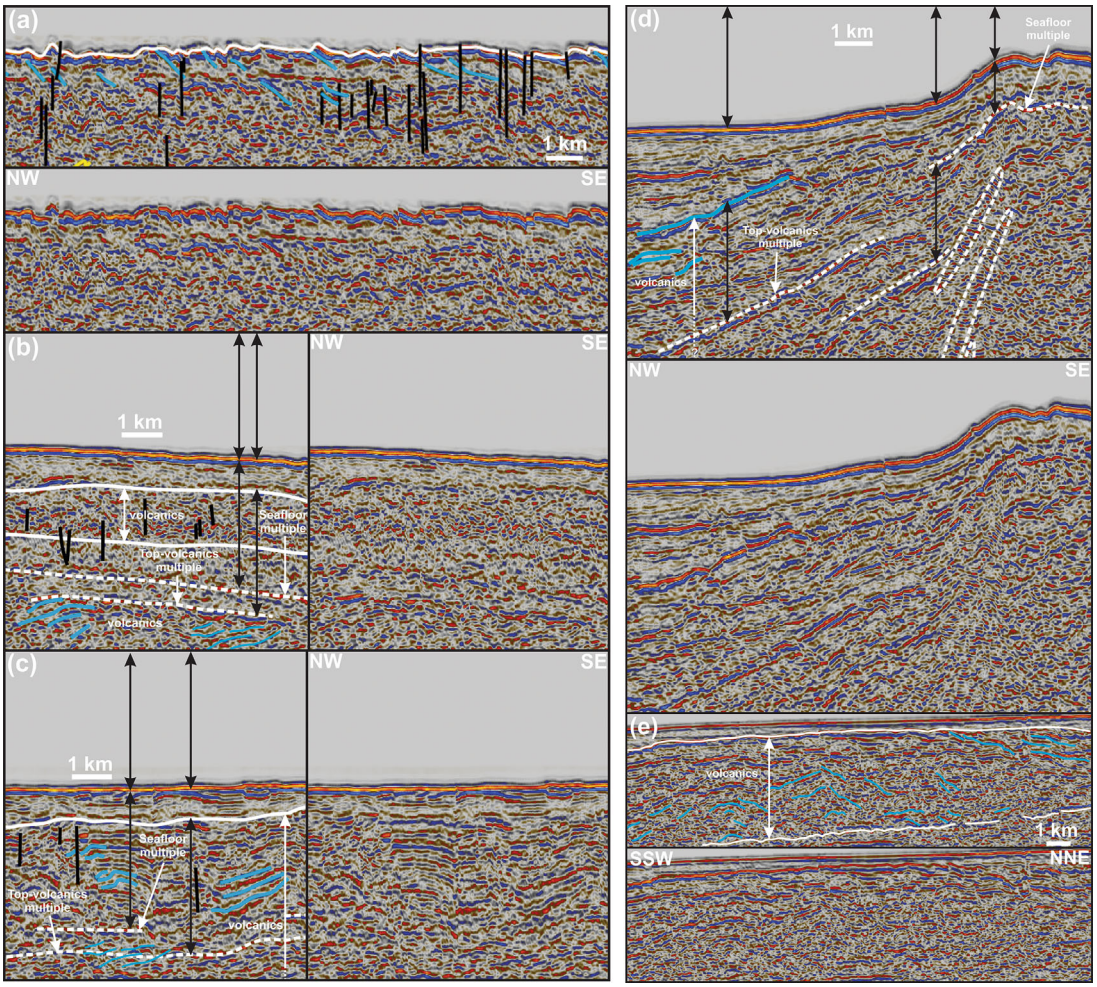


Figure 9. Interpreted (up in a and d–e and left hand side in b–c) and uninterpreted (down in a and d–e and right hand side in b–c) zoom in seismic reflection data showing (a) the rugose geometry of the seafloor on the strandflat southeast of Iceland possibly generated by eroded, seaward-dipping, Cenozoic lava flows, (b–d) km-thick subhorizontal layers consisting in places of chaotic (b) and prograding reflections (b–d) interpreted respectively as Cenozoic lava flows and lava deltas, and (e) oppositely-dipping reflections within the shallow Cenozoic volcanic succession. Notice the occurrence of widespread (seafloor and Top-volcanic) multiples in (b–d) and potential (diffraction-related?) artifacts below the shelf break in (d) (dashed white ovals), of subvertical disruptions possibly reflecting (late?) Cenozoic intrusions in (a–c), and the dome-like shape created by oppositely lava flows potentially suggesting an eruptive center (central volcano?) in (e). Locations are shown in Figure 2a and c–f.

et al., 2022; Koehl *et al.*, 2023a; Koehl *et al.*, 2024a; Koehl, 2025; Koehl & Stokmo, 2024; Koehl, 2025; Koehl et al., 2026), and to modelled asymmetric folds along major shear zones (e.g., Wrona *et al.*, 2020).

The subvertical, < 1.0 second-thick disruptions may represent processing and/or migration artifacts (e.g., vertical data gaps in the upper 2.0–3.5 second TWT of the data; Figure 2a–e), including potential noise attenuation issues (e.g., Li *et al.*, 2022). However, given their non-offsetting character and the extensive magmatic history of the region, it is also possible that they correspond to mafic (feeder) dykes. These subvertical disruptions appear with increased frequency in the hinge of major anticlines and may thus also partly reflect areas with increased sub-vertical fracturing related (e.g., axial fold cleavage).

Upper crust

The rugose geometry of the seafloor near southeastern Iceland is related to erosion of stacks of the shallow, gently to moderately southeast- and northwest-dipping, in place prograding reflections (Figure 2a-e and Figure 9a). The geometry and widespread occurrence of these shallow (≤ 1.5 second deep), gently-dipping reflections between Iceland and the

Table 1. Density average and ranges for common crustal and mantle rocks. Density values significantly higher than that of granitic continental crust and comparable to peridotite are highlighted in red. The corresponding rock types are unlikely to generate a significant contrast in acoustic impedance with mantle peridotite, thus potentially resulting in a diffuse crust–mantle Moho boundary (e.g., Figure 2b–f). In contrast, densities significantly lower than that of mantle peridotite are displayed in blue. These rock types (serpentinite) are likely to generate a significant contrast in acoustic impedance both with mantle peridotite and crustal rocks, thus potentially resulting in a bright Moho reflection like near the coast of southeastern Iceland (e.g., Figure 2b).

Continental crustal rocks	Average density	Density range	Contrast with density 2.8 continental crust (%)	Sources
granite	2.8	2.5–3.1	0.0	Birch, 1960; Eshaghi et al. 2019; Henkel, 1970; Jones, 2015; Smithson, 1971
migmatite	3.0	2.7–3.2	7.1	Eshaghi et al., 2019; Smithson, 1971; Subrahmanyam & Verma, 1981
mylonite	2.8	2.6–3.0	0.0	Christensen & Szymanski, 1988; Eshaghi et al. 2019; Jones & Nur, 1982; McCaffree & Christensen, 1993; Punturo et al., 2014; Smithson, 1971
mafic gneiss	2.9	2.6–3.2	3.6	Eshaghi et al. 2019; Smithson, 1971
mafic granulite	3.0	2.8–3.2	7.1	Ito & Kennedy, 1970; Smithson, 1971; Subrahmanyam & Verma, 1981
felsic granulite	2.7	2.6–2.8 (3.1)	−3.6	Ito & Kennedy, 1970; Subrahmanyam & Verma, 1981
amphibolite	3.0	2.7–3.2	7.1	Christensen, 1965; Eshaghi et al. 2019; Henkel, 1991; Smithson, 1971
eclogite	3.4	3.2–3.5 (3.7)	21.4	Cao et al., 2013; Coleman & Lanphere, 1971; Henkel, 1991; Ito & Kennedy, 1970; Ringwood & Green, 1966; Van der Straaten, 2008; Ye et al., 2022
charnockite	3.0	2.6–3.4	7.1	Birch, 1960; Subrahmanyam & Verma, 1981
blueschist	3.0	2.7–3.3	7.1	Cao et al., 2013; Coleman & Lanphere, 1971; Ott et al., 2024; Van der Straaten, 2008
pseudotachylyte	2.7	2.6–3.0	−3.6	Eshaghi et al. 2019
Oceanic crustal rocks				
gabbro	3.0	2.7–3.1	7.1	Birch, 1960; Birch, 1961; Eshaghi et al. 2019; Glen et al., 2007; Henkel, 1970; Hyndman & Drury, 1977; Nilsen, 1973; Ringwood & Green, 1966
basalt	2.9	2.6–3.1	3.6	Birch, 1960; Birch, 1961; Eshaghi et al., 2019; Hyndman & Drury, 1977; Ito & Kennedy, 1970
diorite	2.9	2.6–3.1	3.6	Eshaghi et al. 2019; Glen et al., 2007; Henkel, 1970; Henkel, 1976; Jones, 2015
anorthosite	2.9	2.6–3.0 (3.3)	3.6	Birch, 1960; Birch, 1961; Eshaghi et al., 2019; Jones, 2015; Smithson, 1971; Subrahmanyam & Verma, 1981
Mantle rocks				
serpentinite	2.6	2.4–2.8	−7.1	Birch, 1960; Birch, 1961; Hyndman & Drury, 1977
peridotite	3.3	3.1–3.4	17.9	Boyd & McCallister, 1976; Ye et al., 2022

Faroe Islands (e.g., Figure 9a–e) suggest that they reflect Cenozoic lava flows and/or hyaloclastites, possibly including some interbedded sedimentary rocks. This is supported by the results of DSDP 38 at site 336, which penetrated 43 ± 3.3 Ma basalt (Talwani *et al.*, 1976) and by seismic refraction data suggesting a 1.5 km thickness for this upper

crustal basalt layer (Bohnhoff & Makris, 2004). The alternating dip and prograding character of the lavas indicate that they locally form deltas (Figure 9b–d).

The 0.2–1.0 second-thick, up to hundred km wide, pinching-out layers of chaotic reflections occur at a comparable depth as the gently- to moderately-dipping lava flows (≤ 1.5 second depth) and may correspond to more chaotic magmatic endmembers, e.g., hyaloclastites, volcaniclastics, or lava flows intruded by numerous dykes (e.g., Geoffroy *et al.*, 2022; Phillips & McCaffrey, 2019; Walker *et al.*, 2022). However, considering the large number of migration artifacts, multiples, and potential seismic noise in the shallow portion of the data (e.g., Figure 9b–d), they may as well be regular lavas with interbedded sedimentary rocks.

Considering the thick character of Cenozoic lavas around the Faroe Islands (c. 3–10 km thick; Ólavsdóttir *et al.*, 2016; Ólavsdóttir *et al.*, 2021; Richardson *et al.*, 1998; Waagstein *et al.*, 1982) and Iceland (≥ 4.8 km; Friðleifsson *et al.*, 2017; Tryggvason & Båth, 1961), the upper 2.0 seconds below seafloor may realistically consist dominantly of Cenozoic lavas. Using the seismic velocities obtained by Bohnhoff & Makris (2004; 4.7–5.0 km.s^{-1}), Cenozoic lavas at the Iceland–Faroe Ridge may thus amount for up to c. 5 km of crustal thickness. However, this is an upper estimate considering the large number of migration artifacts and multiples that make it challenging to differentiate lavas from sedimentary rocks in the upper 2.0–3.0 second (TWT) of the analyzed seismic reflection data and the thinning of the lava succession towards Iceland (Figure 2a–e and Figure 9b–d).

Magnetic data

Description

The Reykjanes Ridge oceanic crustal domain of the northeastern Atlantic Ocean is characterized by hundreds to a thousand kilometers long, NE–SW-striking, rectilinear magnetic anomalies (Figure 10a–d). These anomalies are continuous on the edge of the Reykjanes oceanic crustal domain near Rockall Bank and Greenland and semi-continuous to disrupted in places near the Reykjanes Ridge (Figure 10a–d and Figure 11a–b). The central and northeastern parts of the Reykjanes Ridge oceanic crustal domain show subsidiary N–S-striking, medium- to high-amplitude anomalies, which extend into southwestern Iceland and the Greenland–Iceland Ridge (Figure 10a–d and Figure 11a–b). In the south and southwest, N–S-trending anomalies are widespread but show a low amplitude and high frequency.

The Greenland–Iceland Ridge and Iceland–Faroe Ridge are both characterized by generally broad (≥ 10 km wide), arcuate to undulating and discontinuous (≤ 100 km long) magnetic anomalies (Figure 10a–d and Figure 11a–b). In places, two anomalies merge and form triangular, dominantly ʌ- and subsidiary V-shaped anomalies. In addition to the dominant NE–SW to NNE–SSW strike, magnetic anomalies at the Greenland–Iceland Ridge strike subsidiarily N–S. In contrast at the Iceland–Faroe Ridge, anomalies strike dominantly WNW–ESE, whereas NE–SW- and N–S-striking anomalies are subsidiary (Figure 10a–d). Furthermore, the central part of the Iceland–Faroe Ridge is characterized by circular to oval dominantly positive and subsidiarily negative magnetic anomalies.

Iceland is characterized by overall arcuate, discontinuous (≤ 100 km long), NE–SW- to NNE–SSW-striking anomalies, which bend into a N–S strike northwards (Figure 10a–d and Figure 11a–b). In central and eastern Iceland, some anomalies display Λ-like geometries and align along NE–SW- to NNE–SSW-striking undulating axes (Figure 10a–d and Figure 11a–b). Furthermore, southernmost and southeasternmost Iceland are dominated by a series of tens to hundred km long, WNW–ESE- to E–W-striking anomalies, i.e., orthogonal to the northeastern Atlantic rift system. These anomalies are similar to the dominant anomaly trend in the Iceland–Faroe Ridge (Figure 10a–d).

At the Ægir Ridge oceanic domain, moderate-amplitude magnetic anomalies display an overall arcuate shape, bending from an ENE–WSW strike in the southwest to a NNE–SSW strike in the northeast. In this region, they are discontinuous to semi-continuous and of low amplitude.

In contrast, magnetic anomalies at the Kolbeinsey Ridge oceanic crustal domain are continuous, rectilinear to mildly undulating, NNE–SSW-striking moderate-amplitude anomalies on the edges and right-stepping, high-amplitude in the basin center around the Kolbeinsey Ridge (Figure 10a–d).

In between the oceanic crustal domains of the Kolbeinsey and Ægir ridges, continental crust of the Jan Mayen Microcontinent Complex is characterized by dominantly low- up to moderate-amplitude anomalies, some of which display dominantly Λ- and subsidiary V-like shapes aligning along NNE–SSW-striking axes, especially towards the center of the Jan Mayen continental crustal domain (Figure 10a–d and Figure 11c–d). The main Λ-shaped anomaly coincides in the northeast with the location of the Jan Mayen Archipelago (Figure 10a–d and Figure 11c–d).

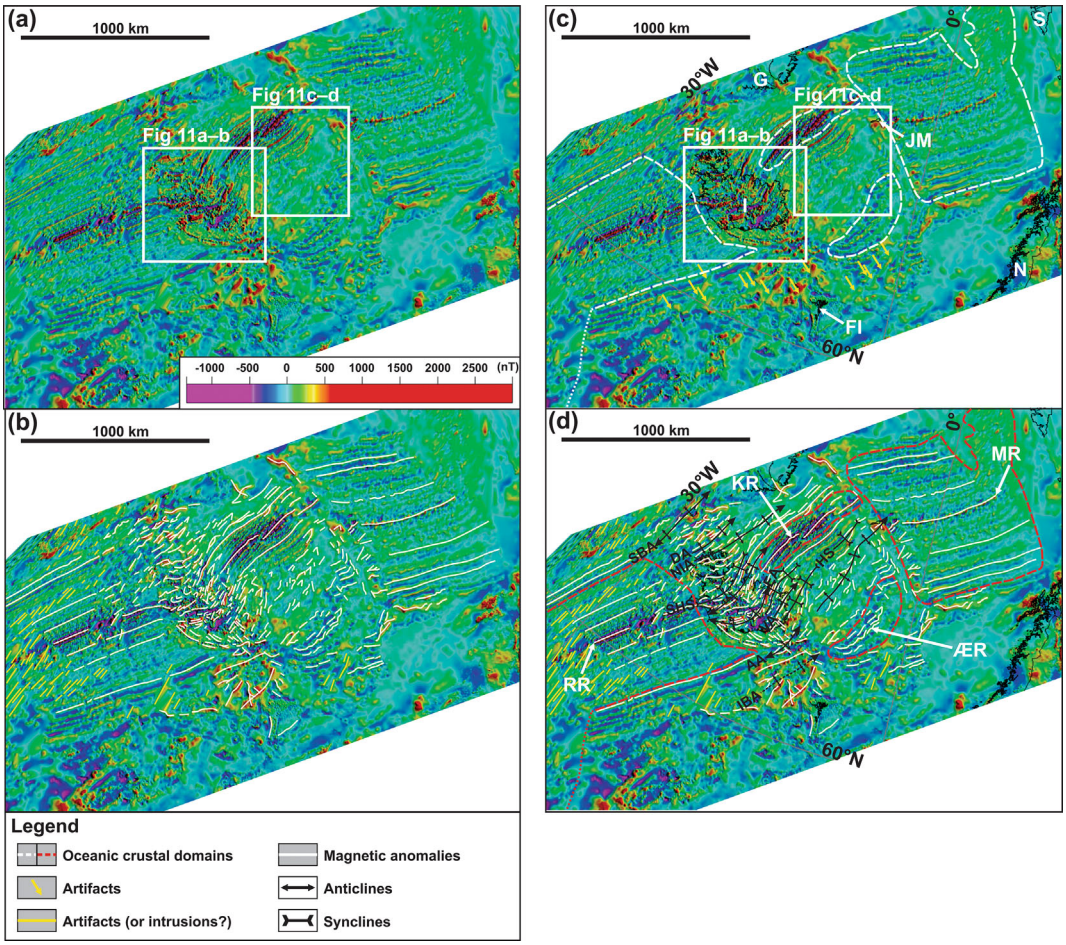


Figure 10. (a) Uninterpreted and (b–d) interpreted magnetic anomaly map in the northeastern Atlantic Ocean (Gaina et al., 2017; Hopper et al., 2014; Nasuti & Olesen, 2014a; Nasuti & Olesen, 2014b). (b) shows the interpreted magnetic anomalies without the coastlines to illustrate the contrast between the Greenland–Iceland–Faroe Ridge and adjacent oceanic crustal domains shown in (c). (d) shows interpreted tectonic fold structures in continental crustal domains. The continent–ocean boundary (dashed white lines in (c) and dashed red lines in (d)) is from the present study at the Greenland–Iceland–Faroe Ridge, Dumais et al. (2020) in the Fram Strait, Geoffroy et al. (2021) at the Reykjanes oceanic segment, and based on Gernigon et al. (2021) off mid-Norway. Abbreviations: AA: Austurbrún Anticline; DA: Djúpáll Anticline; EA: Eyjafjörður Anticline; FI: Faroe Islands; G: Greenland; HS: Héraðsflói Syncline; I: Iceland; IBA: Iceland Basin Anticline; JM: Jan Mayen; KR: Kolbeinsey Ridge; MR: Mohns Ridge; N: Norway; NIA: NW Iceland Anticline; RR: Reykjanes Ridge; S: Svalbard; SBA: Strede Bank Anticline; SHS: Snæfellsnes–HúnaflóI Syncline; VA: Vopnafjörður Anticline; ÆR: Ægir Ridge.

Farther northeast, the Mohns Ridge oceanic crustal domain is characterized by a similar pattern as the Reykjanes Ridge domain with anomalies showing increasing disruptions towards the active mid-ocean ridge (Figure 10a–d).

Interpretation

The NE–SW-striking rectilinear anomalies in the Reykjanes and Mohns oceanic domains are parallel to the Reykjanes and Mohns ridges and to V-shaped valleys along the Reykjanes Ridge and, thus, are likely the product of the variations of the magnetic field intensity and polarity and seafloor spreading off these mid-ocean ridges. As suggested by recent studies of magnetic and seismic reflection data in the area and other rifted margins, the more proximal NE–SW-striking (pseudo-) rectilinear anomalies are interpreted as intrusions in thinned continental crust, e.g., outer seaward-dipping reflectors (Geoffroy *et al.*, 2021; Geoffroy *et al.*, 2022). The arcuate, moderate-amplitude, ENE–WSW- to NNE–SSW-striking and NNE–SSW-striking anomalies at the Ægir and Kolbeinsey oceanic domains are interpreted to result from seafloor spreading. In both the Ægir and the Kolbeinsey oceanic domains, the magnetic anomalies converge toward the active

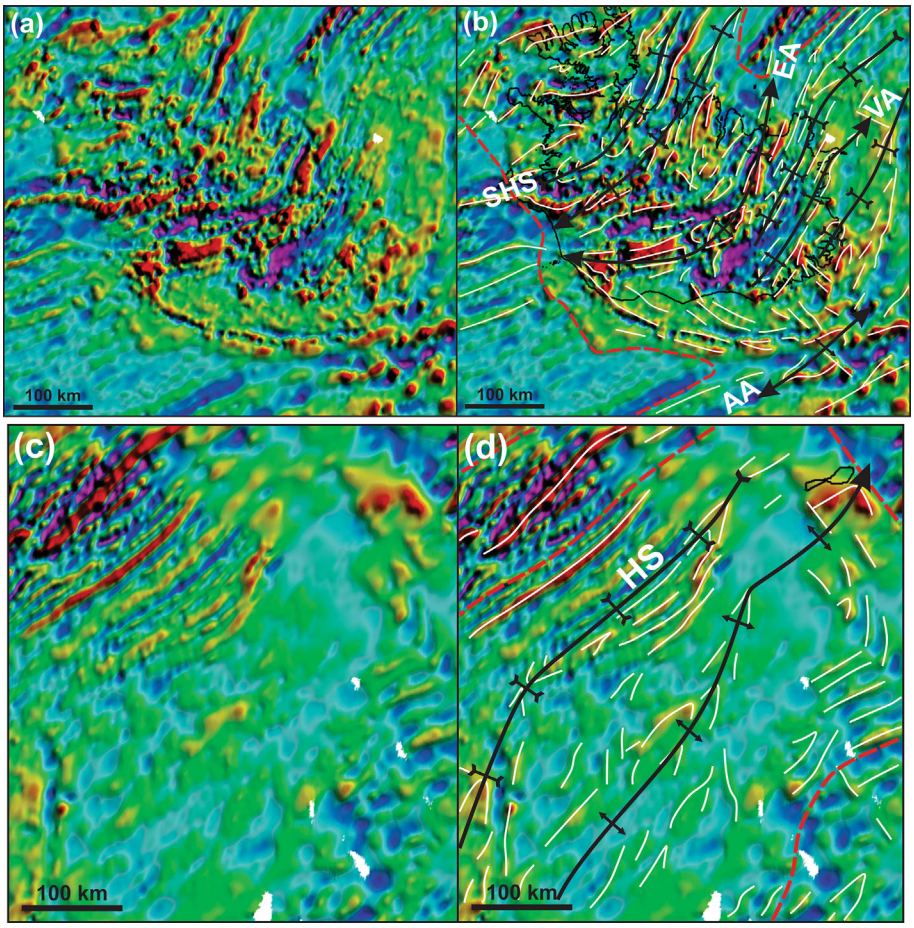


Figure 11. (a & c) Uninterpreted and (b & d) interpreted zoom in magnetic anomaly map in Iceland and the Jan Mayen Microcontinent Complex showing Λ- and V-shaped magnetic anomalies interpreted as overall NE–SW-striking Caledonian folds. Locations are shown in Figure 10a and c. Legend is the same as Figure 10. Abbreviations: AA: Austurbrún Anticline; EA: Eyjafjörður Anticline; HS: Héraðsflói Syncline; SHS: Snæfellsnes–HúnaflóI Syncline; VA: Vopnafjörður Anticline.

spreading center in the northeast (Mohns Ridge) either by counterclockwise bending (Ægir domain) or right stepping (Kolbeinsey domain; Figure 10a–d).

The N–S-striking low- to high-amplitude anomalies in the Reykjanes oceanic domain, Greenland–Iceland–Faroe Ridge, and adjacent continental margins parallel the mid-ocean ridge farther south between the Charlie Gibbs and Bight transform fault zones (Figure 1a). The high-amplitude endmember of these anomalies may correspond to local ultramafic intrusions in oceanic or mafic–ultramafic intrusions in continental crust. In contrast, the low-amplitude, high-frequency endmember could either reflect artifacts related to acquisition or processing issues, or intrusions along high-frequency, N–S-striking fractures that propagated northwards from the Charlie Gibbs–Bight oceanic domain due to local stress propagation. An interpretation as processing artifacts is also suggested for high-amplitude N–S-striking anomalies on the UK–Faroe continental margin, where they appear to distort nearby NE–SW-striking anomalies (yellow arrows in Figure 10a).

The geometry of NE–SW- to NNE–SSW-striking anomalies in the Greenland–Iceland–Faroe Ridge significantly differs from similarly striking continuous and rectilinear anomalies in the adjacent Rekjanes, Ægir, and Kolbeinsey oceanic crustal domains (Figure 10a–d and Figure 11a–b). Their discontinuous, arcuate character is more consistent with (folded? bending?) mafic–ultramafic intrusions in continental crust (e.g., Koehl *et al.*, 2019; Koehl & Stokmo, 2024; Nasuti *et al.*, 2015).

The triangular anomalies in the Greenland–Iceland–Faroe Ridge, Jan Mayen Microcontinent Complex, and southeastern Greenland margin are similar to gently- to moderately-plunging contractional folds in continental crust on magnetic data, e.g., in the Barents Sea and northern Norway, which are produced by folded mafic intrusions and highly-magnetic metasedimentary beds (Koehl *et al.*, 2019; Koehl *et al.*, 2022; Koehl & Stokmo, 2024; Roberts & Siedlecka, 2013; Roberts & Williams, 2013). The Λ-shaped magnetic anomaly in the Iceland–Faroe Ridge (Figure 10a–d) coincides with the location of the hinge of the hundred-km-wide, NE–SW-striking Austurbrún Anticline observed on seismic reflection data (present study and Hjartarson *et al.*, 2017; Figure 2a–e). Considering the extensive Cenozoic magmatism in Iceland and nearby margins, the triangular magnetic anomalies are interpreted to reflect mafic–ultramafic intrusions along northeast- to NNE-plunging and southwest-plunging anticlines.

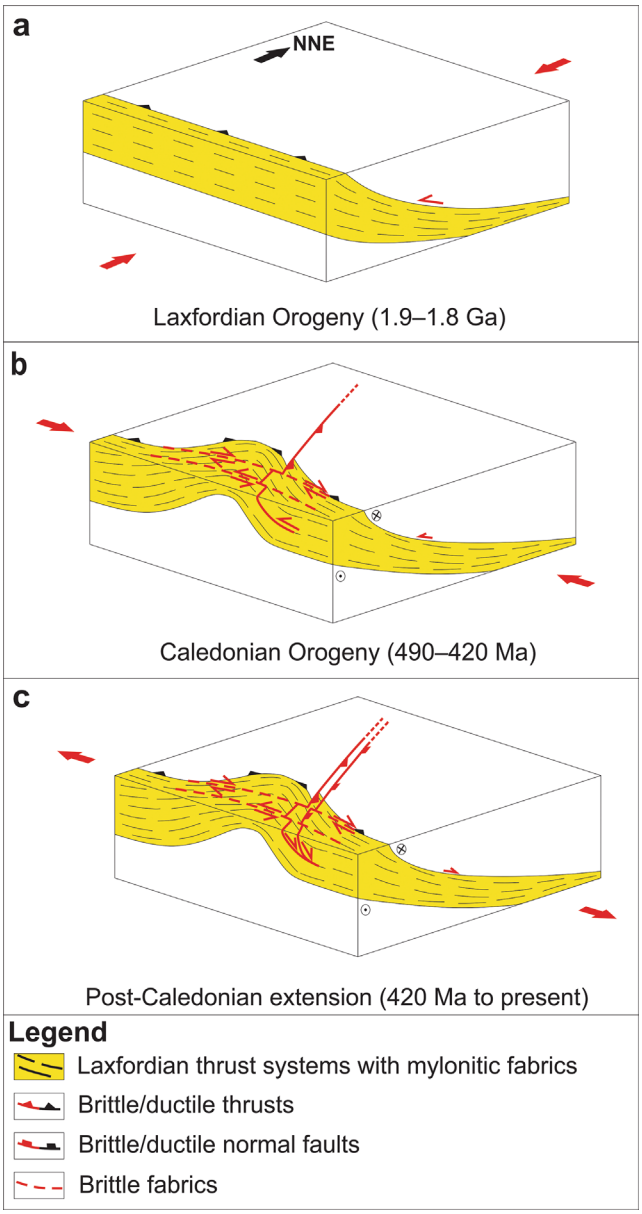


Figure 12. (a) Formation of top-SSW thrust systems during the (Neoarchean?–) late Paleoproterozoic (Badcallian–Inverian event and/or) Laxfordian Orogeny. (b) Reworking of the thrust systems into hundred km wide, open, NNE–SSW-striking folds during the Caledonian Orogeny. Notice the potential formation of Caledonian thrusts on the limbs of the folded Paleoproterozoic thrust systems. (c) Post-Caledonian (i.e., Devonian–Permian and possibly Mesozoic–Cenozoic) inversion of Laxfordian and Caledonian structures. Modified after Koehl et al. (2024a).

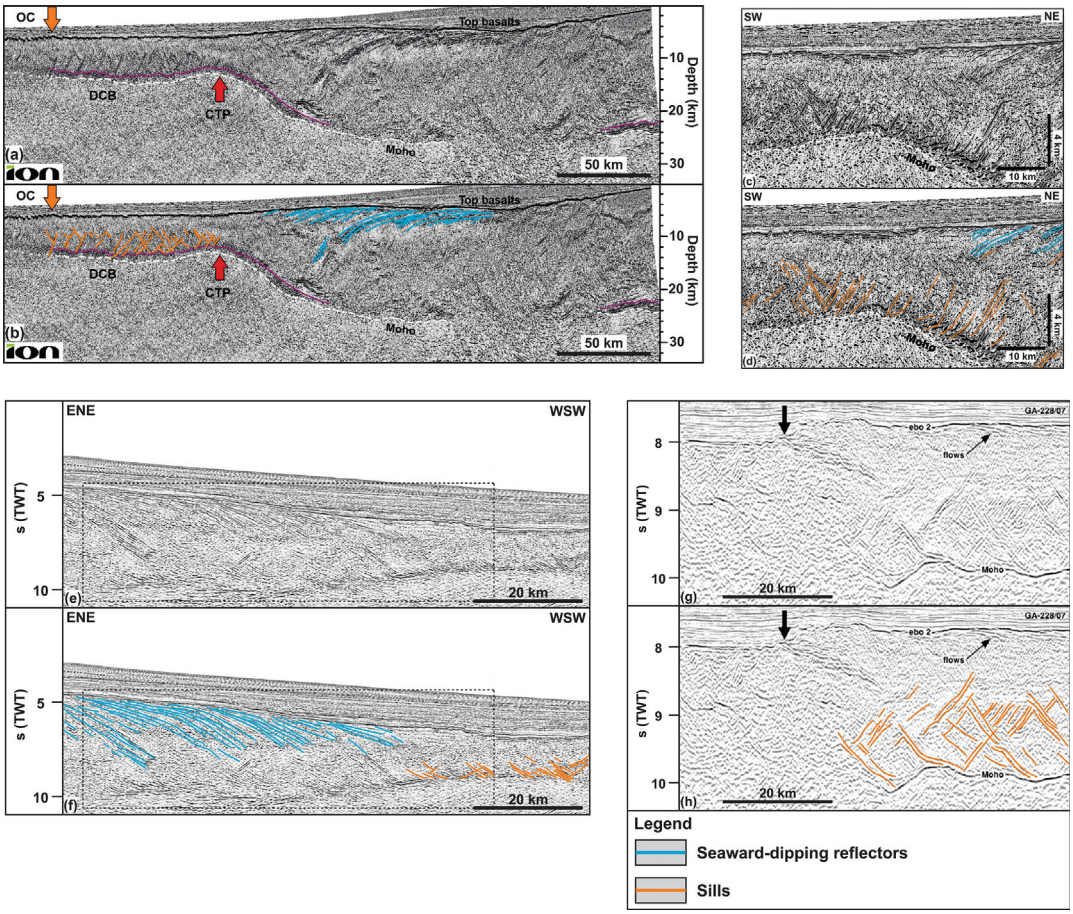


Figure 13. (a, c, e, and g) Uninterpreted and (b, d, f, and h) interpreted seismic sections at the continent–ocean boundary at rifted margins in (a–f) Namibia and (g–h) Antarctica showing lower-crustal intrusions (orange lines) characteristic of 7–8 km-thick Penrose-like oceanic crust and seaward-dipping reflectors (blue lines) onto adjacent thinned continental crust. The interpretation shown in (b, d, e, g, and i) is by the authors of the present study. Earlier interpretations are found in (a–d) Geoffroy et al. (2022; their Figure 3a and 4e), (e–f) Sapin *et al.* (2021; their Figure 5), and (g–h) Sinha (2024; their Figure 6.8).

In the Iceland–Faroe Ridge and southernmost and southeasternmost Iceland, WNW–ESE-striking anomalies strike sub-orthogonal to nearby active and extinct mid-ocean ridges (Figure 10a–d and Figure 11a–b). In contrast, they are parallel to in the Iceland–Faroe Ridge (present study; Figure 2a–f). Thus, these rift-orthogonal anomalies are interpreted as potential intrusions along WNW–ESE-striking faults.

Circular to oval anomalies at the Iceland–Faroe Ridge align both along WNW–ESE- and NE–SW-trending axes. Some of these circular anomalies coincide with known igneous centers around the Faroe Islands (e.g., Jolley *et al.*, 2021; Kimbell *et al.*, 2005; Stoker *et al.*, 2015). They are thus interpreted as mafic–ultramafic Cenozoic igneous centers, possibly at the intersection of NE–SW- and WNW–ESE-striking faults. While those displaying negative anomalies likely intruded coeval with the bulk of the igneous centers in the Rockall region (Kimbell *et al.*, 2005; Waddams & Cordingley, 1999) when the magnetic field was reversed (ca. 63–53.5 Ma), those correlating with positive magnetic anomalies possibly intruded during the previous and/or following period with normal magnetic field (i.e., at ca. 65–63 Ma and/or 53.5–45.5 Ma or even down to ca. 36 Ma; Figure 10a–d; Walker & Geissmann, 2022). Given the 62.15–43.3 Ma ages obtained for igneous rocks of the North Atlantic Igneous Province in the Faroe Islands, Greenland–Iceland–Faroe Ridge, and southeastern Greenland (Bohnhoff & Makris, 2004; Brooks, 2011; Hansen & Ganerød, 2023; Larsen *et al.*, 2014; Storey *et al.*, 2007; Talwani *et al.*, 1976; Tegner & Duncan, 1999; Tegner *et al.*, 2008; Wilkinson *et al.*, 2016), their position closer to the active spreading centers in Iceland, and the 43 ± 3.3 Ma ages obtained for basalts in the Iceland–Faroe Ridge (Bohnhoff & Makris,2004; Talwani *et al.*, 1976), a 53.5 to 36 Ma age is proposed for the igneous centers at the Iceland–Faroe Ridge (Figure 10a–d).

Discussion

Tectonic structures at the Greenland–Iceland–Faroe Ridge

The interpretation of seismic reflection and magnetic data suggest the existence of hundred-km-long, top-SSW thrust systems and hundred-km-wide, NE–SW- to NNE-SSW-striking folds at the Greenland–Iceland–Faroe Ridge and under Iceland (Figure 2a–f, Figure 10a–d, and Figure 11a–d). The NNE-dipping thrust systems are characterized by WNW–ESE-striking anomalies at the Iceland–Faroe Ridge, probably reflecting along-strike (ultra) mafic intrusions (Figure 10a–d), and tens of km wide, top-SSW thrusts and SSW-verging folds in seismic reflection data (Figure 2f). The widespread, WNW–ESE-striking, rift-related faults and zones of seismicity onshore Iceland (e.g., Southern Iceland Seismic Zone; Bergerat & Angelier, 2008; Khodayar *et al.*, 2018a; Khodayar *et al.*, 2018b; Khodayar *et al.*, 2020; Villemin *et al.*, 1994), which parallel these NNE-dipping thrust systems in the Iceland–Faroe Ridge and correlate with their northwestward continuation, are thus interpreted as rift overprints and reactivation of these thrust systems.

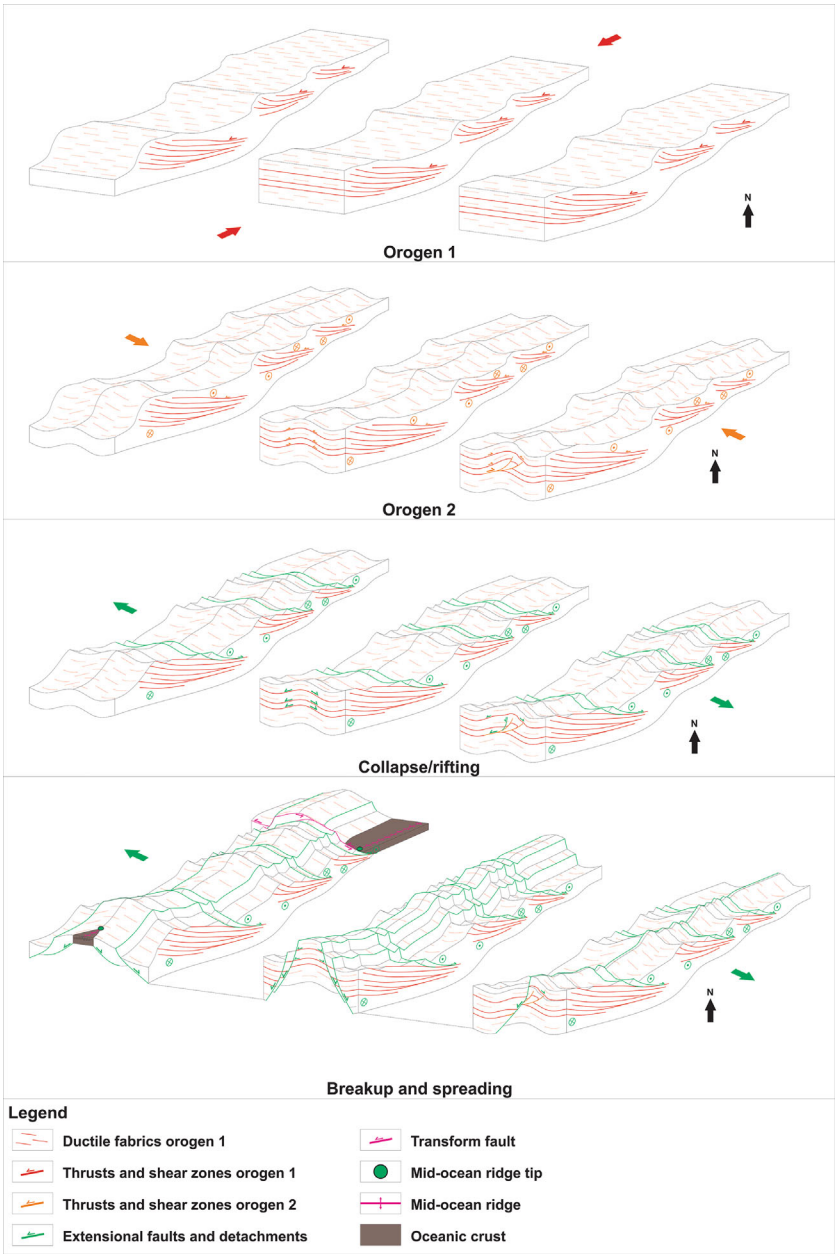


Figure 14. Caption continued on next page.

The coincidence of the hinge zone of anticlines in seismic reflection data with triangular (dominantly Λ-shaped) magnetic anomalies suggests that the top-SSW thrust systems are reworked into dominantly NNE-plunging folds (e.g., Austurbrún and Iceland Basin anticlines; Figure 2a–f, Figure 10a–d, and Figure 11a–d). This relationship is also valid for the Greenland–Iceland Ridge, onshore Iceland, and Jan Mayen Microcontinent Complex, where the Djúpáll and Strede Bank anticlines (Hjartarson *et al.*, 2017 based on seismic reflection data), the NW Iceland, Eyjafjörður, and Vopnafjörður anticlines and the Snæfellsnes–HúnaflóI and Héraðsflói synclines (Jóhannesson & Sæmundsson, 2009 based on onshore structural data), and the main ridge of the Jan Mayen Microcontinent Complex (Péron-Pinvidic *et al.*, 2012 and Blischke *et al.*, 2016 based on seismic reflection and gravimetric data) correlate with NE–SW- to NNE–SSW-striking alignments of triangular magnetic anomalies of matching, hundred-km-wide width (Figure 10a–d, and Figure 11a–d). In places, the alignment of both V- and Λ-shaped magnetic anomalies indicates a dome- or trough-shaped (i.e., both SSW- and NNE-plunging) geometry for the NE–SW- to NNE–SSW-striking folds (Figure 10a–d and Figure 11a–d). These double-plunging folds typically extend across (perpendicular to) the Greenland–Iceland–Faroe Ridge for c. 400–500 km and terminate at the Rekjanes and Kolbeinsey oceanic domains (Figure 10a–d, and Figure 11a–b).

The dominant top-SSW vergence of the thrust systems and related asymmetric folds in NNE–SSW-trending seismic cross section (Figure 2f) is comparable to that of late Paleoproterozoic Laxfordian structures in basement rocks around the Faroe Islands (Koehl *et al.*, 2024a) and northern Scotland (Beach, 1974; Coward *et al.*, 1980; Coward & Park, 1987). In NW–SE-trending cross section, the alternating top-southeast and top-northwest vergence of hundreds of meters- to km-wide asymmetric folds respectively on the northwestern and southeastern limb of the major, hundred-km-wide anticlines (e.g., Austurbrún and Iceland Basin anticlines) and their increased symmetry in the large anticlines' hinge zone (Figure 2a–e) also mimics the attitude of WNW–ESE-striking late Paleoproterozoic Laxfordian thrust systems around the Faroe Islands and onshore northern Scotland, which were reworked into hundred-km-wide, open, dominantly NNE-plunging folds during the Caledonian Orogeny and extend beyond seaward-dipping reflectors and feeder dyke complexes northwest of the Faroe Islands (Koehl *et al.*, 2024a; Figure 12a–b). In addition, the top-southeast, top-northwest, and top-SSW vergence of asymmetric folds and thrust surfaces in seismic reflection data (yellow and red lines in Figure 2a–f) are consistent with the dominantly NNE-plunging character of the anticlines in magnetic data (Figure 10a–d and Figure 11a–d). The tens of km wide, mid–lower crustal disruption surfaces and related asymmetric folds (Figure 2a–f, Figure 5g, i–j, and l–n, Figure 6c and e, Figure 7a–j, and Figure 8a–h) are therefore interpreted as hundreds (to thousand) km long, tens of km wide, overall WNW–ESE-striking and NNE-dipping Laxfordian thrust systems reworked during the Caledonian Orogeny (Figure 12a–c; see also Koehl *et al.*, 2024a their Figure 5a–c). The thrust systems mapped in the present study (Figure 2a–f) are tentatively correlated with the Suðurøy and West Faroe fault zones of Koehl *et al.* (2024a).

Figure 14. Schematic model showing the critical steps in the development of orogenic bridges through two orogeneses whose main stress directions (σ_1) are perpendicular, repeated extension along extensional faults and detachments and inherited orogenic structures, and breakup along inherited, reactivated/overprinted orogenic structures. Note that any number of additional orogeneses and/or extension (collapse/rifting) may be added in between these events. (a) First orogenesis deforming the crust, e.g., in the present case with a WNW–ESE-oriented maximum stress (Badcallian–Inverian event and/or Laxfordian Orogeny). (b) New period of orogenesis deforming the crust with the maximum stress oriented perpendicular to the first orogeny (i.e., NNE–SSW), thus resulting in reworking of preexisting orogenic structures, tightening of deformation, formation of new orogenic structures with highly oblique to perpendicular strike to those formed during the first orogeny, and further thickening and locking of the crust. Note that it is not necessary that the orogenic keel of the first orogeny be preserved as extensional collapse is likely to occur between the two orogenies. (c) Episode of extensional collapse and/or rifting thinning the crust through reactivation and overprinting of preexisting orogenic structures. Note that the crust is easier to thin at anticlines (uplift leading to increased erosion compared to synclines) and therefore it is easier to exhume the mantle there. Also note the strike-slip kinematic reactivation component of preexisting structures formed during the first orogeny. (d) Breakup occurs at non-orogenic or less tightly deformed portions of the crust, propagating towards tightly deformed crust. There, breakup is stalled because the crust is tightly deformed and "locked" by two sub-orthogonal structural trends, one of which is unsuitably oriented to thin the crust (structural fabrics formed during the first orogeny). This results in a scissor-like geometry at that end of the mid-ocean ridge (e.g., Reykjanes Ridge). The rift may then step sideways (e.g., opening of the Labrador Sea) and/or bypass the orogenically thickened crust, thus resulting in the formation of a major transform fault between the locked continental crust and the oceanic crustal domain (e.g., Tjörnes fault zone in northern Iceland). The portion of locked orogenic continental crust is hereby referred to as an "orogenic bridge" because it remains as a bridge of continental crust connecting two diverging continental plates (e.g., Greenland and Europe), while breakup has occurred on either side of the orogenic bridge, i.e., where the crust was not orogenically locked and, thus, was relatively quickly thinned down to breakup. The orogenic bridge may eventually rupture once enough extension has occurred (e.g., Newfoundland defining a continental salient into oceanic crustal domain denoting the existence of ruptured early–mid Paleozoic orogenic bridge related to the Appalachian–Caledonian Orogen; Koehl & Foulger, 2025).

Complementarily, given the occurrence of circular–oval igneous centers in the Iceland–Faroe Ridge and their alignment along both WNW–ESE- and NE–SW- to NNE–SSW-striking axes (Figure 10a–d), it is probable that the core of the hundreds km wide anticlines also consist of Cenozoic intrusions. This is suggested by the subvertical disruptions in the hinge of the anticlines, which may correspond to feeder dykes along Caledonian axial fold cleavage (black lines in Figure 2a–e), and by the c. 10-km-wide, 8.5–9.5 second-deep, high-amplitude, undulating reflections possibly reflecting lower-crustal (plutonic?) intrusions (fuchsia lines in Figure 2a–e). These suggests that both Laxfordian and Caledonian structures acted as magma pathways in the crust.

Asymmetric folds are also found at depth > 8.0–9.0 seconds (TWT; Figure 2a–f). This suggests that the mantle has also been involved in contractional folding. This further supports a long-lived tectonic history and, thus, a continental nature for both the crust and lithospheric (cratonic?) mantle at the Iceland–Faroe Ridge.

In the northwesternmost part of the Iceland–Faroe Ridge, some of the interpreted asymmetric reflections occur up to 0.5 second (TWT) below the seabed, thus suggesting a thinning of Cenozoic lava flows (Figure 2a–e). The present interpretation as contractional structures could thus possibly be tested via drilling of these shallow occurrences.

A late Paleoproterozoic age for the WNW–ESE-striking thrust systems at the Iceland–Faroe Ridge is a conservative estimate since Laxfordian fabrics reactivated Neoarchean–earliest Paleoproterozoic WNW–ESE-striking Badcallian–Inverian fabrics (Attfield, 1987; Barooah & Bowes, 2009; Coward & Park, 1987; Evans & Lambert, 1974; Park, 1970; Storey *et al.*, 2010; Zirkler *et al.*, 2012).

Nature of the crust at the greenland–iceland–faroe ridge

Difference with oceanic crust

Typical oceanic crustal transects in seismic reflection data at various rifted margins worldwide are displayed in Figure 13a–h. The crustal thickness at the Greenland–Iceland–Faroe Ridge is ≥23 km and up to 40 km (e.g., Bohnhoff & Makris, 2004; Darbyshire *et al.*, 1998; Foulger *et al.*, 2003; Funck *et al.*, 2014), i.e., significantly thicker than Penrose-like oceanic crust (c. 7–8 km; Vine & Moores, 1972; Christeson et al., 2019; Figure 13a–h). The lower part of oceanic crust typically includes sets of crisscrossed (conjugate?), margin-parallel, 5–10 km wide, planar to gently-undulating, moderate–high-amplitude reflections (Figure 13a–h). These likely reflect magmatic sills in the gabbroic–dioritic lower oceanic crust (e.g., Hoggard *et al.*, 2017 their Figure 2a–f; Reeve et al., 2021 their seismic facies 3; Sinha, 2024 his Figure 6.8; Vasileiou *et al.*, 2023 their Figure 5a and 6a; oceanic crustal layer 3 of Vine & Moores, 1972). A magmatic origin for these reflections is supported by the absence of offset across these features (Figure 13a–h). The relatively high acoustic impedance contrast produced by the sills may be explained either by relatively (ultra-) mafic intrusions in relatively isotropic gabbroic–dioritic lower oceanic crust, or by mafic–ultramafic intrusions in hyperextended continental crust (e.g., Geoffroy *et al.*, 2022; Reeve *et al.*, 2021).

Such lower crustal, crisscrossed sills and related high- to moderately-amplitude reflections are absent at the Greenland–Iceland–Faroe Ridge (Figure 2a–f). Instead, saucer-shaped sills occur in upper crustal sedimentary strata (e.g., Koehl *et al.*, 2024a their Figure 2e). Furthermore, lower crustal magmatic sills in oceanic crust are typically broader (5–10 km wide) and display higher amplitudes (moderate to high; Figure 13a–h) than the interpreted, low- to moderate-amplitude, hundreds of meters to km-scale, mid to lower crustal asymmetric folds at the Greenland–Iceland–Faroe Ridge (Figure 2a–f). In addition, the intrusions in hyperextended continental crust and Penrose-like oceanic crust are associated with relatively planar, i.e., undeformed, reflections (Figure 13a–h; Geoffroy *et al.*, 2022; Reeve *et al.*, 2021; Sapin *et al.*, 2021), whereas the curving and disrupted character of the mid–lower crustal asymmetric reflections at the Greenland–Iceland–Faroe Ridge suggests a long-lived history and involvement in tectonic deformation (Figure 2a–f, Figure 3, Figure 4a–b, Figure 5a–n, Figure 6a–j, Figure 7a–j, and Figure 8a–h). Thus, despite the ≤5 km of upper crustal lavas, the crust at the Greenland–Iceland–Faroe Ridge is interpreted to be continental (Figure 2a–f).

Possible analogs for the hundreds km wide, NE–SW- to NNE–SSW-striking anticlines at the Greenland–Iceland–Faroe Ridge are potential magmatic domes at rifted margins (e.g., Péron-Pinvidic, 2025) and abandoned spreading centers in oceanic crust (e.g., Ding *et al.*, 2018). However, the radiant and crisscrossed reflection patterns observed at magmatic domes and interpreted as sheeted dykes (Péron-Pinvidic, 2025) are absent in the Greenland–Iceland–Faroe Ridge. In addition, there is no evidence of high-amplitude, subhorizontal reflections interpreted as axial, subaxial, or off-axis magmatic lenses as seen along and off the East Pacific Rise, Galappagos, and Juan de Fuca spreading centers (e.g., Boddupalli & Canales, 2019; Carbotte *et al.*, 2021; Nedimović *et al.*, 2005). Furthermore, the crust in these areas is 6–7.5 km thick, i.e., in the range of that of oceanic crust (Vine & Moores, 1972; Christeson et al., 2019).

A partial local similarity with lower oceanic crust is observed for the lowermost crust (depth of 6.0–9.0 seconds; TWT) at the Iceland–Faroe Ridge near southeastern Iceland, where the Moho appears more well-defined (Figure 2a–e). There, lowermost crustal lensoidal reflection packages suggest the occurrence of relatively isotropic rock units, i.e., possible plutons (Figure 2a–e). If such is the case, the relatively higher acoustic impedance contrast between the lower crustal rocks and mantle peridotites may result from the occurrence of young, relatively less dense, gabbroic–dioritic (density of c. 2.9–3.0), anorthosite (c. 2.9), or granitic plutons (c. 2.8) instead of high-density, continental, lower crustal rocks (e.g., eclogite and migmatite; density of c. 3.2–3.4; e.g., Birch, 1960; Birch, 1961; Cao *et al.*, 2013; Coleman & Lanphere, 1971; Eshaghi et al., 2019; Glen *et al.*, 2007; Henkel, 1976; Henkel, 1991; Hyndman & Drury, 1977; Ito & Kennedy, 1970; Jones, 2015 and references therein; Nilsen, 1973; Smithson, 1971; Ringwood & Green, 1966; Subrahmanyam & Verma, 1981; van der Straaten, 2008; Ye *et al.*, 2022; Table 1), the latter of which are probably responsible for the diffuse Moho in the rest of the ridge towards the Faroe Islands (Figure 2a–f). This further suggests a continental nature for the crust at the Greenland–Iceland–Faroe Ridge.

Migmatite and ptygmatic folds

The early Cenozoic magmatic record of the North Atlantic Igneous Province at the Greenland–Iceland–Faroe Ridge, including igneous centers, thick lava flows, intrusions (e.g., dykes and sills), and seaward-dipping reflectors (e.g., Davison *et al.*, 2010; Hitchen, 2004; Jolley *et al.*, 2021; Koehl *et al.*, 2024a; Parson *et al.*, 1988; Smythe, 1983; Spence *et al.*, 1989), and ongoing magmatism in Iceland (e.g., Harðarson *et al.*, 2008; Sæmundsson, 1979) suggest a rich magmatic activity in the region. It is therefore necessary to consider the possibility that the interpreted asymmetric folds in seismic reflection data at the Iceland–Faroe Ridge are (partly?) of magmatic origin, e.g., partially molten rocks (migmatite).

Migmatites reflect partial melting of the bedrock due to increased pressure and temperature conditions (e.g., Mehnert, 1968). These typically include structures such as ptygmatic folds (Ghosh, 1966; Godfrey, 1954), whose origin has been debated. Ptygmatic folds occur when a relatively competent layer bounded by or within less competent rocks becomes folded. Their apparently chaotic organization and geometry with regard to other tectonic structures (e.g., foliation, folds, and shear zones) and nearby rock units may, in places, appear to be random (e.g., Ghosh, 1966 his Figure 14; Ramberg, 1959 his Figure 10), and in outcrop it may be tricky to measure the strike of ptygmatic folds and to compare it to that of other tectonic structures (Llorens *et al.*, 2013).

Nevertheless, modern studies have shown that ptygmatic folding typically occurs under tectonic stress and consistently reflects the direction of maximum stress (e.g., Bathaeian, 2018). Thus, apparently chaotic, incoherent folding in migmatitic rocks is simply the result of the high viscosity contrast between the partially melted portion of the bedrock (neosome) and the remaining (unmelted) competent portion of the bedrock (mesosome) during coeval magmatic and tectonic processes. This way, the partially molten character (i.e., less competent) of the country rock offers less resistance to more competent rock layers, which can thus deform rapidly into relatively tight geometries under relatively low tectonic stress, i.e., similarly to competent layers in weak, mobile evaporite successions (e.g., Rowan *et al.*, 2019). Thus, the geometry of ptygmatic folds is of tectonic origin and related to the dominant tectonic stress orientation during partial melting and/or follows the geometry of inherited tectonic crustal structures, which may create local stress perturbations. Alternatively, post-migmatization ptygmatic folding may result from the viscosity (competence) contrast of the leucosome, melanosome, and mesosome components of the bedrock, i.e., anyway of tectonic origin. Thus, despite a possible influence of magmatic processes (e.g., late Paleoproterozoic to present-day migmatization) on the formation of the interpreted hundreds of meters to km-scale, lower crustal fold structures at the Iceland–Faroe Ridge, their origin is more likely to be primarily tectonic, thus supporting a continental origin of the crust there.

Deep conductive layer under Iceland

Despite the lack of seismic reflection coverage over Iceland, the suggested presence of a high-grade metamorphic continental crust at the Greenland–Iceland–Faroe Ridge opens new possibilities. A continental nature of the lower crust under Iceland is suggested by the character of the deep conductive layer, which likely consists of iron- and titanium-rich and/or hydrated minerals such as amphibole (Arnason *et al.*, 2025). It is possible that the higher conductivity in a WNW–ESE direction is related to magmatic-flow-related fabrics in gabbroic lower crust as observed in lower oceanic crustal rocks (e.g., Dilek *et al.*, 1998; Trutner, 2016; VanTongeren *et al.*, 2015). However, this would suggest a different nature for the lower 20 km of the Icelandic crust (i.e., below the 5–20-km-deep deep conductive layer), which show much lower conductivity (Arnason *et al.*, 2025).

Iron-rich minerals include biotite (e.g., annite), which is common in high-pressure metamorphic rocks such as metapelite (e.g., in Scotland and Greenland; Lamont *et al.*, 2025; Lang & Gilotti, 2015 – and elsewhere worldwide; e.g., Faryad, 1999; Mposkos, 1989). Biotite is also typically found in (mylonitic) shear zones and foliation where it can also be enriched in titanium (e.g., Pe-Piper *et al.*, 2004).

Other iron- and titanium-rich rocks include mafic to ultramafic intrusions and anorthosite, the latter of which typically contains ilmenite and titanomagnetite (e.g., Charlier *et al.*, 2014; Duchesne, 1999; Owens & Dymek, 1992; Årebäck & Stigh, 2000). Anorthosite is typical in Archean–Paleoproterozoic basement rocks in Greenland and Europe (e.g., Sotiriou & Polat, 2023), including in the late Paleoproterozoic Laxfordian Orogen in northern Scotland (Bergh *et al.*, 2012; Frazer, 1977; Mason *et al.*, 2004; Tarney & Weaver, 1987) and Ammassalit Belt in southeastern Greenland (Bridgewater *et al.*, 1973; Moorlock et al., 1972; Nunes *et al.*, 1974), i.e., the two continental margins bounding the Greenland–Iceland–Faroe Ridge (Figure 1a–b). Both in northern Scotland and southeastern Greenland, Archean anorthosite is involved in late Paleoproterozoic, WNW–ESE-striking ductile foliation and (mylonitic) shear zones (Bridgewater & Myers, 1979; Bridgewater *et al.*, 1973; Frazer, 1977; Nunes *et al.*, 1974; Weaver & Tarney, 1980). Some anorthosites have been ascribed to partial melting of continental granulite (e.g., Moorlock *et al.*, 1972; Oliver, 1977; Weaver & Tarney, 1980), and/or granulite protolith (e.g., charnockite; Mukherjee & Das, 2002), and/or contamination by continental crust (e.g., Ghose *et al.*, 2008). Granulite and charnockite are dominant rock types both in the Lewisian Complex in northern Scotland and the Ammassalik Belt in southeastern Greenland (Bridgewater & Myers, 1979; Chadwick *et al.*, 1989; Evans & Lambert, 1974; Frazer, 1977; Kalsbeek *et al.*, 1993a; Park, 1970; Sutton & Watson, 1950; Tarney & Weaver, 1987; Weaver & Tarney, 1980).

These suggest the presence of continental crust with well-developed, WNW–ESE-striking, (mylonitic) ductile fabrics in high-grade metamorphic rocks (e.g., granulite and anorthosite) under Iceland. These fabrics are proposed to represent the continuation of the late Paleoproterozoic Laxfordian Orogen (Lewisian Complex) and Ammassalik Belt (Figure 1a–b). This is further supported by the deep conductive layer's higher conductivity in the extension direction (WNW–ESE; Arnason *et al.*, 2025), i.e., parallel to the (Neoarchean?–) late Paleoproterozoic structures and fabrics in southeastern Greenland and northern Scotland (Bergh *et al.*, 2012; Bridgewater & Myers, 1979; Chadwick *et al.*, 1989; Mason *et al.*, 2004) and in the Iceland–Faroe Ridge (Figure 2a–f; present study and Koehl *et al.*, 2024a), and its occurrence at a 5–20 km depth (Arnason *et al.*, 2025), i.e., comparable to that of the potential thrust systems mapped in the Iceland–Faroe Ridge in the present study (Figure 2a–f). It is also supported by the doming of the deep conductive layer under volcanic centers and geothermal fields, which mimics the attitude of the interpreted Caledonian anticlines interpreted in seismic and magnetic data (Figure 2a–e, Figure 10a–d, and Figure 11a–d), which also rework Precambrian basement rocks in Greenland and Scotland (e.g., Andresen *et al.*, 2007; Coward, 1980).

A continental nature of the lower crust under Iceland could also explain the occurrence of anorthosite inclusions in Cenozoic dolerite in western Iceland (Snæfellsnes Volcanic Zone; Figure 1b; Griffin *et al.*, 1974; Kristmannsdóttir, 1971) given the possible continental affinities of anorthosites (e.g., Ghose *et al.*, 2008; Moorlock *et al.*, 1972; Mukherjee *& Das*, 2002; Oliver, 1977; Weaver & Tarney, 1980) and presence of anorthosite in both northern Scotland and southeastern Greenland (Bergh *et al.*, 2012; Bridgewater *et al.*, 1973; Frazer, 1977; Mason *et al.*, 2004; Moorlock et al., 1972; Nunes *et al.*, 1974; Tarney & Weaver, 1987).

Differential thinning of the crust at the greenland–iceland–faroe ridge

A continental nature of the crust at the Greenland–Iceland–Faroe Ridge adds a new challenge to reconstructing plate tectonics in the northeastern Atlantic region. It suggests that, despite ongoing extension (e.g., Sigmundsson *et al.*, 2020), breakup may not be complete or has occurred significantly later in Iceland than at the Reykjanes and Ægir–Kolbeinsey rift segments (Figure 1a–b).

A possible way to reconcile delayed breakup at the Greenland–Iceland–Faroe Ridge with seafloor-spreading at adjacent rift segments and ongoing extension in Iceland is an initially relatively thicker continental crust at the Greenland–Iceland–Faroe Ridge. This is possible given the presence of late Paleoproterozoic thrust systems of the Laxfordian Orogen off the Faroe Islands and within the (Greenland–) Iceland–Faroe Ridge (Figure 2a–f). A thickened orogenic keel is unlikely to have been preserved for 1.8 billion years, but a hypothesis of relatively thicker crust at the Greenland–Iceland–Faroe Ridge prior to the opening of the northeastern Atlantic does not require the continental crust to have been 70–80 km thick at the onset of rifting in the latest Cretaceous–early Cenozoic. The crust had already been thinned repeatedly, e.g., during late–post-Caledonian collapse and Permian and Jurassic–Early Cretaceous extension (e.g., Clift *et al.*, 2004; Kimbell *et al.*, 2016; Musgrove & Mitchener, 1996; Waddams & Cordingley, 1999). Thus, the hypothesis of relatively thicker continental crust at the Greenland–Iceland–Faroe Ridge simply requires a more efficient thinning of the orogenic crust at

the Reykjanes and Ægir–Kolbeinsey rift segments than at the Greenland–Iceland–Faroe Ridge during these extensional episodes.

A thicker crust at the Greenland–Iceland–Faroe Ridge is supported by crustal thickness variations in northern Europe (e.g., Funck *et al.*, 2014 their Figure 6.6; Kimbell *et al.*, 2016 their Figures 3–4). Late Paleozoic collapse and Jurassic–Early Cretaceous extension had significantly thinned the crust to 5–6 km in the Southern Rockall and Møre basins, while the crust at the Greenland–Iceland–Faroe Ridge and nearby areas in northern Europe (Faroe Islands, Shetland Islands, Northern Rockall Basin, northern Scotland) is generally >10 km thick (except under the Faroe–Shetland Basin where it is down to 6–7.5 km; Funck *et al.*, 2014; Kimbell *et al.*, 2016).

Preserving a relatively thicker continental crust at the Greenland–Iceland–Faroe Ridge and delayed breakup in Iceland were likely facilitated by the orientation and geometry of 5–10 km thick, late Paleoproterozoic thrust systems (present study and Koehl *et al.*, 2024a). Their WNW–ESE strike (i.e., perpendicular to the NE–SW-striking rift axis) was unsuitable to thin the crust, and their low-angle geometry was unsuitable to accommodate (transform-related) strike-slip faulting (Figure 2a–f).

In addition, the dominantly diffuse Moho below the Iceland–Faroe Ridge (Figure 2a–e) suggests that the crust is mechanically stronger and that these inherited thrusts consist of high-density rocks (i.e., density comparable to mantle peridotite), which are relatively resistant to further deformation (e.g., eclogite, granulite, and migmatite). A mechanically stronger crust under the Greenland–Iceland–Faroe Ridge, Faroe Islands, and northern Scotland is also supported by the northward step in the Mesozoic rift system between the Southern Rockall Basin and the Northern Rockall Basin, which coincides with the Scottish Hebrides where prominent, late Paleoproterozoic, WNW–ESE-striking Laxfordian shear zones are well known onshore (Beach, 1974; Coward & Park, 1987).

The well-developed, long-lived, late Paleoproterozoic (to Neoarchean?), rift-orthogonal orogenic fabrics at the Greenland–Iceland–Faroe Ridge formed prior to the occurrence of all known tectonic episode with NW–SE-oriented main stress in the region, e.g., rifting of Iapetus (?), Caledonian Orogeny, late–post-Caledonian collapse, Variscan Orogeny (?), and Permian, Jurassic–Early Cretaceous, and Cenozoic rifting. Given their unsuitable orientation to contribute to thinning or thickening the crust under NW–SE-oriented stress and their probably relatively resistant constitution (e.g., eclogite, migmatite, granulite, and/or anorthosite), WNW–ESE-striking, preexisting, rift-orthogonal structures are believed to have locally hindered the development of NNE–SSW- to NE–SW-striking fabrics during subsequent tectonic episodes with NW–SE-oriented main stress. Thus, while rifting has efficiently used well-developed, rift-parallel (NNE–SSW-striking) Caledonian structures off the (north-) western coast of Norway and northern coast of Ireland (e.g., Clift *et al.*, 2004; Doré *et al.*, 1999; Musgrove & Mitchener, 1996; Norton *et al.*, 1987; Péron-Pinvidic & Osmundsen, 2020), which led to early breakup and seafloor spreading northeast and southwest of Iceland, the lack of well-developed rift-parallel, pre-rift structures delayed these processes at the Greenland–Iceland–Faroe Ridge.

The present interpretation can be further tested by acquiring new WNW–ESE- to NW–SE- and NE–SW-striking seismic reflection transects over Iceland and/or potentially by reprocessing the KRISE seismic reflection transect north of Iceland. The latter is, however, less ideal because oriented E–W and only partially overlapping the Greenland–Iceland–Faroe Ridge. Drilling the lower crust in Iceland and the Iceland–Faroe Ridge and/or Greenland–Iceland Ridge would also provide additional constraints on the nature and composition of the crust.

Assuming a pre-rift crustal thickness of c. 35 km at the Greenland–Iceland–Faroe Ridge, Faroe Islands, and northern Scotland (e.g., Funck *et al.*, 2014), a ≥ 23 km thick crust at the Greenland–Iceland–Faroe Ridge at present (Bohnhoff & Makris, 2004; Darbyshire *et al.*, 1998; Foulger *et al.*, 2003), and an average 5 km cap of lava flows (i.e., ≥ 18 km thick mid–lower crust), a maximum of 17 km crustal thinning has occurred pending no contribution from diking (i.e., magma intrusions and resulting crustal growth along sub-vertical fractures).

Stretching of the middle to lower crust in the Iceland–Faroe Ridge is apparent from localized inversion of the main thrust surfaces and S–C-like fabrics within WNW–ESE-striking thrust systems (e.g., extensional duplexes), especially where reworked as NNE–SSW-striking folds (Figure 2a–f and Figure 8a–h and Koehl *et al.*, 2024a their Figure 3e).

Other indications of Cenozoic extension in the mid–lower crust at the Iceland–Faroe Ridge include potential NNE–SSW-striking dykes intruded in the hinge zone of NNE–SSW-striking Caledonian anticlines (i.e., potential diking along Caledonian axial fold cleavage?; Figure 2a–e and Figure 4a) and similarly striking sills intruded perpendicular to inverted portions of WNW–ESE-striking thrust systems, e.g., Wyville–Thomson fault zone (Koehl *et al.*, 2024a their Figure 3e; Figure 1b), possibly in response to (tensile?) fracturing during extensional inversion. Swarms of magmatic sills intruded

perpendicular to an inverted major thrust system also occur in Svalbard (Koehl *et al.*, 2022 their Figure 3e and 6d–e, Koehl *et al.*, 2024b their Figures 3–7), thus suggesting this is not an isolated phenomenon and should be further investigated to evaluate the influence of the inversion of crustal-scale thrust systems on partial melting and swarms of magmatic intrusions.

Orogenic bridges and implications for plate tectonics

Transform margins have been known for their relatively abrupt continent–ocean transition (e.g., Lundin *et al.*, 2022; Mercier de Lépinay *et al.*, 2016). Lundin et al. (2022) proposed that the abrupt transition from thick continental to thin oceanic crust at transform margins suggests very limited pre-breakup lithospheric thinning at such margins. This contrasts with evidence from the geological record in the northeastern Atlantic region. In the Fram Strait, at least two episodes of post-Caledonian, pre-Cenozoic extension were recorded in the latest Silurian–earliest Permian (Braathen *et al.*, 2018; Chorowicz, 1992; Gudlaugsson *et al.*, 1998; Koehl & Muñoz-Barrera, 2018; Koehl *et al.*, 2022; Koehl *et al.*, 2023b; McCann & Dallmann, 1996; Roy, 2007; Stemmerik *et al.*, 1991; Strachan, 1994) and Late Jurassic–Early Cretaceous (Faleide et al., 1984; Faleide *et al.*, 1993; Indrevær et al., 2013; Blaich et al., 2017). The Greenland–Iceland–Faroe Ridge margins recorded at least three pre-breakup tectonic episodes, including late–post-Caledonian collapse and Permian–Triassic and Jurassic–Early Cretaceous extension (Clift *et al.*, 2004; Kimbell *et al.*, 2016; Musgrove & Mitchener, 1996; Waddams & Cordingley, 1999). It is therefore probable that some lithospheric thinning did occur but was less efficient at these transform margins.

A model that reconciles repeated extension at transform margins with their abrupt continent–ocean transition is that of orogenic bridges, i.e., the hindering of crustal thinning and breakup by rift-oblique orogenic structures and fabrics (Koehl & Foulger, 2025; Figure 14a–d). Orogenic bridges consist of intensely deformed continental crust tightened into at least two orogenic episodes with sub-orthogonal main stress (Figure 14a–b). The crust is then thinned during several episodes of late–post-orogenic collapse and rifting (Figure 14c). Breakup then occurs at inherited, rift-parallel orogenic structures and major transform faults develop at inherited, rift-orthogonal orogenic structures (Figure 14d; Koehl & Foulger, 2025).

An interpretation of the Greenland–Iceland–Faroe Ridge as thinned (orogenic) continental crust implies that the presumed mantle plume under Iceland is not responsible for the anomalously thick (25–40 km) crust at the Greenland–Iceland–Faroe Ridge.

A continental nature of the crust at the Greenland–Iceland–Faroe Ridge fits the interpreted seismic reflection and magnetic data (Figure 2a–f, Figure 10a–d, and Figure 11a–d). It is also in agreement with seismic attenuation under Iceland, which suggests a relatively cold lower crust (Menke & Levin, 1994), the strong continental affinities of lavas in eastern Iceland (Torsvik *et al.*, 2015), and possibly explains why the distance between some of the oldest lavas onshore Iceland is about twice larger than what is predicted by the full-plate spreading rate (Foulger, 2006).

The interpretation of a continuous late Paleoproterozoic (to Neoarchean?) orogenic belt between the Faroe Islands and Iceland suggests a potential extended link (ca. 1.8 Ga up to 2.6 Ga) between Laurentia, Baltica, and Avalonia. This is also suggested by new constraints on the late Neoproterozoic Timanian Orogen in northern Laurentia (Estrada *et al.*, 2018a; Estrada *et al.*, 2018b; Rosa *et al.*, 2016) and northern Baltica (Klitzke *et al.*, 2019; Koehl, 2020; Koehl *et al.*, 2022; Koehl, 2025; Koehl & Mottram, 2025). These new anchors significantly reduce the possible paleo plate movements of these three cratons relative to one another and as a whole in the past 1.8 Gyr. The similar WNW–ESE strike of late Paleoproterozoic structures in Greenland (Bridgewater & Myers, 1979; Chadwick & Vasudev, 1989), the UK (Attfield, 1987; Beach, 1974; Coward et al., 1980; Coward & Park, 1987; Evans, 1965), and Scandinavia (Bergh *et al.*, 2012; Nordgulen & Saintot, 2008; Saintot *et al.*, 2011) indicates that plate models and paleogeographic reconstructions involving rotation (e.g., Cocks & Torsvik, 2002; Merdith *et al.*, 2021; Rehnström *et al.*, 2002; Torsvik & Rehnström, 2001) are not realistic and that all three cratons have most likely remained in a configuration similar to present day for the past 1.8 Gyr (e.g., Cao *et al.*, 2021). In addition, pinning these three cratons to one another for the past 1.8 Gyr reduces the realm of their possible movements as a whole due to the increased size.

The present model of orogenic bridge should be tested at other margins where mantle plumes were proposed to explain anomalously thick crust, e.g., Walvis Ridge (Bai *et al.*, 2024; Fromm *et al.*, 2015), Rio Grande Rise (Hoyer *et al.*, 2022), Mozambique Ridge (Jacques *et al.*, 2019; O'Connor *et al.*, 2019), Madagascar Ridge (Sato *et al.*, 2022). Additional long-lived connections between other cratons (e.g., late Neoproterozoic Damara Belt in Namibia and Dom Feliciano Belt in South America and possibly at the Walvis Ridge and Rio Grande Rise; Koehl & Foulger, 2025) would further reduce the uncertainty around paleo plate reconstructions and provide new constraints on future plate movements and related geohazards and distribution of natural (e.g., hydrocarbon, hydrogen, geothermal, mineral) resources.

Conclusions

1) Seismic reflection and magnetic data suggest that the Greenland–Iceland–Faroe Ridge consists of a continental mid–lower crust crosscut by old, late Paleoproterozoic (to Neoarchean?) orogenic structures, which represent the possible continuation of the Laxfordian Orogen (and/or Badcallian–Inverian belt).

2) The late Paleoproterozoic (to Neoarchean?) thrust systems at the Greenland–Iceland–Faroe Ridge were reactivated during the Neoproterozoic, reworked into hundreds of km folds during the early–mid Paleozoic Caledonian Orogeny, and repeatedly inverted during post-Caledonian collapse and subsequent rifting episodes, e.g., opening of the northeastern Atlantic.

3) Late Paleoproterozoic thrust systems hindered the development of prominent NE–SW-striking fabrics and structures during subsequent tectonic episodes, which significantly delayed crustal thinning and continental breakup at the Greenland–Iceland–Faroe Ridge.

4) Both Laxfordian and Caledonian folds and thrusts possibly acted as crustal magma pathways.

5) The Greenland–Iceland–Faroe Ridge forms an elongated, rift-orthogonal ribbon of thinned, old orogenic crust flanked on either side by oceanic crustal domains with active seafloor spreading, i.e., an orogenic bridge.

6) The Greenland–Iceland–Faroe orogenic bridge suggests a long-term, 1.8 (up to 2.6?) Gyr connection between Laurentia and Avalonia–Baltica, thus providing new robust anchors for future paleo plate reconstructions.

Ethics and consent

Ethical approval and consent were not required.

Acknowledgements

The authors thank TGS and the British Geological Survey for access and permission to publish seismic reflection data at the Greenland–Iceland–Faroe Ridge.

Data availability

Underlying data

The Faroe–Iceland Ridge Experiment (FIRE) seismic reflection profiles acquired by the British Institutes Reflection Profiling Syndicate (BIRPS) were provided by the British Geological Survey (https://metadata.bgs.ac.uk/geonetwork/srv/api/records/c425c9fc-cb6d-352c-e044-0003ba9b0d98). The data can be accessed for academic research and teaching purposes under an academic license for free. To access the data, any prospective user may contact the British Geological Survey (digitaldata@bgs.ac.uk).

Repository name: BGS Metadata Catalogue. https://metadata.bgs.ac.uk/geonetwork/srv/api/records/c425c9fc-cb6d-352c-e044-0003ba9b0d98

The project contains the following underlying data:

BIRPS_FIRE_FinalStack_SEGYdata (folder):

- LINES (folder):
  - 31927.Y1 (SEG-Y file for FIRE-1 seismic profile).
  - 31927.Y2 (SEG-Y file for FIRE-2 seismic profile).
  - 31927.Y3 (SEG-Y file for FIRE-2A seismic profile).
  - 31927.Y4 (SEG-Y file for FIRE-3 seismic profile).
  - 31927.Y5 (SEG-Y file for FIRE-2 N seismic profile).
- NAVFILES (folder):

    - 31940.a27 (Text file containing shotpoint GPS locations).

- SIDELAB (folder):
    - FIRE.tif (Data location map).

- FIXES.txt (Details on each seismic reflection profile and fixes).

- INDEX.txt (Seismic profile list).

- LEGAL.txt (Copyright statement).

- README.txt (ReadMe file).

The copyright of materials contained in this dataset is vested in the Natural Environment Research Council [NERC]. Use of NERC data is restricted under the Copyright Designs and Patents Act 1988; however, permission is granted for use of these data for research purposes. No part of these data may be commercially sold, used to provide a value-added commercial product nor form part of a commercial data package. Any commercial use of products derived from these data requires prior written permission of the copyright holder and must acknowledge the source as being publicly available at the cost of reproduction from the British Geological Survey.

The rest of the seismic reflection data was provided by TGS (https://www.tgs.com/; see also Methods chapter of the manuscript). This data is private and subject to a data privacy agreement (cannot be shared, published, or showed without consent of TGS). TGS allowed us access to the data and gave us permission to publish the data (Academic License Agreement number NA0509–366). Any interested party may contact TGS directly with a research project proposal and be granted access to the data. Access to the data is free of charge for academic research purposes.

The magnetic data used in the study is from the NAG-TEC consortium (Tectonostratigraphic Atlas of the North-East Atlantic Region; Hopper *et al.*, 2014; Nasuti & Olesen, 2014a). The data can be accessed for free under CC-BY-4.0 license in the Dataverse online repository of the Geological Survey of Denmark and Greenland (GEUS; https://dataverse.geus.dk/dataset.xhtml?persistentId=doi:10.22008/FK2/CPODOR).

Repository name: GEUS Dataverse. https://dataverse.geus.dk/dataset.xhtml?persistentId=doi:10.22008/FK2/CPODOR

The project contains the following underlying data:

- mag_geo.nc (netcdf gridded file of the magnetic anomaly in geographic coordinates. Datum: WGS84).

- mag_geo.xyz (XYZ ascii grid of the magnetic anomaly in geographic coordinates. Datum: WGS84).

- mag_lam.nc (netcdf gridded file of the magnetic anomaly in the original projection coordinates used by the project. Lambert Conic Conformal: central meridian - 40°W, standard parallels - 55°N, 75°N. Datum: WGS84).

- mag_lam.xyz (XYZ ascii grid of the magnetic anomaly in the original projection coordinates used by the project. Lambert Conic Conformal: central meridian - 40°W, standard parallels - 55°N, 75°N. Datum: WGS84).

- tilt_derivative_geo.nc (netcdf gridded file of the tilt derivative in geographic coordinates. Datum: WGS84).

- tilt_derivative_geo.xyz (XYZ ascii grid of the tilt derivative in geographic coordinates. Datum: WGS84).

- tilt_derivative_lam.nc (netcdf gridded file of the tilt derivative in the original projection coordinates used by the project. Lambert Conic Conformal: central meridian - 40°W, standard parallels - 55°N, 75°N. Datum: WGS84).

- tilt_derivative_lam.xyz (XYZ ascii grid of the tilt derivative in the original projection coordinates used by the project. Lambert Conic Conformal: central meridian - 40°W, standard parallels - 55°N, 75°N. Datum: WGS84).

The data are available under the terms of the Creative Commons Attribution 4.0 International (CC-BY 4.0).

Extended data

Zenodo: High-resolution versions of the figures for "Inverted rift-orthogonal thrust systems in the Greenland–Iceland–Faroe Ridge: implications for the nature of the crust and plate tectonics", https://doi.org/10.5281/zenodo.20606344, [Koehl, J.B.P., 2026].

The project contains the following extended data:

- 00_ReadMe.txt
- Figure_1a.jpg
- Figure_1b.jpg
- Figure_2a.jpg
- Figure_2b.jpg
- Figure_2c.jpg
- Figure_2d.jpg
- Figure_2e.jpg
- Figure_2f.jpg
- Figure_3.jpg
- Figure_4a–b.jpg
- Figure_5a–f.jpg
- Figure_5g–l.jpg
- Figure_5m–n.jpg
- Figure_6a–e.jpg
- Figure_6f–j.jpg
- Figure_7a–c.jpg
- Figure_7d–j.jpg
- Figure_8a–c.jpg
- Figure_8d–h.jpg
- Figure_9a–c.jpg
- Figure_9d–e.jpg
- Figure_10a–b.jpg
- Figure_10c–d.jpg
- Figure_11a–b.jpg

- Figure_11c–d.jpg
- Figure_12a–c.jpg
- Figure_13a–b.jpg
- Figure_13c–d.jpg
- Figure_13e–f.jpg
- Figure_13g–h.jpg
- Figure_14a–d.jpg

Data are available under the terms of the Creative Commons Attribution 4.0 International license (CC-BY 4.0).

DataverseNO: Extended data for "Impact of sub-basalt thrust systems on the Faroe continental shelf for the late Paleoproterozoic–Cenozoic tectonic evolution of the margin", doi.org/10.18710/780M9P, 2024.

The project contains the following extended data:

- 00_ReadMe.txt
- Figure_2a.jpg
- Figure_2b.jpg
- Figure_2c.jpg
- Figure_2d.jpg
- Figure_2e.jpg
- Figure_2f.jpg
- Figure_2g.jpg
- Figure_2h.jpg
- Figure_2i.jpg

Data are available under the terms of the Creative Commons Attribution 4.0 International license (CC-BY 4.0).

References

Anderson DL: **The Thermal State of the Upper Mantle; No Role for Mantle Plumes.** *Geophys. Res. Lett.* 2000; **27**(22): 3623–3626.
Publisher Full Text

Andresen A, Rehnström EF, Holte M: **Evidence for simultaneous contraction and extension at different crustal levels during the Caledonian orogeny in NE Greenland.** *J. Geol. Soc.* 2007; **164**: 869–880.
Publisher Full Text

Arnason K, Gibert B, Bouligand C, *et al.*: **The deep conductive layer in the Icelandic crust.** *Earth Sci. Rev.* 2025; **270**: 105198.
Publisher Full Text

Årebäck H, Stigh J: **The nature and origin of an anorthosite associated ilmenite-rich leuconorite, Hakefjorden Complex, south-west Sweden.** *Lithos.* 2000; **51**: 247–267.
Publisher Full Text

Attfield P: **The structure history of the Canisp Shear Zone.** *Evolution of the Lewisian and comparable Precambrian high-grade terrains.* Park RG, Tarney J, editors. London: Geological Society; 1987; **27**: 165–173. Special Publications.
Publisher Full Text

Bai Y, Cheng K, Dong D, *et al.*: **Mantle plume – mid ocean ridge interactions revealed from hotspot melt production rate along the Walvis Ridge-Rio Grande Rise.** *EPSL.* 2024; **648**: 119102.
Publisher Full Text

Bamford D: **Seismic constraints on the deep geology of the Caledonides of northern Britain.** *The Caledonides of the British Isles — reviewed.* Harris AL, Holland CH, Leake BE, editors. London: Geological Society; 1979; **8**: 93–96. Special Publication.
Publisher Full Text

Barooah BC, Bowes DR: **Multi-episodic modification of high-grade terrane near Scourie and its significance in elucidating the history of the Lewisian Complex.** *Scott. J. Geol.* 2009; **45**(1): 19–41.
Publisher Full Text

Bathaeian I: *Meshfree Simulation of Problems in Soil Mechanics: Laboratory Tests Shear Bands – Punching – Cone Penetration - Turbulence in Granular Solids – Ptygmatic Folds.* Innsbruck, Germany: University of Innsbruck; 2018. Ph.D. Thesis.
Publisher Full Text

Beach A: **The measurement and significance of displacements on Laxfordian shear zones, North-West Scotland.** *Proc. Geol. Assoc.* 1974; **85**(1): 13–IN1.
Publisher Full Text

Berg SE: *Silicic Magma Genesis in Basalt dominated Oceanic Settings.* Uppsala, Sweden: Uppsala University; 2016; 1–54. Ph.D. Thesis.
Reference Source

Bergerat F, Angelier J: **Immature and mature transform zones near a hot spot: The South Iceland Seismic Zone and the Tjörnes Fracture Zone (Iceland).** *Tectonophysics.* 2008; **447**: 142–154.
Publisher Full Text

Bergh SG, Corfu F, Myhre PI, *et al.*: **Waas the precambrian basement of Western Troms and Lofoten-Vesterålen in Northern Norway linked to the Lewisian of Scotland? A comparison of crustal components, tectonic evolution and amalgamation history.** *Tectonics - Recent Advances.* Sharkov E, editor. InTech; 2012.
Publisher Full Text

Birch F: **The Velocity of Compressional Waves in Rocks to 10 Kilobars, Part 1.** *J. Geophys. Res.* 1960; **65**(4): 1083–1102.
Publisher Full Text

Birch F: **The Velocity of Compressional Waves in Rocks to 10 Kilobars, Part 2.** *J. Geophys. Res.* 1961; **66**(7): 2199–2224.
Publisher Full Text

Bird PC, Cartwright JA, Davies TL: **Basement reactivation in the development of rift basins: an example of reactivated Caledonide structures in the West Orkney Basin.** *J. Geol. Soc.* 2016; **172**: 77–85.
Publisher Full Text

Blaich OA, Tsikalas F, Faleide JI: **New insights into the tectono-stratigraphic evolution of the southern Stappen High and its transition to Bjørnøya Basin, SW Barents Sea.** *Mar. Pet. Geol.* 2017; **85**: 89–105.
Publisher Full Text

Blischke A, Gaina C, Hopper JR, *et al.*: **The Jan Mayen microcontinent: an update of its architecture, structural development and role during the transition from the Ægir Ridge to the mid-oceanic Kolbeinsey Ridge.** *The NE Atlantic Region: A Reappraisal of Crustal Structure, Tectonostratigraphy and Magmatic Evolution.* Péron-Pinvidic G, Hopper JR, Stoker MS, *et al.*: London: Geological Society; 2016; **447**: 299–337. Special Publications.

Boddupalli B, Canales JP: **Distribution of Crustal Melt Bodies at the Hot Spot-Influenced Section of the Galápagos Spreading Centre From Seismic Reflection Images.** *Geophys. Res. Lett.* 2019; **46**: 4664–4673.
Publisher Full Text

Bohnhoff M, Makris J: **Crustal structure of the southeastern Iceland-Faeroe Ridge (IFR) from wide aperture seismic data.** *J. Geodyn.* 2004; **37**: 233–252.
Publisher Full Text

Bourgeois O, Dauteuil O, Hallot E: **Rifting above a mantle plume: structure and development of the Iceland Plateau.** *Geodin. Acta.* 2005; **18**(1): 59–80.
Publisher Full Text

Boyd FR, McCallister RH: **Densities of fertile and sterile garnet peridotite.** *Geophys. Res. Lett.* 1976; **3**(9): 509–512.
Publisher Full Text

Boyer SE, Elliott D: **Thrust systems.** *AAPG Bull.* 1982; **66**(9): 1196–1230.
Publisher Full Text

Boðvarsson G, Walker GPL: **Crustal Drift in Iceland.** *Geophys. J. Int.* 1964; **8**(3): 285–300.
Publisher Full Text

Braathen A, Osmundsen PT, Maher HD, *et al.*: **The Keisarhjelmen detachment records Silurian-Devonian extensional collapse in Northern Svalbard.** *Terra Nova.* 2018; **30**(1): 34–39.
Publisher Full Text

Bransðóttir B, Menke WH: **The seismic structure of Iceland.** *Jökull.* 2008; **58**: 17–34.
Publisher Full Text | **Reference Source**

Brewer JA, Smythe DK: **MOIST and the continuity of crustal reflector geometry along the Caledonian-Appalachian orogen.** *J. Geol. Soc.* 1984; **141**: 105–120.
Publisher Full Text

Bridgewater D, Myers JS: **Outline of the Nagssugtoqidian mobile belt of East Greenland.** *Rapport Grønlands Geologisks Undersøkelse.* 1979; **89**: 9–18.
Publisher Full Text

Bridgewater D, Watson J, Windley BF: **The Archaean craton of the North Atlantic region.** *Phil Trans R Soc Lond A.* 1973; **273**: 493–512.
Publisher Full Text | **Reference Source**

Brooks CK: **The East Greenland rifted volcanic margin.** *Geol Surv Den Greenl Bull.* 2011; **24**: 1–96.
Publisher Full Text

Burchardt S, *et al.*: **Geology of a Neogene caldera cluster in the Borgarfjörðureystri–Loðmundarfjörður area, Eastern Iceland.** *Volcanica.* 2022; **5**(1): 133–161.
Publisher Full Text

Calvert AJ, Doublier MP: **Migration of reflector orientation attributes in deep seismic profiles: evidence for decoupling of the Yilgarn Craton lower crust.** *Solid Earth.* 2019; **10**: 637–645.
Publisher Full Text

Cao Y, Jung H, Song S: **Petro-fabrics and seismic properties of blueschist and eclogite in the North Qilian suture zone, NW China: Implications for the low-velocity upper layer in subducting slab, trench-parallel seismic anisotropy, and eclogite detectability in the subduction zone.** *J. Geophys. Res.* 2013; **118**: 3037–3058.
Publisher Full Text

Cao X, Flament N, Müller RD: **Coupled evolution of plate tectonics and basal mantle structure.** *Geochem. Geophys. Geosyst.* 2021; **22**(1): e2020GC009244.
Publisher Full Text

Carbotte SM, Marjanović M, Arnulf AF, *et al.*: **Stacked Magma Lenses Beneath Mid-Ocean Ridges: Insights From New Seismic Observations and Synthesis With Prior Geophysical and Geologic Findings.** *JGR Solid Earth.* 2021; **126**: e2020JB021424.
Publisher Full Text

Chadwick B, Dawes PR, Escher JC, *et al.*: **The proterozoic mobile belt in the Ammassalik region, South-East Greenland (Ammassalik mobile belt): an introduction and re-appraisal.** *Rapport Grønlands Geologisks Undersøkelse.* 1989; **146**(5–12): 5–12.
Publisher Full Text

Chadwick B, Vasudev VN: **Some observations on the structure of the early Proterozoic, Ammassalik mobile belt in the Ammassalik region, South-East Greenland.** *Rapport Grønlands Geologisks Undersøkelse.* 1989; **146**: 29–40.
Publisher Full Text

Charlier B, Namur O, Bolle O, *et al.*: **Fe–Ti–V–P ore deposits associated with Proterozoic massif-type anorthosites and related rocks.** *Earth Sci. Rev.* 2014; **141**: 56–81.
Publisher Full Text

Chorowicz J: **Gravity-induced detachment of Devonian basin sediments in northern Svalbard.** *Nor Teol Tidsskr.* 1992; **72**: 21–25.

Christensen NI: **Compressional wave velocities in metamorphic rocks at pressures to 10 kilobars.** *J. Geophys. Res.* 1965; **70**(24): 6147–6164.
Publisher Full Text

Christensen NI, Szymanski DL: **Origin of Reflections From the Brevard Fault Zone.** *J. Geophys. Res.* 1988; **93**(B2): 1087–1102.
Publisher Full Text

Christeson GL, Goff JA, Reece RS: **Synthesis of Oceanic crustal structure from two-dimensional seismic profiles.** *Rev. Geophys.* 2019; **57**(2): 504–529.
Publisher Full Text

Clift PD, Dewey JF, Draut AE, *et al.*: **Rapid tectonic exhumation, detachment faulting and orogenic collapse in the Caledonides of western Ireland.** *Tectonophysics.* 2004; **384**: 91–113.
Publisher Full Text

Cocks LRM, Torsvik TH: **Earth geography from 500 to 400 million years ago: a faunal and palaeomagnetic review.** *J. Geol. Soc.* 2002; **159**: 631–644.
Publisher Full Text

Coleman RG, Lanphere MA: **Distribution and Age of High-Grade Blueschists, Associated Eclogites, and Amphibolites from Oregon and California.** *GSA Bull.* 1971; **82**: 2397–2412.
Publisher Full Text

Corfu F, Heaman LM, Rogers G: **Polymetamorphic evolution of the Lewisian complex, NW Scotland, as recorded by U-Pb isotopic compositions of zircon, titanite and rutile.** *Contrib. Mineral. Petrol.* 1994; **117**: 215–228.
Publisher Full Text

Coward MP: **The Caledonian thrust and shear zones of N.W. Scotland.** *J. Struct. Geol.* 1980; **2**(1–2): 11–17.
Publisher Full Text

Coward MP: **The Precambrian, Caledonian and Variscan framework to NW Europe.** *Tectonic events responsible for Britain's oil and gas reserves.* Hardman RFP, Brooks J, editors. London: Geological Society; 1990; **55**: 1–34. Special Publications.
Publisher Full Text

Coward MP, Enfield MA, Fischer MW: **Devonian basins of Northern Scotland: extension and inversion related to late Caledonian – Variscan tectonics.** *Inversion Tectonics.* Cooper MA, Williams GD, editors. London: Geological Society; 1989; **44**: 275–308. Special Publications.
Publisher Full Text

Coward MP, Kim JH, Parke J: **A correlation of Lewisian structures and their displacement across the lower thrusts of the Moine Thrust zone, NW Scotland.** *Proc. Geol. Assoc.* 1980; **91**(4): 327–337.
Publisher Full Text

Coward MP, Park RG: **The role of mid-crustal shear zones in the early Proterozoic evolution of the Lewisian.** *Evolution of the Lewisian and comparable Precambrian and high-grade terrains.* Park RG, Tarney J, editors. Geological Society 1987; **27**: 127–138. Special Publication.
Publisher Full Text

Dahl-Jensen T, Holbrook WS, Hopper JR, *et al.*: **Seismic investigation of the East Greenland volcanic rifted margin.** *Geol. Greenl. Surv. Bull.* 1997; **176**: 50–54.
Publisher Full Text

Darbyshire FA, Bjarnason IT, White RS, *et al.*: **Crustal structure above the Iceland mantle plume imaged by the ICEMELT refraction profile.** *Geophys. J. Int.* 1998; **135**(3): 1131–1149.
Publisher Full Text

Davison I, Stasiuk S, Nuttall P, *et al.*: **Sub-basalt hydrocarbon prospectivity in the Rockall, Faroe–Shetland and Møre basins, NE Altantic.** *Petroleum Geology: From Mature Basins to New Frontiers – Proceedings of the 7 th Petroleum Geology Conference.* Vining BA, Pickering SC, editors. London: Geological Society; 2010; **7**: 1025–1032.
Publisher Full Text

Dawes PR, Soper NJ, Eschel JC, *et al.*: **The northern boundary of the Proterozoic (Nagssugtoqidian) mobile belt of South-East Greenland.** *Rapp. Grønl. Geol. Unders.* 1989; **146**: 54–65.
Publisher Full Text

Day JMD: **Evidence against an ancient non-chondritic mantle source for North Atlantic Igneous Province lavas.** *Chem. Geol.* 2016; **440**: 91–100.
Publisher Full Text

Dickin AP: **Evidence for an early Proterozoic crustal province in the North Atlantic region.** *J. Geol. Soc. Lond.* 1992; **149**: 483–486.
Publisher Full Text

Dilek Y, Moores EM, Furnes H: **Structure of Modern Oceanic Crust and OOphiolites and Implications for Faulting and Magmatism at Oceanic Spreading Centers.** *Faulting and Magmatism at Mid-Ocean Ridges.* Buck WR, Delaney PT, Karson JA, *et al.*, editors. 1998; **106**: 219–265. Geophysical Monograph Series.
Publisher Full Text

Ding W, Sun Z, Dadd K, *et al.*: **Structures within the oceanic crust of the central South China Sea basin and their implications for oceanic accretionary processes.** *EPSL.* 2018; **488**: 115–125.
Publisher Full Text

Doré AG, Lundin ER, Jensen LN, *et al.*: **Principal tectonic events in the evolution of the northwest European Atlantic margin.** *Petroleum Geology of Northwest Europe: Proceedings of the 5th Conference.* Doré AG, Lundin ER, Jensen LN, *et al.*, editors. Petroleum Geology; 1999; **5**: 41–61.
Publisher Full Text

Du Z, Foulger GR: **Variation in the crustal structure across central Iceland.** *Geophys. J. Int.* 2001; **145**: 246–264.
Publisher Full Text

Duchesne JC: **Fe-Ti deposits in Rogaland anorthosites (South Norway): geochemical characteristics and problems of interpretation.** *Mineral. Deposita.* 1999; **34**: 182–198.
Publisher Full Text

Dumais MA, Gernigon L, Johansen SE, *et al.*: **New interpretation of the spreading evolution of the Knipovich Ridge derived from aeromagnetic data.** *Geophys. J. Int.* 2020; **224**(2): 1422–1428.
Publisher Full Text

Edwards JWF: **Development of the Hatton–Rockall Basin, North-East Atlantic Ocean.** *Mar. Pet. Geol.* 2002; **19**: 193–205.
Publisher Full Text

Ellefsen M, Boldreel LO, Larsen M: **Intra-basalt units and base of the volcanic succession east of the Faroe Islands exemplified by interpretation of offshore 3D seismic data.** *Petroleum Geology: From Mature Basins to New Frontiers – Proceedings of the 7th Petroleum Geology Conference.* Vinning BA, Pickering SC, editors. Geological Society London; 2009; **7**: 1033–1042.
Publisher Full Text

Eshaghi E, Smith RS, Ayer J: *Petrophysical characterisation (i.e. density and magnetic susceptibility) of major rock units within the Abitibi Greenstone Belt.* Laurentian University Mineral Exploration Research Centre; 2019; vol. **MERC-ME-2019-144**: 1–86.
Reference Source

Estrada S, Mende K, Gerdes A, *et al.*: **Proterozoic to Cretaceous evolution of the western and central Pearya Terrane (Canadian High Arctic).** *J. Geodyn.* 2018b; **120**: 45–76.
Publisher Full Text

Estrada S, Tessensohn F, Sonntag BL: **A Timanian island-arc fragment in North Greenland: the Midtkap igneous suite.** *J. Geodyn.* 2018a; **118**: 140–153.
Publisher Full Text

Evans CR: **Geochronology of the Lewisian basement near Lochinver, Sutherland.** *Nature.* 1965; **207**: 54–56.
Publisher Full Text

Evans CR, Lambert RSJ: **The Lewisian of Lochinver, Sutherland; the type area for the Inverian metamorphism.** *J. Geol. Soc.* 1974; **130**: 125–150.
Publisher Full Text

Faleide JI, Gudlaugsson ST, Jacquart G: **Evolution of the western Barents Sea.** *Mar. Pet. Geol.* 1984; **1**: 123–150.
Publisher Full Text

Faleide JI, Vågnes E, Gudlaugsson ST: **Late Mesozoic-Cenozoic evolution of the south-western Barents Sea in a regional rift-shear tectonic setting.** *Mar. Pet. Geol.* 1993; **10**(3): 186–214.
Publisher Full Text

Faryad SW: **Metamorphic evolution of the Precambrian South Badakhshan block, based on mineral reactions in metapelites and metabasites associated with whiteschists from Sare Sang (Western Hindu Kush, Afghanistan).** *Precambrian Res.* 1999; **98**: 223–241.
Publisher Full Text

Fazlikhani H, Bauer W, Stollhofen H: **Variscan structures and their control on latest to post-Variscan basin architecture: insights from the westernmost Bohemian Massif and southeastern Germany.** *Solid Earth.* 2022; **13**(2): 393–416.
Publisher Full Text

Fazlikhani H, Fossen H, Gawthorpe RL, *et al.*: **Basement structure and its influence on the structural configuration of the northern North Sea rift.** *Tectonics.* 2017; **36**(6): 1151–1177.
Publisher Full Text

Fitz-Diaz E, Hudleston P, Tolson G: **Comparison of tectonic styles in the Mexican and Canadian Rocky Mountain Fold-Thrust Belt.** *Kinematic Evolution and Structural Styles of Fold-and-Thrust Belts.* Poblet J, Lisle RJ, editors. Geological Society of London Special Publication; 2011; **349**: 149–167.
Publisher Full Text

Foulger GR: **Older crust underlies Iceland.** *Geophys. J. Int.* 2006; **165**(2): 672–676.
Publisher Full Text

Foulger GR: **The origin of Iceland: current hypotheses.** *ZDGG–J App Reg Geol.* 2025; **176**: 3–27.
Publisher Full Text

Foulger GR: **The Plate Theory for Volcanism.** *Encyclopedia of Geology.* Alderton D, Elias SA, editors. Academic Press;Second Edition. 2021; 879–890.
Publisher Full Text

Foulger GR, Doré T, Emeleus CH, *et al.*: **The Iceland microcontinent and a continental Greenland-Iceland-Faroe Ridge.** *Earth Sci. Rev.* 2020; **206**: 102926.
Publisher Full Text

Foulger GR, Du Z, Julian BR: **Icelandic-type crust.** *Geophys. J. Int.* 2003; **155**(2): 567–590.
Publisher Full Text

Foulger GR, Gernigon L, Geoffroy L: **Icelandia.** *In the Footsteps of Warren Hamilton: New Ideas in Earth Science.* Foulger GA, Hamilton LC, Jurdy DM, *et al.*, editors. Geological Society of America; 2021; **553**: 1–12. Special Paper.
Publisher Full Text

Fountain DM, Hurich CA, Smithson SB: **Seismic reflectivity of mylonite zones in the crust.** *Geology.* 1984; **12**(4): 195–198.
Publisher Full Text

Frazer FM: *The Lewisian and Torridonian geology of Iona.* St Andrews, UK: University of St Andrews; 1977; 1–275. Ph.D. Thesis.
Reference Source

Freeman B, Klemperer SL, Hobbs RW: **The deep structure of northern England and the Iapetus Suture zone from BIRPS deep seismic reflection profiles.** *J. Geol. Soc. Lond.* 1988; **145**: 727–740.
Publisher Full Text

Friend PF, Harland WB, Hudson JD: **The Old Red Sandstone and the Highland Boundary in Arran, Scotland.** *TEGS.* 1963; **19**: 363–425.
Publisher Full Text

Friðleifsson GO, Elders WA, Zierenberg RA, *et al.*: **The Iceland Deep Drilling Project 4.5km deep well, IDDP-2, in the seawater-recharged Reykjanes geothermal f ield in SW Iceland has successfully reached its supercritical target.** *Sci. Drill.* 2017; **23**: 1–12.
Publisher Full Text

Friðleifsson IB: **The Iceland Research Drilling Project in Relation to the Geology of Iceland.** *J. Geophys. Res.* 1982; **87**(B8): 6363–6370.
Publisher Full Text

Fromm T, Planert L, Jokat W, *et al.*: **South Atlantic opening: A plume-induced breakup?.** *Geology.* 2015; **43**(10): 931–934.
Publisher Full Text

Funck T, Hopper JR, Fattah RA, *et al.*: **Chapter 6: Crustal Structure. In: Tectonostratigraphic Atlas of the North-East Atlantic Region.** edited by: Hopper JR, Funck T, Stoker MS, *et al.*, editors. Copenhagen, Denmark: Geological Survey of Denmark and Greenland (GEUS); 2014; 69–128.
Publisher Full Text

Gaina C, Nasuti A, Kimbell G, *et al.*: **Break-up and seafloor spreading domains in the NE Atlantic.** *The NE Atlantic region: a reappraisal of crustal structure, tectonostratigraphy and magmatic evolution.* Péron-Pinvidic G, Hopper JR, Stoker MS, *et al.*, editors. London: Geological Society; 2017; **447**: 393–417. Special Publications.
Publisher Full Text

Garcia S, Arnaud NO, Angelier J, *et al.*: **Rift jump process in Northern Iceland since 10 Ma from 40Ar/39Ar geochronology.** *EPSL.* 2003; **214**: 529–544.
Publisher Full Text

Garcia S, Angelier J, Bergerat F, *et al.*: **Influence of rift jump and excess loading on the structural evolution of northern Iceland.** *Tectonics.* 2008; **27**: TC1006.
Publisher Full Text

GEBCO Compilation Group: **GEBCO 2023 Grid.** 2023.
Publisher Full Text

Geldart LP, Sheriff RE: **Problems in exploration seismology and their solutions.** *Society of Exploration Geophysicists, Geophysical References Series.* 2004; **14**: 181–220.
Publisher Full Text

Geoffroy L: **Volcanic passive margins.** *CR Geoscience.* 2005; **337**: 1395–1408.
Publisher Full Text

Geoffroy L, Chauvet F, Ringenbach JC: **Middle-lower continental crust exhumed at the distal edges of volcanic passive margins.** *Commun. Earth Environ.* 2022; **3**: 95.
Publisher Full Text

Geoffroy L, Gernigon L, Foulger GR: **Linear magnetic anomalies and the limits of oceanic crust in oceans.** *In the footsteps of Warren B. Hamilton: New Ideas in Earth Science.* Foulger GR, Hamilton LC, Jurdy DM, *et al.*, editors. Geological Society of America Special Paper; 2021; 553.
Publisher Full Text

Gernigon L, Zastrozhnov D, PLanke S, *et al.*: **A digital compilation of structural and magmatic elements of the Mid-Norwegian continental margin (version 1.0).** *Nor. J. Geol.* 2021; **101**: 202112.
Publisher Full Text

Ghose NC, Chatterjee N, Mukherjee D, *et al.*: **Mineralogy and Geochemistry of the Bengal Anorthosite Massif in the Chotanagpur Gneissic Complex at the Eastern Indian Shield Margin.** *J. Geol. Soc. India.* 2008; **72**: 263–277.
Publisher Full Text

Ghosh SK: **Experimental tests of buckling folds in relation to strain ellipsoid in simple shear deformations.** *Tectonophysics.* 1966; **3**(3): 169–185.
Publisher Full Text

Glen RA, Spencer R, Willmore A, *et al.*: **Junee–Narromine Volcanic Belt, Macquarie Arc, Lachlan Orogen, New South Wales: components and structure.** *Aust. J. Earth Sci.* 2007; **54**: 215–241.
Publisher Full Text

Godfrey JD: **The Origin of Ptygmatic Structures.** *J. Geol.* 1954; **62**(4): 375–387.
Publisher Full Text | **Reference Source**

Goscombe B, Foster DA, Gray D, *et al.*: **Deformation correlations, stress field switches and evolution of an orogenic intersection: The Pan-African Kaoko-Damara orogenic junction, Namibia.** *Geosci. Front.* 2017; **8**: 1187–1232.
Publisher Full Text

Griffin WL, Sundvoll B, Kristmannsdottir H: **Trace element composition of anorthosite plagioclase.** *EPSL.* 1974; **24**: 213–223.
Publisher Full Text

Guarnieri P: **Analysis of Palaeogene strike-slip tectonics along the southern East Greenland margin (Sødalen area).** *Geol Surv Den Greenl Bull.* 2011; **23**: 65–68.
Publisher Full Text

Gudlaugsson ST, Faleide JI, Johansen SE, *et al.*: **Late Palaeozoic structural development of the South-western Barents Sea.** *Mar. Pet. Geol.* 1998; **15**(1): 73–102.
Publisher Full Text

Hansen DM, Cartwright JA, Thomas D: **3D seismic analysis of the geometry of igneous sills and sill junction relationships.** *3D Seismic Technology: Application to the Exploration of Sedimentary. Basins.* Davies RJ, Cartwright JA, Stewart SA, *et al.*, editors. Geological Society, London Memoirs; 2004; **29**: 299–208.
Publisher Full Text

Hansen J, Ganerød M: **On the Timing and Nature of Magmatism in the North Atlantic Igneous Province: New Implications from Basaltic Rocks of the Faroe Islands.** *Earth Sci.* 2023; **12**(5): 121–139.
Publisher Full Text

Harðarson BS, Fitton JG, Hjartarson A: **Tertiary volcanism in Iceland.** *Jökull.* 2008; **58**: 161–178.
Publisher Full Text

Harðarson BS, Fitton JG, Ellam RM, *et al.*: **Rift relocation — a geochemical and geochronological investigation of a palaeo-rift in northwest Iceland.** *EPSL.* 1997; **153**: 181–196.
Publisher Full Text

Hedin P, Almqvist B, Berthet T, *et al.*: **3D reflection seismic imaging at the 2.5 km deep COSC-1 scientific borehole, central Scandinavian Caledonides.** *Tectonophysics.* 2016; **689**: 40–55.
Publisher Full Text

Henkel H: **Density measurements on Precambrian basement rocks from the Uppsala region.** *Meddelande från geodetiska institutionen vid Upsala universitet.* 1970; **9**: 1–23.

Henkel H: **Studies of Density and Magnetic Properties of Rocks from Northern Sweden.** *Pageoph.* 1976; **114**: 235–249.
Publisher Full Text

Henkel H: **Petrophysical properties (density and magnetization) of rocks from the northern part of the Baltic Shield.** *Tectonophysics.* 1991; **192**: 1–19.
Publisher Full Text

Hitchen K: **The geology of the UK Hatton-Rockall margin.** *Mar. Pet. Geol.* 2004; **21**: 993–1012.
Publisher Full Text

Hitchen K, Stoker MS: **Mesozoic rocks from the Hebrides Shelf and implications for hydrocarbon prospectivity in the northern Rockall Trough.** *Mar. Pet. Geol.* 1993; **10**: 246–254.
Publisher Full Text

Hitchen K, Morton AC, Mearns EW, *et al.*: **Geological implications from geochemical and isotopic studies of Upper Cretaceous and Lower Tertiary igneous rocks around the northern Rockall Trough.** *J. Geol. Soc.* 1997; **154**: 517–521.
Publisher Full Text

Hjartarson A: *The Skagafjörður unconformity north Iceland and its geological history* Copenhagen, Denmark: University of Copenhagen; 2003; 1–248. Ph.D. Thesis.
Reference Source

Hjartarson A, Erlendsson Ö, Blischke A: **The Greenland–Iceland–Faroe ridge complex.** *The NE Atlantic region: a reappraisal of crustal structure, tectonostratigraphy and magmatic evolution.* Péron-Pinvidic G, Hopper JR, Stoker MS, *et al.*, editors. London: Geological Society; 2017; **447**: 127–148. Special Publications.
Publisher Full Text

Hoggard MJ, Winterbourne J, Czarnota K, *et al.*: **Oceanic residual depth measurements, the plate cooling model, and global dynamic topography.** *JGR Solid Earth.* 2017; **122**: 2328–2372.
Publisher Full Text

Hole MJ, Natland JH: **Magmatism in the North Atlantic Igneous Province; mantle temperatures, rifting and geodynamics.** *Earth Sci. Rev.* 2020; **206**: 102794.
Publisher Full Text

Hopper JR, Lizarralde D, Larsen HC: **Seismic investigations offshore South-East Greenland.** *Geol Surv Den Greenl Bull.* 1998; **180**: 145–151.
Publisher Full Text

Hopper JR, Funck T, Stoker MS, *et al.*: *Tectonostratigraphic Atlas of the North-East Atlantic Region.* Copenhagen, Denmark: Geological Survey of Denmark and Greenland (GEUS); 2014; 1–338.
Publisher Full Text

Hovikoski J, Fyhn MBW, Nøhr-Hansen H, *et al.*: **Paleocene-Eocene volcanic segmentation of the Norwegian-Greenland seaway reorganized high-latitude ocean circulation.** *Commun. Earth Environ.* 2021; **2**: 172.
Publisher Full Text

Hoyer PA, Haase KM, Regelous M, *et al.*: **Mantle plume and rift-related volcanism during the evolution of the Rio Grande rise.** *Commun. Earth*

Environ. 2022; **3**(18): 1–10.
Publisher Full Text

Hurich CA, Smithson SB, Fountain DM, *et al.*: **Seismic evidence of mylonite reflectivity and deep structure in the Kettle dome metamorphic core complex, Washington.** *Geology.* 1985; **13**(8): 577–580.
Publisher Full Text

Hyndman RD, Drury MJ: **13. Physical properties of basalts, gabbros, and ultramafic rocks from DSDP Leg 37.** *Initial Rep. Deep Sea Drill. Proj.* 1977; **37**: 395–401.
Publisher Full Text

Indrevær K, Bergh SG, Koehl JB, *et al.*: **Post-Caledonian brittle fault zones on the hyperextended SW Barents Sea margin: New insights into onshore and offshore margin architecture.** *Nor. J. Geol.* 2013; **93**: 167–188.

Ito K, Kennedy GC: **The fine structure of the basalt-eclogite transition.** *Mineral Soc Amer Spec Pap.* 1970; **3**: 77–83.
Reference Source

Jacques G, Hauff F, Hoernle K, *et al.*: **Nature and origin of the Mozambique Ridge, SW Indian Ocean.** *Chem. Geol.* 2019; **507**(5): 9–22.
Publisher Full Text

Jancin M, Young KD, Voight B, *et al.*: **Stratigraphy and K/Ar ages across the west flank of the northeast Iceland axial rift zone, in relation to the 7 Ma volcano-tectonic reorganization of Iceland.** *J. Geophys. Res.* 1985; **90**(B12): 9961–9985.
Publisher Full Text

Johannesson H: **Jarðlagaskipan og þróun rekbelta á Vesturlandi.** *Náttúrufræðingurinn.* 1980; **50**(1): 13–31.
Reference Source

Jóhannesson H, Sæmundsson K: *Geological Map of Iceland. Tectonics. 1:600 000.* Reykjavik, Iceland: Iceland GeoSurvey (ÍSOR); 2009.

Johannesson H: *Geological map of Iceland – bedrock geology 1:600 000.* Icelandic Institute of Natural History;2nd ed. 2014.
Reference Source | **Reference Source**

Johnson H, Ritchie JD, Hitchen K, *et al.*: **Aspects of the Cenozoic deformational history of the Northeast Faroe-Shetland Basin, Wyville-Thomson and Hatton Bank areas.** *Petroleum Geology: North-West Europe and Global Perspectives—Proceedings of the 6 th Petroleum Geology Conference.* Doré AG, Vinning BA, editors. London: Geological Society; 2005; 993–1007.
Publisher Full Text

Jolley DW, Millett JM, Schofield N, *et al.*: **Stratigraphy of volcanic rock successions of the North Atlantic rifted margin: the offshore record of the Faroe-Shetland and Rockall basins.** *Earth Environ. Sci. Trans. R. Soc. Edinb.* 2021; **112**(2): 61–88.
Publisher Full Text

Jonasson K: **Silicic volcanism in Iceland: Composition and distribution within the active volcanic zones.** *J. Geodyn.* 2007; **43**: 101–117.
Publisher Full Text

Jones MQW: **Thermophysical properties of rocks from the Bushveld Complex.** *South Afr Inst Min Metall.* 2015; **115**: 153–160.
Publisher Full Text | **Reference Source**

Jones T, Nur A: **Seismic velocity and anisotropy in mylonites and the reflectivity of deep crustal fault zones.** *Geology.* 1982; **10**: 260–263.
Publisher Full Text

Kallweit RS, Wood LC: **The limits of resolution of zero-phase wavelets.** *Geophys.* 1982; **47**(7): 1035–1046.
Publisher Full Text

Kalsbeek F, Austrheim H, Bridgewater D, *et al.*: **Geochronology of Archaean and Proterozoic events in the Ammassalik area, south-east Greenland, and comparisons with the Lewisian of Scotland and the Nagssugtoqidian of west Greenland.** *Precambrian Res.* 1993a; **62**(3): 239–270.
Publisher Full Text

Kalsbeek F, Nutman AP, Taylor PN: **Palaeoproterozoic basement province in the Caledonian fold belt of North-East Greenland.** *Precambrian Res.* 1993b; **63**: 163–178.
Publisher Full Text

Kalsbeek F, Thrane K, Higgins AK, *et al.*: **Polyorogenic history of the East Greenland Caledonides.** *The Greenland Caledonides: Evolution of the Northeast Margin of Laurentia.* Higgins AK, Gilotti JA, Smith MP, editors. Geological Society of America Memoir; 2008; **202**: 55–72.
Publisher Full Text

Kästner F, Pierdominici S, Elger J, *et al.*: **Correlation of core and downhole seismic velocities in high-pressure metamorphic rocks: a case study for the COSC-1 borehole, Sweden.** *Solid Earth.* 2020; **11**(2): 607–626.
Publisher Full Text

Khodayar M: **Shift of a rift by a transform zone: a case from the northern Rift Zone and Tjörnes Fracture Zone of Iceland.** *Pet. Geosci.* 2018; **24**: 414–424.
Publisher Full Text

Khodayar M, Einarsson P: **Strike-slip faulting, normal faulting, and lateral dike injections along a single fault: Field example of the Gljúfurá fault near a Tertiary oblique rift-transform zone, Borgarfjörður, west Iceland.** *J. Geophys. Res.* 2002; **107**(B5): 2103.
Publisher Full Text

Khodayar M, Björnsson S, Guðnason EA, *et al.*: **Tectonic Control of the Reykjanes Geothermal Field in the Oblique Rift of SW Iceland: From Regional to Reservoir Scales.** *Open J Geol.* 2018a; **08**: 333–382.
Publisher Full Text

Khodayar M, Björnsson S, Kristinsson SG, *et al.*: **Tectonic Control of the Theistareykir Geothermal Field by Rift and Transform Zones in North Iceland: A Multidisciplinary Approach.** *Open J Geol.* 2018b; **08**: 543–584.
Publisher Full Text

Khodayar M, Björnsson S, Vikingsson S, *et al.*: **Unstable Rifts, a Leaky Transform Zone and a Microplate: Analogues from South Iceland.** *Open J Geol.* 2020; **10**: 317–367.
Publisher Full Text

Kimbell GS, Ritchie JD, Johnson H, *et al.*: **Controls on the structure and evolution of the NE atlantic margin revealed by regional potential field imaging and 3D modelling.** *Petroleum Geology: North-West Europe and Global Perspectives—Proceedings of the 6 th Petroleum Geology Conference.* Doré AG, Vinning BA, editors. London: Geological Society; 2005; **6**: 933–945.
Publisher Full Text

Kimbell GS, Stewart MA, Gradmann S, *et al.*: **Controls on the location of compressional deformation on the NW European margin.** *The NE Atlantic Region: A Reapraisal of Crustal Structure, Tectonostratigraphy and Magmatic Evolution.* London: Geological Society; 2016; **447**: 249–278. Special Publications.
Publisher Full Text

Klitzke P, Franke D, Ehrhardt A, *et al.*: **The Paleozoic evolution of the Olga Basin region, northern Barents Sea: a link to the Timanian orogeny.** *Geochem. Geophys. Geosyst.* 2019; **20**(2): 614–629.
Publisher Full Text

Koehl JBP: **Impact of Timanian thrusts on the phanerozoic tectonic history of Svalbard.** *Keynote lecture, EGU General Assembly, May 3rd–8th, Vienna, Austria.* 2020.
Publisher Full Text

Koehl JBP: **Early Cenozoic Eurekan strain partitioning and decoupling in central Spitsbergen Svalbard.** *Solid Earth.* 2021; **12**(5): 1025–1049.
Publisher Full Text

Koehl JBP: **Extended data for: "Impact of sub-basalt thrust systems on the Faroe continental shelf for the late Paleoproterozoic–Cenozoic tectonic evolution of the margin".** *DataverseNO.* 2024; **4**: 10.18710/780M9P.
Publisher Full Text

Koehl JBP: **The myth of the De Geer Zone [version 2; peer review: 1 approved, 2 approved with reservations, 1 not approved].** *Open Res Europe.* 2025; **4**: 1.
PubMed Abstract | **Publisher Full Text** | **Free Full Text**

Koehl J-BP: **High-resolution versions of the figures for "Inverted rift-orthogonal thrust systems in the Greenland–Iceland–Faroe Ridge: implications for the nature of the crust and plate tectonics" [Figure].** *Open Research Europe (Version 1.0). Zenodo.* 2026.
Publisher Full Text

Koehl JBP, Gallardo Jara RE, Ortiz J, *et al.*: **Onshore surface–subsurface correlation of orogenic structures and the continuation of the late Paleozoic Gondwanides in the Tierra del Fuego fold-and-thrust belt, southern Patagonia**. *Open Res Europe.* 2026.

Koehl JBP, Allaart L, Noormets R: **Devonian–Carboniferous extension and Eurekan inversion along an inherited WNW–ESE-striking fault system in Billefjorden, Svalbard [version 2; peer review: 2 approved, 1 not approved].** *Open Res Eur.* 2023b; **3**: 124.
PubMed Abstract | **Publisher Full Text** | **Free Full Text**

Koehl JBP, Bergh SG, Henningsen T, *et al.*: **Middle to late Devonian–Carboniferous collapse basins on the Finnmark platform and in the southwesternmost Nordkapp basin, SW Barents Sea.** *Solid Earth.* 2018; **9**(2): 341–372.
Publisher Full Text

Koehl JBP, Bergh SB, Indrevær I, *et al.*: **Late Devonian-Carboniferous faulting and controlling structures and fabrics in NW Finnmark.** *Nor. J. Geol.* 2019; **99**(3): 1–40.
Publisher Full Text

Koehl JBP, Foulger GR: **Orogenic bridge theory: towards a predicting tool for past and future plate tectonics [version 2; peer review: 3 accepted with reservations, 5 not accepted].** *Open Res Europe.* 2025; **4**(76).
Publisher Full Text

Koehl JBP, Jolley DW, Peace AL, *et al.*: **Impact of sub-basalt thrust systems on the Faroe continental shelf for the late Paleoproterozoic-Cenozoic tectonic evolution of the margin [version 2; peer review: 2 approved].** *Open Res Eur.* 2024a; **4**: 181.
PubMed Abstract | **Publisher Full Text** | **Free Full Text**

Koehl JBP, Magee C, Anell IM: **Impact of Timanian thrust systems on the late Neoproterozoic–Phanerozoic tectonic evolution of the Barents**

Sea and Svalbard. *Solid Earth.* 2022; **13**(1): 85–115.
Publisher Full Text

Koehl JBP, Mottram CM: **Proof of concept for Orogenic Bridge Theory in the Fram Strait using U–Pb geochronology of syn-kinematic carbonates [version 1; peer review: 1 approved].** *Open Res Europe.* 2025; **5**: 231.
Publisher Full Text

Koehl JBP, Muñoz-Barrera JM: **From widespread Mississippian to localized Pennsylvanian extension in central Spitsbergen, Svalbard.** *Solid Earth.* 2018; **9**: 1535–1558.
Publisher Full Text

Koehl JBP, Foulger GR, Peace AL: **Introduction to Orogenic Bridge Theory. EGU General Assembly 2025, Vienna, Austria, 27 Apr–2 May 2025, EGU25–2604.**
Publisher Full Text

Koehl JBP, Polonio I, Rojo L: **Timanian fold-and-thrust belt and Caledonian overprint in the Selis Ridge imaged by new 3D seismic attributes and spectral decomposition.** *Tektonika.* 2023a; **1**(1): 76–100.
Publisher Full Text

Koehl JBP, Stokmo EMB: **Caledonian reactivation and reworking of Timanian thrust systems and implications for latest Mesoproterozoic to mid-Paleozoic tectonics and magmatism in Northern Baltica [version 2; peer review: 1 approved, 2 approved with reservations, 1 not approved].** *Open Res Europe.* 2024; **4**: 30.
PubMed Abstract | Publisher Full Text | Free Full Text

Koehl JBP, Tappe S, Foulger GR, *et al.*: **Devonian–Mississippian magmatism related to extensional collapse in Svalbard: implications for radiating dyke swarms [version 1; peer review: 2 approved].** *Open Res Europe.* 2024b; **4**: 262.
PubMed Abstract | Publisher Full Text | Free Full Text

Kristmannsdóttir H: **Anorthosite inclusions in Tertiary dolerite from the island groups Hrappsey and Purkey, West Iceland.** *J. Geol.* 1971; **79**: 741–748.
Publisher Full Text | Reference Source

Lamont TN, McCarthy W, Strachan R, *et al.*: **Late Ordovician regional high-pressure metamorphism in Scotland, UK: Caledonian metamorphic climax predated the closure of the Iapetus Ocean.** *GSA Bull.* 2025; **138**: 977–992.
Publisher Full Text

Lang HM, Gilotti JA: **Modeling the exhumation path of partially melted ultrahigh-pressure metapelites, North-East Greenland Caledonides.** *Lithos.* 2015; **226**: 131–146.
Publisher Full Text

Larsen HC, Jakobsdottir S: **Distribution, crustal properties and significance of seawards-dipping sub-basement reflectors off E Greenland.** *Early Tertiary Volcanism and the Opening of the NE Atlantic.* Morton AC, Parson LM, editors. Geological Society Special Publication; 1988; **39**: 95–114.
Publisher Full Text

Larsen LM, Watt WS, Watt M: **Geology and petrology of the Lower Tertiary plateau basalts of the Scoresby Sund region, East Greenland.** *Bull. Grønl. Geol. Unders.* 1989; **157**(166): 1–164.
Publisher Full Text

Larsen LM, Waastein R, Pedersen AK, *et al.*: **Trans-Atlantic correlation of the Palaeogene volcanic successions in the Faeroe Islands and East Greenland.** *J. Geol. Soc.* 1999; **156**: 1081–1095.
Publisher Full Text

Larsen LM, Pedersen AK, Tegner C, *et al.*: **Eocene to Miocene igneous activity in NE Greenland: northward younging of magmatism along the East Greenland margin.** *J. Geol. Soc.* 2014; **171**: 539–553.
Publisher Full Text

Layfield LK, Schofield N, Watson D, *et al.*: **3D Seismic reflection evidence for lower crustal intrusions beneath the Faroe–Shetland Basin, NE Atlantic Margin.** *J. Geol. Soc.* 2023; 180.
Publisher Full Text

Li QC, Zhu GM: **Singularity detection of the thin bed seismic sifgnals with wavelet transform.** *Acta Seimol Sin.* 2000; **13**(1): 61–66.
Publisher Full Text

Li W, Wu T, Liu H: **Structure-Preserving Random Noise Attenuation Method for Seismic Data Based on a Flexible Attention CNN.** *Remote Sens.* 2022; **14**: 5240.
Publisher Full Text

Liotta D, Brogi A, Árnadóttir S, *et al.*: **Field evidence of the interplay between rift and transform structures in the Krafla geothermal area, N-Iceland.** *Geothermics.* 2021; **91**: 102039.
Publisher Full Text

Llorens MG, Bons PD, Griera A, *et al.*: **Single layer folding in simple shear.** *J. Struct. Geol.* 2013; **50**: 209–220.
Publisher Full Text

Longman CD, Coward MP: **Deformation around the Beinn an Dubhaich granite.** *Skye. Scott J Geol.* 1979; **15**: 301–311.
Publisher Full Text

Love GJ, Kinny PD, Friend CRL: **Timing of magmatism and metamorphism in the Gruinard Bay area of the Lewisian Gneiss Complex: comparisons with the Assynt Terrane and implications for terrane accretion.** *Contrib. Mineral. Petrol.* 2004; **146**: 620–636.
Publisher Full Text

Luckett R, Baptie B: **Local earthquake tomography of Scotland.** *Geophys. J. Int.* 2015; **200**(3): 1538–1554.
Publisher Full Text

Lundin ER, Doré AG, Naliboff J, *et al.*: **Utilization of continental transforms in break-up: observations, models, and a potential link to magmatism.** *Tectonic Development, Thermal History and Hydrocarbon Habitat Models of Transform Margins: their Differences from Rifted Margins.* Nemcok M, Doran H, Doré AG, *et al.*, editors. Geol Soc London; 2022; **524**: 1–25. Special Publications.
Publisher Full Text

Martin E, Paquette JL, Bosse V, *et al.*: **Geodynamics of rift–plume interaction in Iceland as constrained by new ^{40}Ar/^{39}Ar and in situ U–Pb zircon ages.** *EPSL.* 2011; **311**: 28–38.
Publisher Full Text

Mason AJ, Parrish RR, Brewer TS: **U–Pb geochronology of Lewisian orthogneisses in the Outer Hebrides, Scotland: implications for the tectonic setting and correlation of the South Harris Complex.** *J. Geol. Soc.* 2004; **161**: 45–54.
Publisher Full Text

McCaffree CL, Christensen NI: **Shear Wave Properties and Seismic Imaging of Mylonite Zones.** *J. Geophys. Res.* 1993; **98**(B3): 4423–4435.
Publisher Full Text

McCann AJ, Dallmann WK: **Reactivation of the long-lived Billefjorden Fault Zone in north central Spitsbergen.** *Svalbard. Geol Mag.* 1996; **133**(1): 63–84.
Publisher Full Text

McClay KR: **Glossary of thrust tectonics terms.** McClay KR, editor. *Thrust tectonics.* London: Chapman and Hall; 1992; 419–433.

McClay KR, Insley MW: **Duplex structures in the Lewis thrust sheet, Crowsnest Pass, Rocky Mountains, Alberta, Canada.** *J. Struct. Geol.* 1986; **8**(8): 911–922.
Publisher Full Text

McDougall I, Kristjansson L, Sæmundsson K: **Magnetostratigraphy and geochronology of northwest Iceland.** *J. Geophys. Res.* 1984; **89**(B8): 7029–7060.
Publisher Full Text

Mehnert KR: **Migmatites and the Origin of Granitic Rocks.** *Geol. Mag.* 1968; **106**(2): 222–223.
Publisher Full Text

Menke W, Levin V: **Cold crust in a hot spot.** *Geophys. Res. Lett.* 1994; **21**(18): 1967–1970.
Publisher Full Text

Menke W, Brandsdóttir B, Einarsson P, *et al.*: **Reinterpretation of the RRISP-77 Iceland shear-wave profiles.** *Geophys. J. Int.* 1995; **126**(1): 166–172.
Publisher Full Text

Mercier de Lépinay M, Loncke L, Basile C, *et al.*: **Transform continental margins – Part 2: A worldwide review.** *Tectonophysics.* 2016; **693**: 96–115.
Publisher Full Text

Merdith AS, Williams SE, Collins AS, *et al.*: **Extending full-plate tectonic models into deep time: linking the Neoproterozoic and the Phanerozoic.** *Earth Sci. Rev.* 2021; **214**: 103477.
Publisher Full Text

Moorbath S, Sigurdsson H, Goodwin R: **K-Ar ages of the oldest exposed rocks in Iceland.** *EPSL.* 1968; **4**: 197–205.
Publisher Full Text

Moorlock BSP, Tarney J, Wright AE: **K-Rb ratios of intrusive anorthosite veins from Angmagssalik.** *East Greenland. EPSL.* 1972; **14**: 39–46.
Publisher Full Text

Morgan WJ: **Convection plumes in the lower mantle.** *Nature.* 1971; **230**: 42–43.
Publisher Full Text

Morton AC, Taylor PN: **Geochemical and isotopic constraints on the nature and age of basement rocks from Rockall Bank, NE Atlantic.** *J. Geol. Soc.* 1991; **148**: 631–634.
Publisher Full Text

Mosqueira Gonzalez V, Torres Carbonell PJ, Turienzo MM: **Structural overprinting and style of deformation at sierra Beauvoir and sierra de Apen: A geometric and kinematic model for the evolution of the internal thrust-fold belt, Fuegian Andes, Argentina.** *J. S. Am. Earth Sci.* 2021; **112**(1): 103575.
Publisher Full Text

Mposkos E: **High-Pressure Metamorphism in Gneisses and Pelitic Schists in the East Rhodope Zone (N. Greece).** *Mineral. Petrol.* 1989; **41**: 25–39.
Publisher Full Text

Mukherjee A, Das S: **Anorthosites, Granulites and the Supercontinent Cycle.** *Gondwana Res.* 2002; **5**(1): 147–156.
Publisher Full Text

Musgrove FW, Mitchener B: **Analysis of the pre-Tertiary rifting history of the Rockall trough.** *Pet. Geosci.* 1996; **2**(4): 353–360.
Publisher Full Text

Nasuti A, Olesen O: **Chapter 4: Magnetic Data.** *Tectonostratigraphic Atlas of the North-East Atlantic Region.* Hopper JR, Funck T, Stoker MS, *et al.*, editors. Copenhagen, Denmark: Geological Survey of Denmark and Greenland (GEUS); 2014a; 41–52.
Publisher Full Text

Nasuti A, Olesen O: **Magnetic Anomaly Grids.** *GEUS Dataverse.* 2014b; **V1**.
Publisher Full Text

Nasuti A, Roberts D, Gernigon L: **Multiphase mafic dykes in the Caledonides of northern Finnmark revealed by a new high-resolution aeromagnetic dataset.** *Nor. J. Geol.* 2015; **95**(3–4): 285–298.
Publisher Full Text

Natland JH: **ΔNb and the role of magma mixing at the East Pacific Rise and Iceland.** *Plates, plumes, and planetary processes.* Foulger GR, Jurdy DM, editors. Geological Society of America Special Paper; 2007; **430**: 413–449.
Publisher Full Text

Nedimović MR, Carbotte SM, Harding AJ, *et al.*: **Frozen magma lenses below the oceanic crust.** *Nature.* 2005; **436**: 1149–1152.
PubMed Abstract | **Publisher Full Text**

Nicholson A: **Seismic data re-processing offshore Faroes April 2011-January 2012.** *TGS Final Report. OF9495RE11.* 2012; **624**: 1–75.

Nilsen O: **Petrology of the Hyllingen gabbro complex, Sør-Trøndelag, Norway.** *Nor. Geol. Tidsskr.* 1973; **53**: 213–231.
Reference Source

Nilsen TFD, Brooks CK: **The E Greenland rifted continental margin: an examination of the coastal flexure.** *J. Geol. Soc.* 1981; **138**: 559–568.
Publisher Full Text

Nilsen TH, Kerr DR: **Paleoclimatic and paleogeographic implications of a lower Tertiary laterite (latosol) on the Iceland-Faeroe Ridge, North Atlantic region.** *Geol. Mag.* 1978; **115**(3): 153–182.
Publisher Full Text

Nordgulen Ø, Saintot A: *The character and kinematics of deformation zones (ductile shear zones, fracture zones and fault zones) at Forsmark - report from phase 3.* Stockholm, Sweden: Swedish Nuclear Fuel and Waste Management Co; 2008; P-07-111.

Norton MG, McClay KR, Way NA: **Tectonic evolution of Devonian basins in northern Scotland and southern Norway.** *Nor. Geol. Tidsskr.* 1987; **67**: 323–338.
Reference Source

Nunes PD, Steiger RH, Bridgewater D: **A zircon age from gabbro-anorthosite inclusions in the gneisses of the Angmagssalik area, south-east Greenland.** *Rapp Grønlands Geol. Unders.* 1974; **66**: 21–31.
Publisher Full Text

Ólavsdóttir J, Eidesgaard ÓR, Stoker MS: **The stratigraphy and structure of the Faroese continental margin.** *The NE Atlantic Region: A Reapraisal of Crustal Structure, Tectonostratigraphy and Magmatic Evolution.* Péron-Pinvidic G, Hopper JR, Toker MS, *et al.*, editors. London: Geological Society; 2016; **447**: 1–10. Special Publications.
Publisher Full Text

Ólavsdóttir J, Stoker MS, Riishuus MS, *et al.*: **Discovery of two sub-volcanic basins below the North Atlantic Igneous Province (NAIP), Faroe Platform, NE Atlantic Ocean.** *Tectonics.* 2021; **40**.
Publisher Full Text

Ólavsdóttir J, Stoker MS, Riishuus MS, *et al.*: **Discovery of two sub-volcanic basins below the North Atlantic Igneous Province (NAIP)**, *Faroe Platform, NE Atlantic Ocean*. Tectonics. 2021; **40**(4): e2020TC006589.
Publisher Full Text

Oliver GJH: **Feldspathic Hornblende and Garnet Granulites and Associated Anorthosite Pegmatites From Doubtful Sound, Fiordland, New Zealand.** *Contrib. Mineral. Petrol.* 1977; **65**: 111–121.
Publisher Full Text

Ott JN, Condit CB, Schulte-Pelkum V, *et al.*: **Seismic Anisotropy of Mafic Blueschists: EBSD-Based Constraints From the Exhumed Rock Record.** *JGR Solid Earth.* 2024; **129**: e2023JB027679.
Publisher Full Text

Owens BE, Dymek RF: **Fe-Ti-P-rich rocks and massif anorthosite: problems of interpretation illustrated from the Labrieville and St-Urbain plutons, Québec.** *Can. Mineral.* 1992; **30**: 163–190.
Reference Source

O'Connor JM, Jokat W, Regelous M, *et al.*: **Superplume mantle tracked isotopically the length of Africa from the Indian Ocean to the Red Sea.** *Nat. Commun.* 2019; **10**(1): 5493.
Publisher Full Text

Park RG: **Observations on Lewisian Chronology.** *Scott. J. Geol.* 1970; **6**(4): 379–399.
Publisher Full Text

Parson LMthe ODP Leg 104 Scientific Party: **Dipping reflector styles in the NE Atlantic Ocean.** *Early Tertiary Volcanism and the Opening of the NE Atlantic.* Morton AC, Parson LM, editors. Geological Society; 1988; **39**: 57–68. Special Publication.
Publisher Full Text

Passey SR, Jolley DW: **A revised lithostratigraphic nomenclature for the Palaeogene Faroe Islands Basalt Group, NE Atlantic Ocean.** *Earth Environ. Sci. Trans. R. Soc. Edinb.* 2008; **99**: 127–158.
Publisher Full Text

Pe-Piper G, Reynolds PH, Nearing J, *et al.*: **Early Carboniferous deformation and mineralization in the Cobequid shear zone, Nova Scotia: an ^{40}Ar/^{39}Ar geochronology study.** *Can. J. Earth Sci.* 2004; **41**: 1425–1436.
Publisher Full Text

Péron-Pinvidic G: **Magmatic domes and the initiation of oceanic processes at the Norwegian margin.** *Sci. Rep.* 2025; **15**: 35082.
PubMed Abstract | **Publisher Full Text** | **Free Full Text**

Péron-Pinvidic G, Osmundsen PT: **From orogeny to rifting: insights from the Norwegian 'reactivation phase'.** *Sci. Rep.* 2020; **10**(1): 14860.
PubMed Abstract | **Publisher Full Text** | **Free Full Text**

Péron-Pinvidic G, Gernigon L, Gaina C, *et al.*: **Insights from the Jan Mayen system in the Norwegian–Greenland sea—I. Mapping of a microcontinent.** *Geophys. J. Int.* 2012; **191**: 385–412.
Publisher Full Text

Phillips TB, McCaffrey KJW: **Terrane Boundary Reactivation, Barriers to Lateral Fault Propagation and Reactivated Fabrics: Rifting Across the Median Batholith Zone, Great South Basin, New Zealand.** *Tectonics.* 2019; **38**(11): 4027–4053.
Publisher Full Text

Phillips T, Jackson CAL, Bell RE, *et al.*: **Reactivation of intrabasement structures during rifting: a case study from offshore southern Norway.** *J. Struct. Geol.* 2016; **91**: 54–73.
Publisher Full Text

Punturo R, Cirrincione R, Fazio E, *et al.*: **Microstructural, compositional and petrophysical properties of mylonitic granodiorites from an extensional shear zone (Rhodope Core complex, Greece).** *Geol. Mag.* 2014; **151**(6): 1051–1071.
Publisher Full Text

Ramberg H: **Evolution of ptygmatic folding.** *Nor. Geol. Tidsskr.* 1959; **39**: 99–152.
Reference Source

Reeve MT, Magee C, Bastow ID, *et al.*: **Nature of the Cuvier Abyssal Plain crust, offshore NW Australia.** *J. Geol. Soc.* 2021; **178**: 1–17.
Publisher Full Text

Rehnström EF, Corfu F, Torsvik TH: **Evidence of a Late Precambrian (637 Ma) Deformational Event in the Caledonides of Northern Sweden.** *J. Geol.* 2002; **110**(5): 591–601.
Publisher Full Text

Richardson KR, Smallwood JR, White RS, *et al.*: **Crustal structure beneath the Faroe Islands and the Faroe–Iceland Ridge.** *Tectonophysics.* 1998; **300**(1–4): 159–180.
Publisher Full Text

Ringwood AE, Green DH: **An experimental investigation of the gabbro–eclogite transformation and some geophysical implications.** *Tectonophysics.* 1966; **3**(5): 383–427.
Publisher Full Text

Roberts D, Siedlecka A: **Berggrunnskart HOPSEIDET 2236-1, M 1:50 000, Foreløpig utgave.** *NORG GEOL UNDERS.* 2013.

Roberts D, Williams GD: **Berggrunnskart Kjøllefjord 2236 IV, M 1: 50.000, foreløpig utgave.** *NORG GEOL UNDERS.* 2013.

Roberts DG, Ardus DA, Dearnley R: **Precambrian rocks drilled on the Rockall Bank.** *Nat. Phys. Sci.* 1973; **244**: 21–23.
Publisher Full Text

Robinson PT, Hall JM, Christensen NI, *et al.*: **The Iceland Research Drilling Project: Synthesis of Results and Implications for the Nature of Icelandic and Oceanic Crust.** *J. Geophys. Res.* 1982; **87**(B8): 6657–6667.
Publisher Full Text

Rosa D, Majka J, Thrane K, *et al.*: **Evidence for Timanian-age basement rocks in North Greenland as documented through U–Pb zircon dating of igneous xenoliths from the Midtkap volcanic centers.** *Precambrian Res.* 2016; **275**: 394–405.
Publisher Full Text

Rowan MG, Urai JL, Fiduk JC, *et al.*: **Deformation of intrasalt competent layers in different modes of salt tectonics.** *Solid Earth.* 2019; **10**: 987–1013.
Publisher Full Text

Roy JC: *La géologie du fossé des Vieux Grès Rouges du Spitzberg (archipel du Svalbard, territoire de l'Arctique) : synthèse stratigraphique, conséquences paléogéographiques, paléoenvironnementales et tectoniques synsédimentaires par.* Paris, France: Pierre and Marie Curie University; 2007-15, **2007**;242. Ph.D. thesis.

Rutter E, Brodie K, James T, *et al.*: **Large-scale folding in the upper part of the Ivrea-Verbano zone, NW Italy.** *J. Struct. Geol.* 2007; **29**: 1–17.
Publisher Full Text

Sæmundson K: **Outline of the geology of Iceland.** *Jökull.* 1979; **1**: 7–28.
Reference Source

Saintot A, Stephens MB, Viola G, *et al.*: **Brittle tectonic evolution and paleostress field reconstruction in the Southwestern part of the Fennoscandian Shield, Forsmark, Sweden.** *Tectonics.* 2011; **30**.
Publisher Full Text

Sapin F, Ringenbach JC, Clerc C: **Rifted margins classification and forcing parameters.** *Sci. Rep.* 2021; **11**: 8199.
PubMed Abstract | **Publisher Full Text** | **Free Full Text**

Sato T, Nogi Y, Sato H, *et al.*: **A new tectonic model between the Madagascar Ridge and Del Cano Rise in the Indian Ocean.** *JGR: Solid Earth.* 2022; **127**.
Publisher Full Text

Schilling JG: **Iceland Mantle Plume: Geochemical Study of Reykjanes Ridge.** *Nature.* 1973; **242**: 565–571.
Publisher Full Text

Schuler J, Christie PAF, White RS: **Borehole study of compressional and shear attenuation of basalt flows penetrated by the Brugdan and William wells on the Faroes shelf.** *Geophys. Prospect.* 2013; **62**: 315–332.
Publisher Full Text

Shannon PM, Jacob AWB, O'Reilly BM, *et al.*: **Structural setting, geological development and basin modelling in the Rockall Trough.** *Petroleum Geology of Northwest Europe: Proceedings of the 5th Conference.* Fleet AJ, Boldy SAR, editors. Petroleum Geology; 1999; **86**: 421–431.
Publisher Full Text

Shannon PM, English KL, Hanrahan M: *The Stratigraphic Nomenclature of the Irish Offshore Basins.* Dublin, Ireland: Department of the Environment, Climate and Communications, PAD Special Publication; 2020; vol. **2/21**: 1–95.
Reference Source

Siegesmund S, Kern H, Vollbrecht A: **The effect of oriented microcracks on seismic velocities in an ultramylonite.** *Tectonophysics.* 1991; **186**: 241–251.
Publisher Full Text

Sigmundsson F, Einarsson P, Hjartardóttir AR, *et al.*: **Geodynamics of Iceland and the signatures of plate spreading.** *JVGR.* 2020; **391**: 106436.
Publisher Full Text

Sinha ST: *Factors controlling a microcontinent development during continental breakup- the Elan Bank case study.* Brno, Croatia: Masaryk University; 2024; 1–305. Ph.D. Thesis.
Publisher Full Text

Smallwood JR, White RS, Staples RK: **Deep crustal reflectors under Reydarfjördur, eastern Iceland: crustal accretion above the Iceland mantle plume.** *Geophys. J. Int.* 1998; **134**: 277–290.
Publisher Full Text

Smithson SB: **Densities of metamorphic rocks.** *Geophys.* 1971; **36**(4): 690–694.
Publisher Full Text

Smythe DK: **Faeroe-Shetland escarpment and continental Margin North of the Faeroes.** *Structures and Development of the Greenland-Scotland Ridge. Nato Conference Series.* Bott MHP, Saxov S, Talwani M, *et al.*, editors. Boston, Massachusetts, USA: Springer; 1983; **8**: 109–119.
Publisher Full Text

Sotiriou P, Polat A: **Petrogenesis of anorthosites throughout Earth history.** *Precambrian Res.* 2023; **384**: 106936.
Publisher Full Text

Spence GD, White RS, Westbrook GK, *et al.*: **The Hatton Bank continental margin—I. shallow structure from two-ship expanding spread seismic profiles.** *Geophys. J. R. Astron. Soc.* 1989; **96**(2): 273–294.
Publisher Full Text

Staples RK, White RS, Brandsdóttir B, *et al.*: **Färoe-Iceland Ridge Experiment 1. Crustal structure of northeastern Iceland.** *J. Geophys. Res.* 1997; **102**(B4): 7849–7866.
Publisher Full Text

Stemmerik L, Vigran JO, Piasecki S: **Dating of late Paleozoic rifting events in the North Atlantic: New biostratigraphic data from the uppermost Devonian and Carboniferous of East Greenland.** *Geology.* 1991; **19**: 218–221.
Publisher Full Text

Stoker MS, Smith K, Kimbell GS, *et al.*: *Dynamic evolution of the Faroe-Shetland region, Energy and Marine Geoscience Programme Commissioned Report, CR/15/001.* Edinburgh, UK: British Geological Survey; 2015; 95.

Storey CD, Brewer TS, Parrish RR: **Late-Proterozoic tectonics in northwest Scotland: one contractional orogeny or several?.** *Precambrian Res.* 2004; **134**(3–4): 227–247.
Publisher Full Text

Storey M, Duncan RA, Tegner C: **Timing and duration of volcanism in the North Atlantic Igneous Province: Implications for geodynamics and linksto the Iceland hotspot.** *Chem. Geol.* 2007; **241**: 264–281.
Publisher Full Text

Storey CD, Brewer TS, Anckiewicz R, *et al.*: **Multiple high-pressure metamorphic events and crustal telescoping in the NW Highlands of Scotland.** *J. Geol. Soc.* 2010; **167**: 455–468.
Publisher Full Text

Strachan RA: **Evidence in North-East Greenland for Late Silurian-Early Devonian regional extension during the Caledonian orogeny.** *Geology.* 1994; **22**: 913–916.
Publisher Full Text

Subrahmanyam C, Verma RK: **Densities and Magnetic Susceptibilities of Precambrian Rocks of Different Metamorphic Grade (Southern Indian Shield).** *Geophys.* 1981; **49**(1): 101–107.
Reference Source

Sutton J, Watson J: **The pre-Torridonian metamorphic history of the Loch Torridon and Scourie areas in the north-west Highlands, and its bearing on the chronological classification of the Lewisian.** *QJGS.* 1950; **106**: 241–307.
Publisher Full Text

Sæmundsson K: **Outline of the geology of Iceland.** *Jökull.* 1979; **29**: 7–28.
Publisher Full Text | **Reference Source**

Talwani M, Udintsev GB, White SM: **1. Introduction and explanatory notes, Leg 38, Deep Sea Drilling Project.** *Initial Rep. Deep Sea Drill. Proj.* 1976; **38**: 3–19.
Publisher Full Text

Tarney J, Weaver BL: **Geochemistry of the Scourian complex: petrogenesis and tectonic models.** *Evolution of the Lewisian and Comparable Precambrian High Grade Terrains.* Park RG, Tarney J, editors. Geological Society Special Publication; 1987; **27**: 45–56.
Publisher Full Text

Tegner C, Duncan RA: **^{40}Ar–^{39}Ar chronology for the volcanic history of the southeast Greenland rifted margin.** *Proceedings of the Ocean Drilling Program, Scientific Results.* 1999; **163**: 53–62.
Publisher Full Text

Tegner C, Brooks CK, Duncan RA, *et al.*: **^{40}Ar–^{39}Ar ages of intrusions in East Greenland: Rift-to-drift transition over the Iceland hotspot.** *Lithos.* 2008; **101**: 480–500.
Publisher Full Text

Thordarson T, Larsen G: **Volcanism in Iceland in historical time: Volcano types, eruption styles and eruptive history.** *J. Geodyn.* 2007; **43**: 118–152.
Publisher Full Text

Thrane K: **Palaeoproterozoic age of a basement gneiss complex in the Charcot Land tectonic window, East Greenland Caledonides.** *Geol Surv Den Greenl Bull.* 2004; **6**(57–66): 57–66.
Publisher Full Text

Torsvik TH, Amundsen HEF, Trønnes RG, *et al.*: **Continental crust beneath southeast Iceland.** *Proc. Natl. Acad. Sci. USA.* 2015; **112**(15): E1818–E1827.
Publisher Full Text

Torsvik TH, Rehnström EF: **Cambrian palaeomagnetic data from Baltica: implications for true polar wander and Cambrian palaeogeography.** *J. Geol. Soc. Lond.* 2001; **158**: 321–329.
Publisher Full Text

Trutner SD: *An Investigation of AMS in Oman Ophiolite Gabbros.* Oberlin College, USA: 2016; **247**: 1–40. Bachelor's Thesis.
Reference Source

Tryggvason E: **Seismicity, earthquake swarms, and plate boundaries in the Iceland region.** *BSSA.* 1973; **63**(4): 1327–1348.
Publisher Full Text

Tryggvason E, Båth M: **Upper Crustal Structure of Iceland.** *J. Geophys. Res.* 1961; **66**(6): 1913–1925.
Publisher Full Text

Van der Straaten F: *Retrogression of eclogites to blueschists: a record of fluid infiltration during uplift in subduction zones.* Germany: Christian Albrecht University; 2008; 1–156. Ph.D. Thesis.
Reference Source

VanTongeren JA, Hirth G, Kelemen PB: **Constraints on the accretion of the gabbroic lower oceanic crust from plagioclase lattice preferred orientation in the Samail ophiolite.** *EPSL.* 2015; **427**: 249–261.
Publisher Full Text

Vasileiou A, Gouiza M, Mortimer E, *et al.*: **New insights into the crustal architecture and tectonic evolution of the Eastern Gulf of Mexico.** *Basin Res.* 2023; **36**(1): e12812.
Publisher Full Text

Villemin T, Bergerat F, Angelier J, *et al.*: **Brittle deformation and fracture patterns on oceanic rift shoulders: the Esja peninsula, SW Iceland.** *J. Struct. Geol.* 1994; **16**(12): 1641–1654.
Publisher Full Text

Vine FJ, Moores EM: **A model for the gross structure, petrology, and magnetic properties of oceanic crust.** *Geol. Soc. Am. Mem.* 1972; **132**:

195–208.
Publisher Full Text

Waagstein R, Nielsen PH, Fine S, *et al.*: *Lopra Well No. 1, Suduroy, Faeroe Islands. Geological Well Completion Report.* Faeroe Department, Geological Survey of Denmark; 1982; 1–176.
Publisher Full Text

Waddams P, Cordingley T: **The regional geology and exploration potential of the NE Rockall Basin.** *Petroleum Geology of Northwest Europe: Proceedings of the 5th Conference.* Fleet AJ, Boldy SA, editors. London: Geological Society; 1999; **5**: 379–390.
Publisher Full Text

Walker GPL: **Geological investigations in eastern Iceland.** *Bull. Volcanol.* 1964; **27**: 351–363.
Publisher Full Text

Walker JD, Geissmann JW: *Geologic Time Scale v. 6.0.* Geological Society of America; 2022.
Publisher Full Text

Walker F, Schofield N, Millett J, *et al.*: **Paleogene volcanic rocks in the northern Faroe–Shetland Basin and Møre Marginal High: understanding lava field stratigraphy.** *Cross-Border Themes in Petroleum Geology II: Atlantic Margin and Barents Sea.* Chiarella D, Archer SG, Howell JA, *et al.*, editors. Geological Society London Special Publications; 2022; **495**: 199–235.
Publisher Full Text

Watson J, Dunning FW: **Basement-cover relations in the British Caledonides.** *The Caledonides of the British Isles—reviewed.* Harris AL, Holland CH, Leake BE, editors. Geological Society London, 1979; **8**: 67–91.
Publisher Full Text

Weaver BL, Tarney J: **Rare earth geochemistry of Lewisian granulite-facies gneisses, northwest Scotland: implications for the petrogenesis of the archaean lower continental crust.** *EPSL.* 1980; **51**: 279–296.
Publisher Full Text

Western Geco: *Faeroe Iceland Ridge, Western Atlas.* British Institutes Reflection Profiling Syndicate; 1996.
Reference Source

White RS, McKenzie D: **Mantle plumes and flood basalts.** *J. Geophys. Res.* 1995; **100**(B9): 17543–17585.
Publisher Full Text

Wilkinson CA, Ganerød M, Hendriks BWH, *et al.*: **Compilation and appraisal of geochronological data from the North Atlantic Igneous Province (NAIP).** *The NE Atlantic Region: A Reappraisal of Crustal Structure, Tectonostratigraphy and Magmatic Evolution.* Péron-Pinvidic G, Hopper JR, Stoker MS, *et al.*, editors. London: Geological Society; 2016; **447**: 69–103. Special Publications.
Publisher Full Text

Williamson JP, Ziska H: *A new look at the structure of the Faroe-Shetland Basin southeast of the Faroe Islands, Energy Systems & Basin Analysis Programme Commissioned Report, CR/18/038.* Keyworth, UK: British Geological Survey; 2018; 1–37.

Wrona T, Fossen H, Lecomte I, *et al.*: **Seismic expression of shear zones: Insights from 2-D point-spread-function based convolution modelling.** *J. Struct. Geol.* 2020; **140**: 104121.
Publisher Full Text

Ye Z, Fan D, Li B, *et al.*: **Thermal equation of state of the main minerals of eclogite: Constraining the density evolution of eclogite during the delamination process in Tibet.** *Solid Earth.* 2022; **13**: 745–759.
Publisher Full Text

Young KD, Jancin M, Voight B, *et al.*: **Transform deformation of tertiary rocks along the Tjörnes Fracture zone, north central Iceland.** *J. Geophys. Res.* 1985; **90**(B12): 9986–10010.
Publisher Full Text

Zhang S, Chen J, Pan L, *et al.*: **Seismic structure of Iceland revealed by ambient noise Rayleigh wave tomography.** *Tectonophysics.* 2024; **891**: 230511.
Publisher Full Text

Zirkler A, Johnson TE, White RW, *et al.*: **Polymetamorphism in the mainland Lewisian complex, NW Scotland – phase equilibria and geochronological constraints from the Cnoc an t'Sidhean suite.** *J. Metamorph. Geol.* 2012; **30**: 865–885.
Publisher Full Text